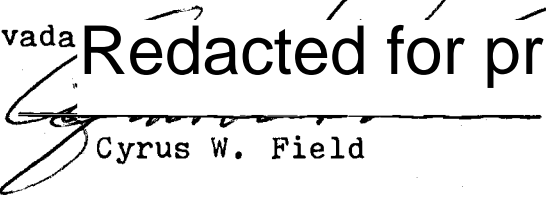


AN ABSTRACT OF THE THESIS OF

John Doucette for the degree of
Master of Science in Geology presented on April 28, 1981.

Title: The geology of the Copper Chief Prospect,
Mineral County, Nevada

Abstract approved: 
Cyrus W. Field

The Copper Chief Prospect is on the south slope of the Gabbs Valley Range, Mineral County, Nevada. It is a scheelite-sulfide deposit associated with skarn-type alteration.

Shales and limestones of the Triassic Luning Formation have been intruded by sills, dikes, and stocks of quartz monzodiorite or granodiorite of Cretaceous (?) age. Reactions between the intrusions, their host rocks, and the associated fluids have resulted in the formation of endoskarns, exoskarns, and contact metamorphic assemblages.

Unaltered samples of the intrusions from the Copper Chief Prospect are porphyritic and contain phenocrysts of plagioclase feldspar in a groundmass of quartz and potassium feldspar with minor amounts of hornblende and biotite and trace quantities of apatite, sphene, and zircon. The intrusions were altered to endoskarns in the high-temperature stages

of hydrothermal alteration. Endoskarns of low alkalinity are characterized by epidote, calcite, and crystals of clinopyroxene that have pseudomorphically replaced hornblende. Those of high alkalinity (periskarns) are characterized by an extreme enrichment in potassium feldspar, which may also be accompanied by wollastonite, garnet, epidote, and crystals of clinopyroxene that replace primary hornblende. Other types of alteration imposed upon the intrusive rocks include: 1) quartz-sericite, and 2) calcite-iron oxide.

Thermal contact metamorphism of the host rocks caused by heat released during the emplacement and crystallization of the intrusions has converted shale to hornfels and limestones to marble. In contrast hydrothermal contact metasomatism of the carbonate host rocks has formed alteration assemblages characterized by wollastonite, garnet, and clinopyroxene-garnet. Garnet exoskarns are the most abundant product of calc-silicate metasomatism at the Copper Chief Prospect. They range from grossularite to andradite in composition but most garnetites have intermediate compositions (grandites).

Alteration of the intrusions and their hosts occurred under the temperature and pressure conditions of the upper hornblende to lower pyroxene hornfels facies (600-800° C, 100-3000 bars) of contact

metamorphism and contact metasomatism.

The ore minerals exhibit a preferred distribution with respect to the alteration assemblages and controls of deposition. Scheelite is localized in clinopyroxene-rich garnetites, whereas the sulfides (chalcopyrite, pyrite, and chalcocite) are most abundant in andradite garnetite, marble, and veins of quartz.

Regional uplift and erosion followed emplacement of the intrusions and deposition of the calc-silicates and ore-bearing minerals. Volcanic activity of middle to late-Tertiary age resulted in the deposition of lava flows and tuffs. Late-Tertiary displacement on the Walker Lane system of faults has cut both the volcanic rocks and the underlying local basement of sedimentary, intrusive, and associated metamorphic rocks.

The Geology of the Copper Chief Prospect,
Mineral County, Nevada

by

John Doucette

A THESIS

submitted to

Oregon State University

in partial fulfillment of
the requirements for the
degree of

Master of Science

Completed April 28, 1981

Commencement June 1981

APPROVED: **Redacted for privacy**

[Signature]

Professor of Geology in charge of major

Redacted for privacy

[Signature]

Chairman of Department of Geology

Redacted for privacy

[Signature]

Dean of Graduate School

Date thesis is presented April 28, 1981

Typed by John Doucette

ACKNOWLEDGEMENTS

I would like to express my thanks to Roney C. Long and Continental Oil Company for suggesting this topic and for providing the financial and technical support that made it possible. I also wish to express my appreciation to Dr. Cyrus W. Field for his support, patience, and criticism of the study. Assistance with specific parts of the thesis problem and manuscript criticism from Dr. W. H. Taubeneck and Dr. E. M. Taylor is gratefully acknowledged. Manuscript criticism by fellow graduate students Paul McCarter, Greg Mack, and Bob Caseceli has been greatly appreciated if not always gracefully recieved. Many hours of geological discussion with Bob Schalla, Mark Bailey, Scott Jenkins, Bill Trojan, Greg Mack, Allan Stockman, Kathleen Benedetto, Celia Greenman, and Ed Shorey were of great assistance. Financial aid at critical points of my education from my mother, Mrs Michael O'Conner, and Col. Sydney and Arkie Smith were invaluable. Finally I would like to acknowledge the aid I recieved from my Uncle Sam in the form of G.I. Bill and guarenteed student loans without which I could have never obtained any college degree.

TABLE OF CONTENTS

<u>Chapter</u>		<u>Page</u>
1	INTRODUCTION	1
	Previous geologic studies	4
	Purpose and methods	5
2	REGIONAL GEOLOGY	8
	Sedimentary and volcanic rocks .	8
	Precambrian(?) or Cambrian.	8
	Paleozoic	10
	Paleozoic and Mesozoic	10
	Mesozoic	11
	Cenozoic	14
	Plutonic rocks	15
	Structure	18
3	SKARNS	25
4	SEDIMENTARY ROCKS	34
5	INTRUSIVE ROCKS	44
	Petrography	51
	Unaltered intrusive rocks .	51
	Endoskarn and periskarn ...	61
	Quartz-sericite alteration.	69
	Calcite alteration	71
	Veined intrusive rocks	73
	Petrochemistry	74
6	METAMORPHIC AND METASOMATIC ROCKS ...	91
	Lithology	94
	Petrography	100
	Petrochemistry	111
7	VOLCANIC ROCKS	125
	Lower volcanic group	129
	Upper volcanic group	137
8	ECONOMIC GEOLOGY	141
	Mineralogy	141
	Trace element chemistry	145

<u>Chapter</u>		<u>Page</u>
9	STRUCTURE	151
10	GEOLOGIC SUMMARY	156
	BIBLIOGRAPHY	162
	APPENDIX	173

LIST OF FIGURES

<u>Figure</u>		<u>Page</u>
1	Location map of the Copper Chief Prospect	3
2	Distribution of the Luning Formation in the Gabbs Valley Range and surrounding areas	12
3	A) Approximate limits of the Sierra Nevada Batholith	16
	B) Potassium-argon age determinations of intrusive rocks in Mineral County, Nevada	16
4	Potassium-argon age determinations for plutonic rocks of the Sierra Nevada Range, White Mountains, and Inyo Range, California, and for plutonic bodies in Mineral County, Nevada	19
5	Major right and left-lateral strike-slip faults of east California and west Nevada, normal faults of the Sierra Nevada fault system, and Basin and Range faults	24
6	Skarn classification	28
7	Measured stratigraphic sections of the Luning Formation in the northeast part of the Copper Chief Prospect ...	35
8	Pink fissile siltstone of the Luning Formation	36
9	Yellowish brown siltstone of the Luning Formation	37
10	Sandy lime packstone with wispy interbeds of cherty material	39
11	Chert pebble conglomerate of the Luning Formation	42
12	Distribution of intrusive bodies at the Copper Chief Prospect	45
13	Inch-scale veins of quartz monzodiorite in calc-silicate host rock	46
14	Red stained joints in pinkish gray intrusive rock	48

FigurePage

15	Locations of samples of plutonic rock collected for petrographic and chemical analyses	50
16	Modal percentages of minerals versus that of plagioclase feldspar in intrusive rocks of the Copper Chief Prospect	53
17	Crystals of potassium feldspar with embroidered borders in aplitic groundmass	56
18	Micropegatitic groundmass	57
19	Characteristics of twins and zones in crystals of plagioclase feldspar from samples of intrusive rock	59
20	Ternary quartz-potassium feldspar-plagioclase feldspar plot of rocks of the Copper Chief Prospect	62
21	Pseudomorph of clinopyroxene after amphibole in a sample of periskarn from the Copper Chief Prospect	65
22	Crystal of wollastonite in a sample of periskarn from the Copper Chief Prospect	67
23	Quartz-sericite alteration of intrusive rock	70
24	Quartz monzodiorite with secondary calcite in groundmass	72
25	Silica variation diagram for intrusive rocks of the Copper Chief Prospect	78
26	Normative Qz-Or-Pfs ternary diagram for the intrusive rocks from the Copper Chief Prospect	81
27	Comparison of the normative Or-Ab-An contents of the intrusive rocks of the Copper Chief Prospect with the granodiorites and adamellites of the Sierra Nevada Range and of world wide occurrences of these rock types	83

<u>Figure</u>		<u>Page</u>
28	Ternary A'KF diagram of plutonic rocks from the Copper Chief Prospect, the east Sierra Nevada Range, and the average granodiorite .	87
29	Ternary ACF diagram for plutonic rocks of the Copper Chief Prospect, average granodiorite, and plutonic rocks from the east Sierra Nevada Range	88
30	Distribution of metamorphic and metasomatic lithotypes at the Copper Chief Prospect	92
31	Siliceous hornfels crosscut by veinlets, some of which have bleached selvages	95
32	Photograph of grossularite garnetite from the Copper Chief Prospect	98
33	Photograph of andradite garnetite from the Copper Chief Prospect	98
34	Photograph of grandite garnetite from the Copper Chief Prospect	99
35	Ideoblastic porphyroblasts of garnet in a groundmass of clinopyroxene and quartz	101
36	Streaky garnet in clinopyroxene-rich groundmass	101
37	Coarsely bladed wollastonite after limestone in the central part of the Copper Chief Prospect	102
38	Locations of samples of metamorphic and metasomatic rock collected for petrographic and chemical analyses ..	104
39	Crystals of andradite	105
40	Crystals of grossularite	105
41	Parallel veinlets of quartz in garnetite	110
42	Retrograde mineralization of garnetite in sample CCP-33	112
43	Sieved porphyroblast of garnet in clinopyroxene-garnet calc-silicate rock	113

<u>Figure</u>		<u>Page</u>
44	Histogram showing gains and losses of metacarbonates from the Copper Chief Prospect	119
45	Ternary ACF plot of samples of carbonate and metacarbonate rocks from the Copper Chief Prospect	122
46	A) Geologic setting of the Copper Chief Prospect	126
	B) Highly schematic cross-section of the Copper Chief Prospect showing generalized locations of major rock types	126
47	Distribution of volcanic rocks at the Copper Chief Prospect	130
48	Quartz monzodiorite non-conformably overlain by pyroclastic tuff	131
49	Photomicrograph of basal pyroclastic unit of lower volcanic group	131
50	Ternary Qz-Or-Pfs plot of volcanic rocks	135
51	Photomicrograph of the middle unit of the lower volcanic group	136
52	Photomicrograph of the upper unit of the lower volcanic group	136
53	Photomicrograph of the middle unit of the upper volcanic group	138
54	Photomicrograph of the upper unit of the upper volcanic group	140
55	Textural relations of ore minerals ..	143
56	Plots of trace element distributions.	147
57	Histogram and log-probability plots of copper and zinc concentrations in samples of carbonate and metacarbonate rocks from the Copper Chief Prospect	149
58	Histogram and log-probability plots of copper and zinc concentrations in samples of plutonic rocks from the Copper Chief Prospect	149

Figure

Page

59	Stereographic projections of sedimentary and relict sedimentary bedding data from exposures of the Luning Formation in the northwest and central sections of the Copper Chief Prospect	152
60	Highly schematic map view of the Copper Chief Prospect showing structural features	153

LIST OF TABLES

<u>Table</u>		<u>Page</u>
1	Rock units and formations that occur in Mineral County	9
2	Genetic types of limy skarn ore deposits	33
3	Fossil collection from the northeast section of the Copper Chief Prospect.	41
4	Alteration state of the intrusive rock samples for which chemical and petrographic data were obtained .	49
5	Modal analyses of samples of intrusive rock samples from the Copper Chief Prospect	52
6	Chemical data for samples of intrusive rocks from the Copper Chief Prospect	75
7	Modal analyses of calc-silicate rocks from the Copper Chief Prospect	108
8	Trace element concentrations in samples of carbonate and metacarbonate host rocks from the Copper Chief Prospect for which major oxide analyses were obtained	114
9	Major oxide percentages and specific gravities of samples of carbonate and metacarbonate rocks from the Copper Chief Prospect, and with gains and losses calculated from these data	115
10	Chemical analyses and normative mineralogy of volcanic rocks from the Copper Chief Prospect	132
11	Maximum and minimum concentrations of trace elements in rocks of the Copper Chief Prospect	146

LIST OF PLATES

<u>Plate</u>		<u>Page</u>
1	Geologic map	in pocket
2	Geologic cross section	in pocket
3	Geologic cross section	in pocket

THE GEOLOGY OF THE COPPER CHIEF PROSPECT,
MINERAL COUNTY, NEVADA

INTRODUCTION

The Copper Chief Prospect is on the south slope of the Gabbs Valley Range, Mineral County, Nevada. It consists of several mine shafts, adits, bulldozer scrapings, and many shallow prospects. The thesis area comprises slightly more than one square mile and includes most or all of these workings.

Little is known of the mining history at Copper Chief. Hand-picked high-grade copper carbonate and zinc oxide samples are present on most waste dumps in the area. The oldest claim found during field mapping was recorded in March of 1904 by R.H. Salter and John Fagin under the name of the "Robert M", but the property may have earlier been known as the "Blue Bird Claim". A town, Smithville, was sited on the Copper Chief property during the time when mining was active (Roney C. Long, personal communication, 1978).

Copper in the form of carbonate ore, was produced from the Santa Fe District, in the Gabbs Valley Range north of Copper Chief, as early as 1883. Mining was active from 1906 to 1909 and during World War I from 1916-1918(?). The largest amount of ore was produced during World War I when the price of metals was high.

During the war period nearly two million dollars worth of copper and associated gold, silver, and lead were extracted from the district (Ross, 1961). In order for an orebody to be profitably mined at that time it had to average no less than four percent copper (Clark, 1922).

In addition to copper and zinc ore, samples of scheelite and powellite occur on at least one waste dump on the Copper Chief Prospect. The waste dump is adjacent to an inclined mine shaft and slit trenches from which the tungsten ore was taken probably during the 1950's.

The Copper Chief Prospect is reached by a county road which intersects U.S. Highway 95 approximately one-half mile north of Mina (Fig. 1). The first two miles of this road are paved. A short distance after the road changes from asphalt to gravel it ascends a low pass between the Gabbs Valley Range to the north and the Pilot Mountains to the south. The Copper Chief Prospect is in this pass about eight miles east of the intersection with Highway 95. Previous mining and exploration activity has provided a number of roads within the boundaries of the prospect and most of these can be traveled by four-wheel drive vehicles.

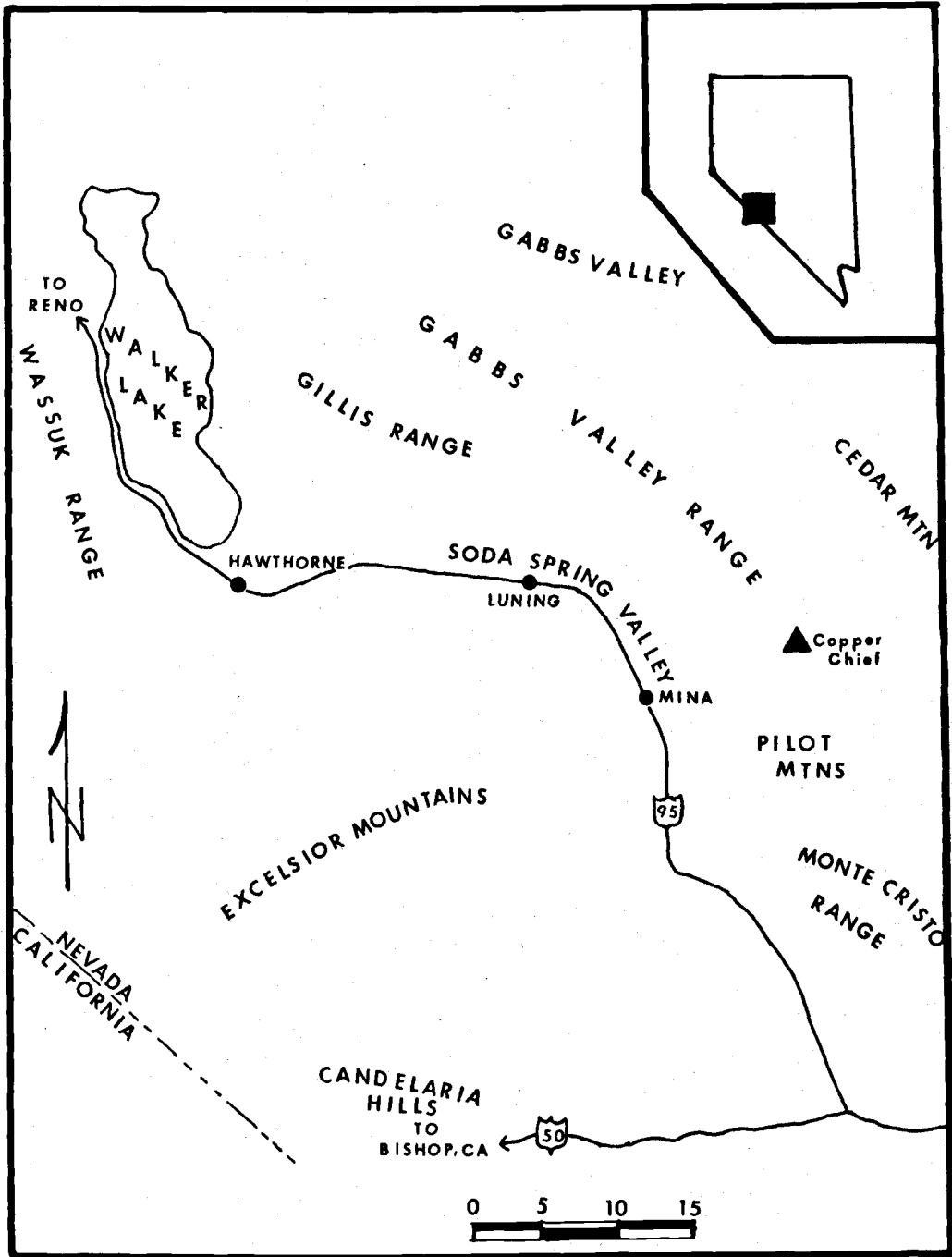


Figure 1. Location map of the Copper Chief Prospect.

Previous Geologic Studies

The geology of Mineral County was first reported in a study by J.D. Whitney (1866) which included a description of Triassic fossils in the Gabbs Valley Range.

James M. Hill visited a number of mining districts in eastern California and western Nevada in 1912. In his report (1915) of this visit, he briefly described many facts concerning the geology of the Santa Fe District. Clark (1922) reported the results of his more detailed field mapping and laboratory studies of rock samples from the Santa Fe District. Other studies of the late nineteenth and early twentieth centuries which mention the geology of Mineral County include: Emmons (1870); Knopf (1921, 1922); Lincoln (1923); and Vanderburg (1937).

Starting in 1922 H.G. Ferguson and S.W. Muller spent many field seasons in Mineral and adjacent Esmeralda Counties. Reports of their geologic investigations are given in Ferguson (1924), Ferguson and Cathcart (1924), and Ferguson and Muller (1949). Ross (1961) contributed a detailed account of the geology and mineral resources of Mineral County.

Geologists of the Continental Oil Company have mapped at detail and reconnaissance scales in Mineral

County, including most of the Gabbs Valley Range (Mangham, 1977). A reconnaissance map of the Copper Chief Prospect was made by D. Frischman (1976).

Purpose and Methods

Copper, zinc, lead, silver, and gold are among the metals commonly associated with intrusive rocks of intermediate to silicic composition. Tungsten is commonly associated with such intrusions that have carbonate or calc-silicate hosts. As the higher grade, or lower grade high-volume ore deposits now being mined are depleted, it is important that new processes be invented for the extraction of ore from lower grade rock or that new ore bodies be found. When viewed under new circumstances, such as different economic or technological conditions, some districts that have been mined in the past become areas of renewed interest or, possibly, of renewed mineral production.

The Copper Chief Prospect includes carbonate and calcareous clastic rocks which are hosts to intrusive rocks of intermediate composition. It is also an area where miners in past years have removed ore of unknown grade, but certainly ore of sufficient grade to justify the development of the considerable amount of surficial and underground workings present at the Copper Chief.

In addition to its potential economic value, the Copper Chief is within a major fault corridor, the Walker Lane. This structure is possibly comparable to the San Andreas Fault although it has not been mapped in as much detail; any biostratigraphic data that can be gathered from within this fault zone should be of some value in determining the sense and amount of movement. The purpose of this thesis is to provide a large-scale geologic map of a restricted area, and to determine the stratigraphy of sedimentary host rocks, petrography and chemistry of intrusive bodies, and the effects of contact metamorphism and metasomatism produced by the intrusive bodies on their sedimentary host rocks.

Fourteen weeks were spent doing field work during the summer of 1978. This included the preparation of a geologic map and the collection of rock samples. Mapping was done at a scale of 1:2400 using mylar overlays on a topographic map supplied by the Continental Oil Company.

Thin sections of 60 rock samples were prepared for microscopic examination and modal analyses were performed using the mechanical stage and point counter (Chayes, 1956). The surfaces of about 130 rock samples were polished for the macroscopic and stereomicroscopic examination of textures and for comparison with thin-

sectioned samples. Acetate peel impressions were made from the surfaces of sixteen limestone samples for the determination of texture and the abundance of clastic components.

Rock chip samples from 213 locations were analyzed for their contents of copper, zinc, molybdenum, gold, silver, and tungsten. Major oxide chemistry was determined for 19 rock samples and the compositions of two samples of garnet were determined.

The analytical methods and chemical laboratories used in this study are listed in the appendix.

REGIONAL GEOLOGY

The geologic record in Mineral County ranges from Precambrian(?) or Cambrian to Quaternary time but not all time periods are represented.

Sedimentary and Volcanic Rocks

The rock units and formations in Mineral County are listed in Table 1 which is compiled from Muller and Ferguson (1939), Ross (1961), and Langenheim and Larson (1973).

Precambrian(?) or Cambrian

Approximately one square mile of the southern tip of Mineral County is underlain by schistose metamorphic rocks in the White Mountains. These rocks are not precisely dated. Fossiliferous Cambrian rocks of somewhat similar lithology occur on the south flank of Miller Mountain about ten miles south of the Mineral County exposures. Anderson (1937) suggested that the schistose rocks of the White Mountains are partly Cambrian but mostly Precambrian in age. However, Anderson's work was of reconnaissance nature and the age estimates must be based on correlations with units many miles from Mineral County. Ross (1961) considered the schistose rocks to be Precambrian(?) or Cambrian

ERA	PERIOD	EPOCH	FORMATION	LITHOLOGY	THICKNESS	
CENOZOIC		Pleistocene		Alluvial gravels and valley fill Older gravels Basalt		
		Pliocene	Gilbert Fm.	Andesite		
		Miocene	Oddie Fm Esmeralda Fm	Rhyolite Tuff, breccia, shale Older lavas - latite and andesite	1000+ feet	
		Oligocene				
		Eocene				
		Paleocene				
		Cretaceous (?)		Granitic intrusive rocks		
	MESOZOIC	Jurassic	Upper			
			Middle			
			Lower	Dunlap Fm Sunrise Fm	Conglomerate, sandstone, and volcanic rocks Limestone, shale, sandstone	5000 feet 1240 feet
Triassic		Upper	Gabbs Fm Luning Fm	Shale, limestone Limestone, dolomite, shale, and conglomerate	420 feet 10000+feet	
		Middle	Excelsior Fm	Volcanics, chert, shale, limestone, conglomerate		
		Lower	Condalaria Fm	Shale, sandstone, conglomerate, limestone	3000 feet	
PALEOZOIC	Permian	Upper	Pablo Fm 1) Diablo Fm 2) Excelsior Fm	Conglomerate, sandstone 1) Dolomite, sandstone 2) Chert, trachyte, andesite	3000 feet 0-3600 feet 3600 feet	
		Lower				
	Pennsylvanian					
	Mississippian					
	Devonian					
	Silurian					
PRECAMBRIAN	Cambrian	Upper	Palmetto Fm	Slate, chert	4000 feet	
		Middle	(precise age unknown)			
		Lower	Miller Mountain Fm	Argilloceous hornfels, calc-hornfels, marble Schist	5600 feet	
	Late					

Table 1. Rock units and formations that occur in Mineral County.

in age until further work in the White Mountains might provide better correlations and better estimates of age.

Paleozoic

Cambrian and Ordovician sedimentary rocks form scattered outcrops in Mineral County. Argillaceous hornfels, calc-hornfels, and marble are the dominant Cambrian rocks whereas slate and chert predominate in Ordovician lithologies.

The Diablo Formation overlies Ordovician rocks with angular unconformity. This formation includes sandstone, conglomerate, and dolomite and contains a distinctive Permian fauna. Major constituents of the Diablo sandstones and conglomerates are quartz and fragments of dark chert which are possibly derived from the underlying Ordovician rocks.

Paleozoic and Mesozoic

The Excelsior Formation crops out in the southern Pilot Mountains. The age of this formation has not been precisely determined. Ross (1961) suggested that rocks belonging to this formation may be of different ages at different locations. He further suggested that the rocks of the formation can be divided into two groups - one correlative with Permian exposures, the other with Triassic exposures. The formation is largely of volcanic

origin but includes lesser amounts of fine-grained clastic rock, conglomerate, and limestone. The volcanic rocks range from rhyolite to andesite in composition and include lava flows, tuffs, and breccias. Epidote is present in most of these volcanic rocks whereas volcanic rocks of Tertiary age do not generally contain this mineral.

Mesozoic

In the Candelaria Mountains, the Candelaria Formation rests with angular unconformity on the Permian Diablo Formation. The Candelaria Formation consists of shale, sandstone, conglomerate, and minor limestone. It contains an ammonite assemblage of Early Triassic age.

The Luning Formation crops out throughout the east half of Mineral County, including the southern Gabbs Valley Range and northern Pilot Mountains. It is of Upper Triassic age. The distribution of exposures of the Luning Formation in the Gabbs Valley Range and surrounding areas is shown in Figure 2. This formation consists largely of limestone and dolomite with lesser shale, argillite, and conglomerate. Muller and Ferguson (1939) divided the formation into three informal units: an upper and a lower unit dominated by limestone and dolomite; and a middle unit

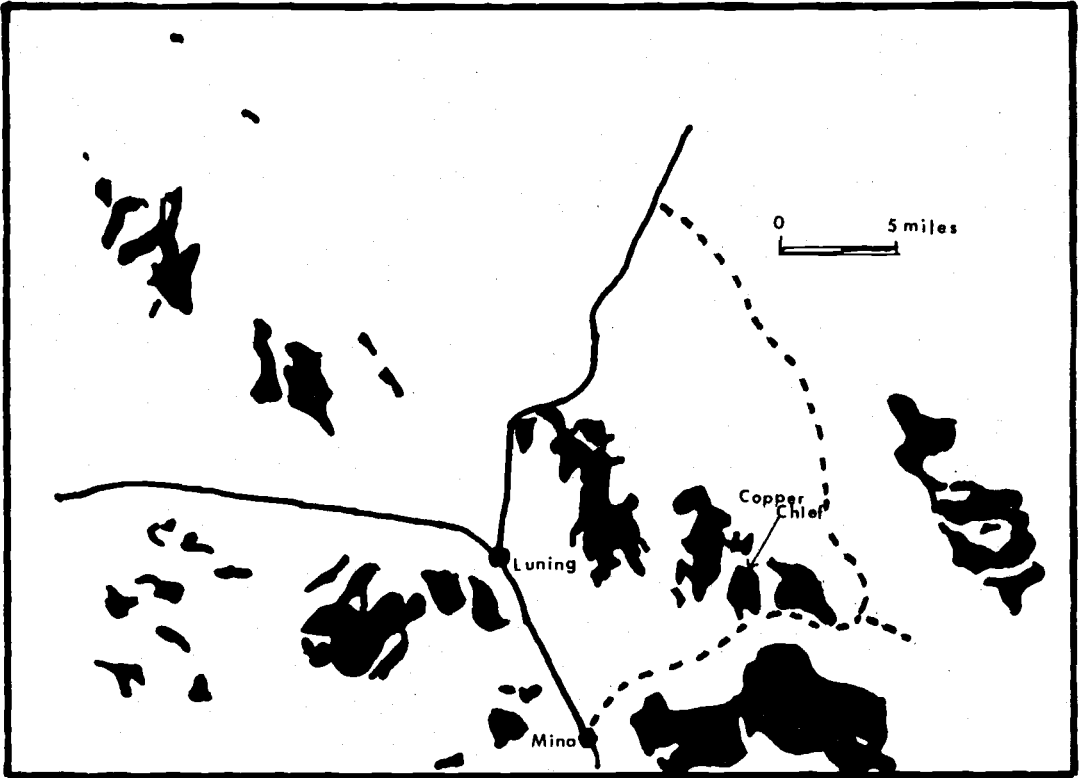


Figure 2. Distribution of the Luning Formation in the Gabbs Valley Range and surrounding areas.

consisting of shale with lesser amounts of limestone and chert pebble conglomerate. They estimated that the thickness of the Luning Formation might approach 10,000 feet. More recent studies by exploration geologists support this figure and indicate that the formation may in fact be thicker than 10,000 feet (Roney C. Long, personal communication, 1978). The Luning Formation lies unconformably on the Excelsior Formation in the Pilot Mountains. Fossil assemblages include a near-shore pelecypod facies, a coral-reef facies, and an offshore ammonite facies. About 40 miles northeast of Copper Chief at the Berlin State Park, Esmeralda County, large plesiosaurs up to 70 feet in length in rocks of the Luning Formation are displayed in quarry by park rangers. The plesiosaurs are among the largest yet discovered in the world.

Stratigraphically overlying the Luning Formation are the Gabbs Formation of Upper Triassic age and the Sunrise Formation of Lower Jurassic age. The two formations have similar lithologies that consist of interbedded dark-colored shale and limestone that vary from a few inches to a few feet in thickness, and with some intercalated beds of impure limestone, sandy shale, and calcareous sandstone. Both formations contain abundant, well-preserved fossils.

The Dunlap Formation of Jurassic age was named

by Ferguson and Muller (1949) for exposures in the northern Pilot Mountains near Dunlap Canyon. This formation is in fault contact with the Luning Formation, and has a maximum thickness of 5000 feet. The Dunlap Formation consists of sandstone, conglomerate, and fanglomerate. Carbonate clasts in the upper part of the formation are perhaps derived from the Luning Formation when the latter was uplifted and eroded. In addition to sedimentary rocks, the upper Dunlap Formation includes volcanic greenstone, greenstone breccia, and tuff.

Cenozoic

Lithologies of Tertiary and Quaternary age include volcanic flows, pyroclastic rocks, and continental clastic rocks. The volcanic rocks range from felsic to mafic in composition. Early Tertiary volcanic rocks are intermediate to felsic and range from rhyolite to andesite. These volcanic rocks are overlain by the Tertiary Esmeralda Formation which consists of sandstone, conglomerate, and rhyolite tuff. The Esmeralda Formation is overlain by Tertiary volcanic rocks of intermediate to felsic composition. Rocks of latest Tertiary and Quaternary age are chiefly mafic volcanics that include flows of latite and trachybasalt (Ross, 1961).

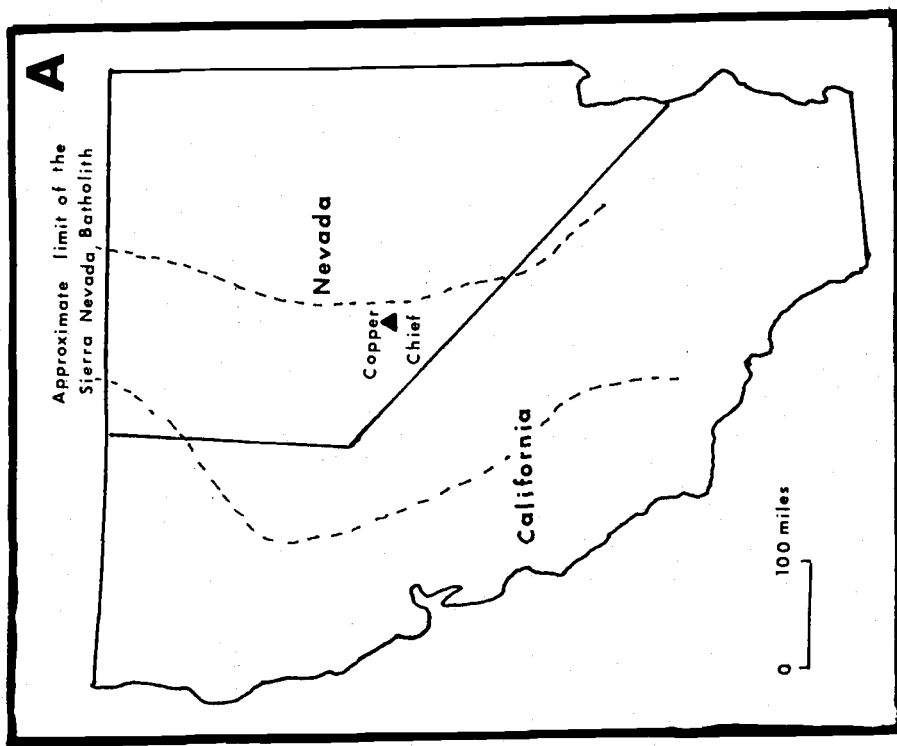
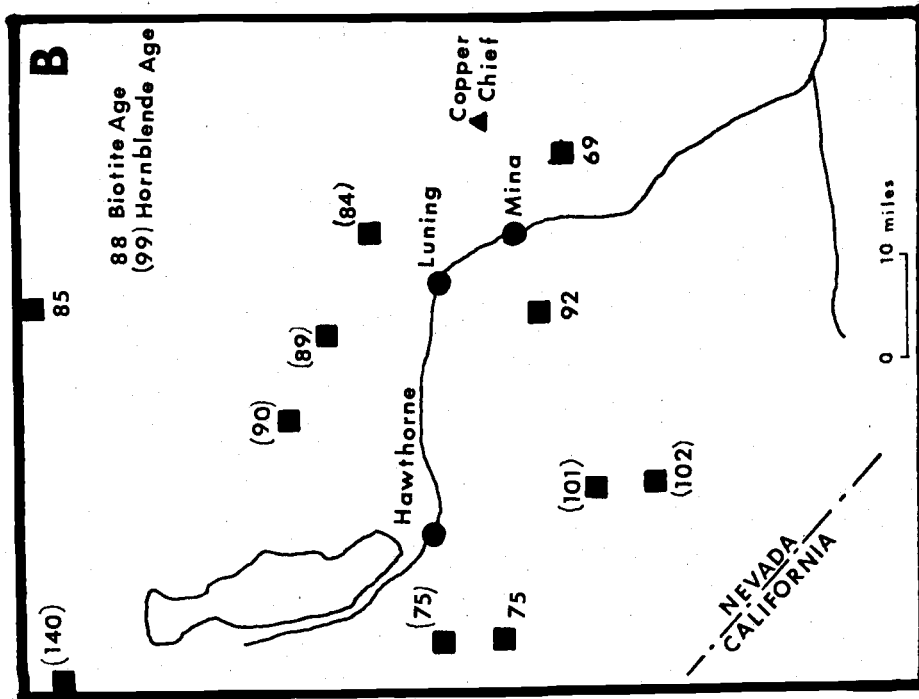
Plutonic Rocks

Intrusive rocks in Mineral County range from peridotite to albite granite. Granitic rocks of intermediate composition are the most widespread of the intrusive types in the county. More than one-half of the Wassuk Range (Figure 1) is underlain by granitic rocks. Plutonic rock exposures become smaller and more scattered in the east part of the county. Compositional similarities to the intrusive rocks of eastern California suggest that the exposures in Mineral County are part of the Sierra Nevada Batholith (Ross, 1961). The intrusive rocks exposed in the Copper Chief Prospect area fall within the approximate limits of the Sierra Nevada Batholith (Fig. 3A) as defined by Crowder and others (1973).

Diorite and hornblende gabbro form small outcrops scattered throughout Mineral County. In the Pilot Mountains, a dike of peridotite is reported to cut both aplite and granodiorite, and is traceable for two and one-half miles (Ferguson and Muller, 1949).

Published potassium-argon age determinations for the hornblende and biotite phases of intrusive rocks in eastern California and western Nevada range from 210 to 68 m.y. (Curtis and others, 1958; Kistler and others, 1965; Schilling, 1965; McKee and Nash, 1967;

- Figure 3. A) Approximate limits of the Sierra Nevada batholith, modified after Crowder and others (1973)
- B) Potassium-argon age determinations of intrusive rocks in Mineral County, Nevada. (See text for sources of data).



Evernden and Kistler, 1970; Crowder and others, 1973; and Kistler and Peterman, 1973). The largest number of ages cluster in the period of 105 to 75 m.y. (Fig. 4). Granitic intrusive rocks in Mineral County range in age from 140 to 69 m.y. (Fig. 3B) and most occur in the range from 105 to 75 m.y.

Structure

Mineral County is near the west border of the Basin and Range physiographic province. As is typical of the province, the topography consists of uplifted horst or tilt-block mountains and down-dropped graben valleys. Throughout most of the Basin and Range province, linear mountain ranges trend either north or north-northeast. However the ranges trend northwest or have sinuous trends (oroflexes, Albers, 1967) in western Nevada and eastern California. One such group of sinuous trending ranges includes the Gillis Range, Gabbs Valley Range, Pilot Mountains, and the Monte Cristo Range (Fig. 1). The Excelsior Range departs more markedly from the normal Basin and Range trend by having an east-west direction of elongation. The junction between normal Basin and Range trends and the anomalous trending ranges was termed the Walker Lane after an explorer who followed a route influenced by the topography of this linear depression (Locke and

Figure 4. Potassium-argon age determinations for plutonic rocks of the Sierra Nevada Range, White Mountains, and Inyo Range, eastern California; and for plutonic bodies in Mineral County. The data are from:

- A) Schilling (1965)
- B) Curtis, Evernden, and Lipson (1958)
- C) Crowder, McKee, Ross, and Krauskopf (1973)
- D) McKee and Nash (1967)
- E) Kistler and Peterman (1973)
- F) Kistler, Bateman, and Brannock (1965), and Evernden and Kistler (1970).

5
0 } Number of age determinations

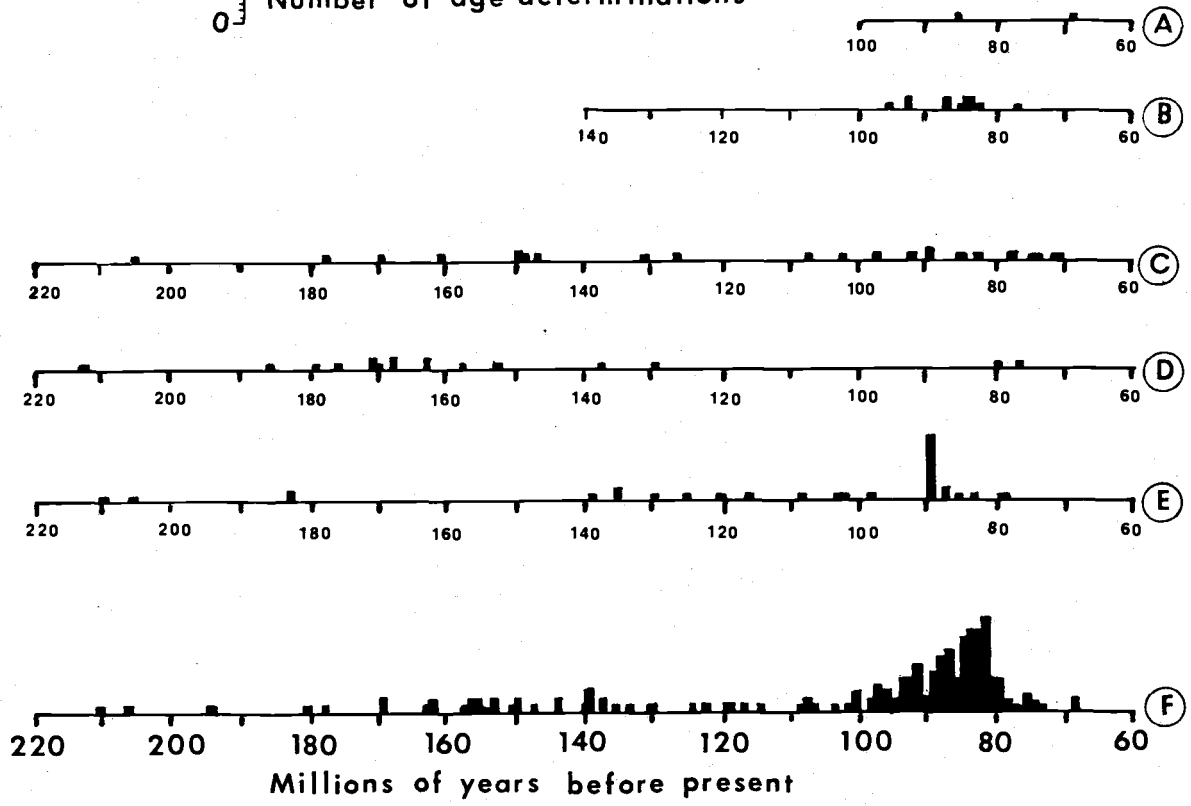


Figure 4.

others, 1940).

Basin and Range structure was defined by Gilbert (1874, 1875) who suggested that it was caused by block faulting accompanied by little or no folding. Other geologists have explained the development of Basin and Range structure in terms of:

- 1) crustal collapse following and, in part, accompanying Tertiary volcanism (LeConte, 1889; Mackin, 1960);
- 2) westward extension and crustal thinning (Thompson, 1959, 1966; Hamilton and Meyers, 1966; Stewart, 1971; and Thompson and Burke, 1973, 1974);
- 3) transfer of subcrustal material toward the Colorado Plateau (Gilluly, 1970); and
- 4) strike-slip faulting accompanied by western extension (Donath, 1959; Shaw, 1965).

The Walker Lane is considered by some geologists to be a profound structure of continental scale (Locke and others, 1940; Neilsen, 1965). Strike-slip faulting along the Walker Lane is estimated to have caused displacements from a few miles (Ferguson and Muller, 1949) to approximately 29 miles (Slemmons and others, 1979). Greensfelder (1965) suggested that continental crust east of the Walker Lane is thinner than continental crust west of the Walker Lane, and that the lane may be the border between two different tectonic provinces. Right-lateral displacement along the Walker

Lane was first suggested by Gianella and Callaghan (1934) following the 1932 earthquake in the Cedar Mountains area. These authors compared the Walker Lane to the San Andreas Fault with regard to scale and trend. Movement along the Walker Lane may have been active:

- 1) for the last 22 million years (Slemmons and others, 1979);
- 2) "probably earlier than Tertiary, and it is still active ..." (Shawe, 1965); or
- 3) Middle or Late Triassic to Recent (Albers, 1967).

Gumber and Scholz (1971) argue that the Walker Lane is not a currently active structure and that the Cedar Mountain earthquake of 1932 was related to a seismic zone which extends from the Owens Valley in eastern California to the Fairview Peak-Dixie Valley area in western Nevada.

There are five en echelon fault strands in the Walker Lake area (Slemmons and others, 1979). One of these, the Battles Well Strand, crosses the northeast border of the Copper Chief Prospect.

South of the study area, right-lateral displacement has been suggested for the Death Valley-Furnace Creek Fault Zone (Stewart and others, 1968; and Wright and Troxel, 1970), for the Las Vegas Valley

Fault Zone (Longwell, 1950), and for the Texas Lineament which Jerome and Cook (1967) have suggested may be a southeasterly extension of the Walker Lane. Illustrated in Figure 5 are major right and left-lateral strike-displacement faults of California and Nevada, normal faults of the eastern Sierra Nevada fault system, and some western Basin and Range faults (modified after Wright and Troxel, 1967).

Ekren and others (1976) proposed four east-west trending lineaments in central Nevada. One of these, the Pancake Lineament, extends through the broad pass between the Gabbs Valley Range and Pilot Mountains, near the site of the Copper Chief Prospect.

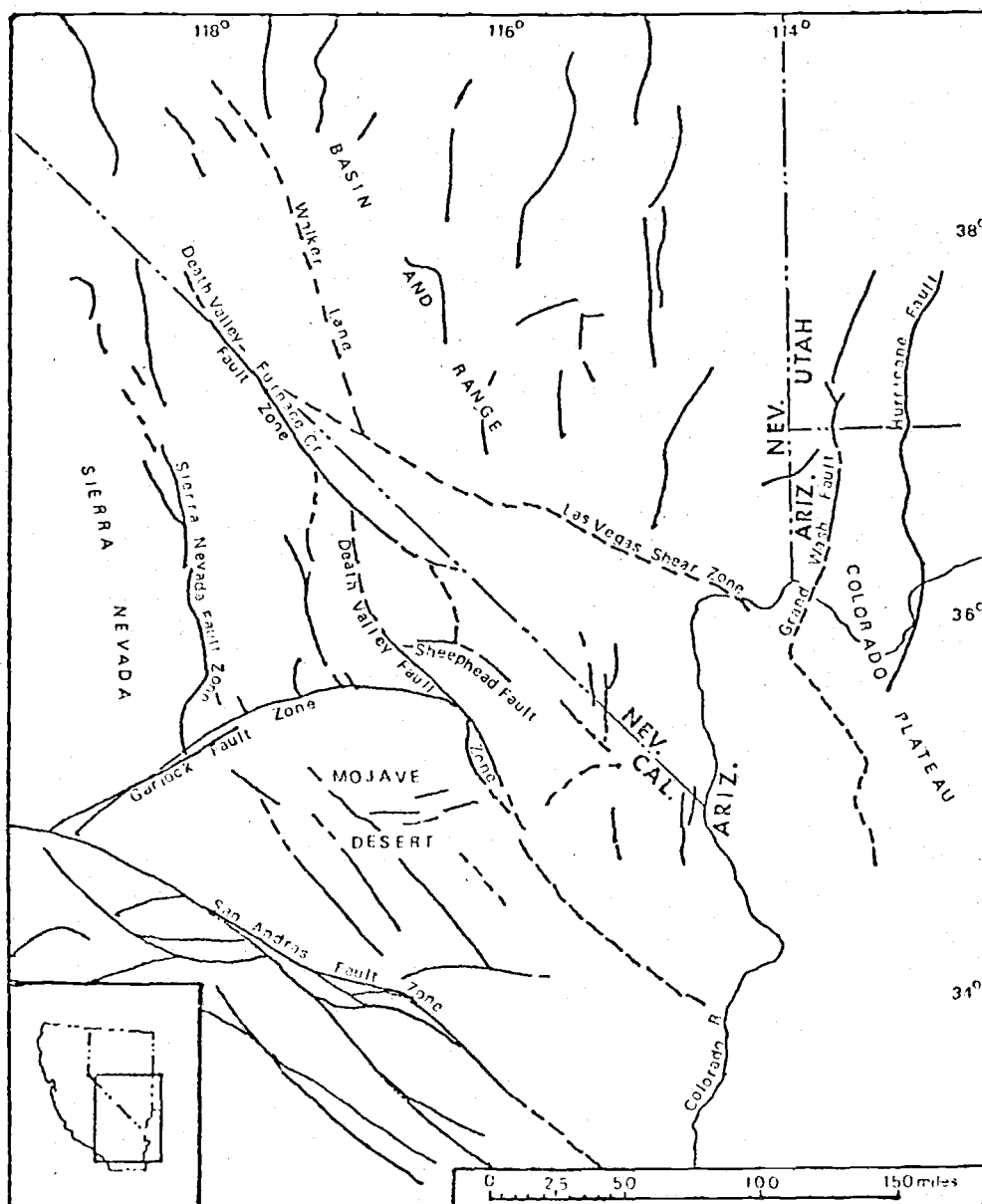


Figure 5. Major right and left-lateral strike-slip faults of eastern California and western Nevada, normal faults of the Sierra Nevada fault system, and Basin and Range faults. (Redrawn after Wright and Troxel, 1967).

SKARNS

The term "skarn" indicates a genetic type of ore deposit, and is the name for the secondary silicate rocks that are associated with the ore. The term, originally used by Swedish miners, was first applied by Suschinskiy (1912) as the general name for ore deposits that had previously been referred to as contact, contact metamorphic, contact metasomatic, pyrometamorphic, or pyrometasomatic. Another term which is synonymous with skarn is "tactite". It was introduced by F.L. Hess (1919) to describe rock formations produced by the metasomatic replacement of carbonate, or other soluble, rocks in the contact zones of invading magmas.

Zharikov (1968) defines skarns as:

"... limy-magnesian-ferruginous metasomatic silicates and aluminosilicates formed in high-temperature zones or contact halos of intrusions by interactions, implemented by magmatogenic solutions, between carbonate rocks and magma or intrusives or other aluminosilicate rocks."

He stresses the point that not all "limy-magnesian-ferruginous silicates" are skarns. The term only includes those mineral deposits that contain ore minerals and that were produced by contact-reactional metasomatism.

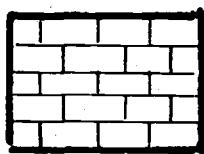
Skarns are formed in the thermal aureoles of

intrusions emplaced at different depths within the earth's crust. Magnesial skarns are formed at all depths but are best developed and most extensive in the aureoles of intrusions emplaced in the catazone. Limy skarns are restricted to the epizone and mesozone because their characteristic calc-silicate minerals are not stable at high pressures. The mineral deposit at the Copper Chief Prospect is of the limy type and, therefore, the following summary of the principles of skarn formation will only include topics generally relevant to limy skarns and will omit those generally applicable only to magnesial skarns.

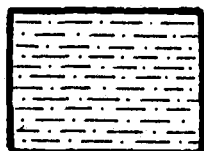
Korshinskii (1965, 1968) distinguishes two limiting methods of metasomatic transfer of components in solution. These are contact-infiltration and diffusion. In the case of pure infiltration, components are transported by the flow of the solution; whereas, in the case of pure diffusion, components in stagnant solutions move in response to concentration gradients. A subtype of the diffusional case, bimetatomatism, involves the simultaneous diffusion in opposite directions of components having contrasting characteristics. Bimetatomatic diffusion could occur, for example, at the contact between a plutonic body and its host carbonates by diffusion of silica and

alumina from the aluminosilicates of the intrusion into the carbonates, and of lime from the sedimentary host rocks into the intrusion. Skarns formed by diffusional processes are characterized by gradational changes in the composition of solid-solution minerals, and in the mineralogy of the assemblages and the number of mineral phases present. Infiltrational skarns are characterized by abrupt changes in the chemical compositions of minerals, and by the formation of essentially monomineralic lithologies. The majority of ore deposits in limy skarns are bimetasomatic or contact-infiltrational. Bimetasomatic skarns are classified on the basis of the composition of the rocks replaced by skarn as: 1) exoskarn - after carbonates, 2) skarnoid - after carbonates but with admixtures of the original aluminosilicate substances (metamorphic skarns; Kerrick, 1977), 3) endoskarn - after the aluminosilicates, and 4) periskarns - endoskarns of essentially feldspathic composition. The contact-infiltrational skarns also have recognizable exoskarns and endoskarns. Additional types of infiltrational skarn are: 1) frontal skarn that is generally formed at the contact between the roofs of large plutonic bodies and overlying carbonate rocks, and 2) vein skarns that range from pipe-shaped bodies to true veins. The types of skarns are shown in Figure 6

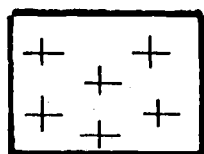
Figure 6. Skarn classification (modified after Zharikov, 1968).



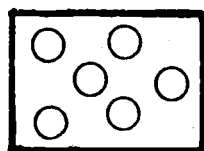
Limestone



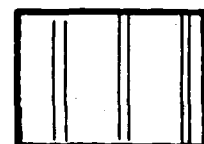
Siltstone



Intrusive rock



Exoskarn



Endoskarn or periskarn



Vein skarn

- A. Contact infiltrational - vein type
- B. Bimetasomatic
- C. Contact infiltrational - frontal type

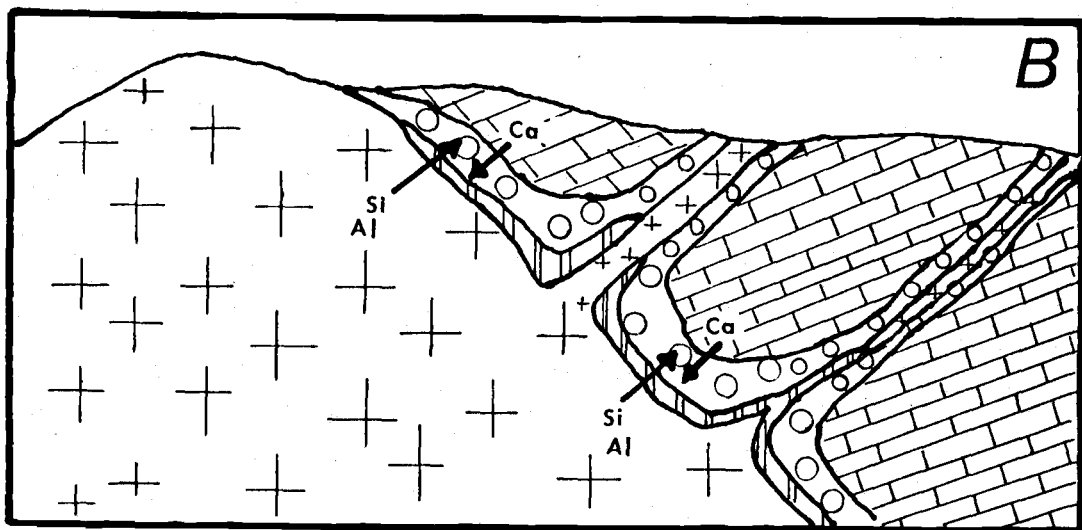
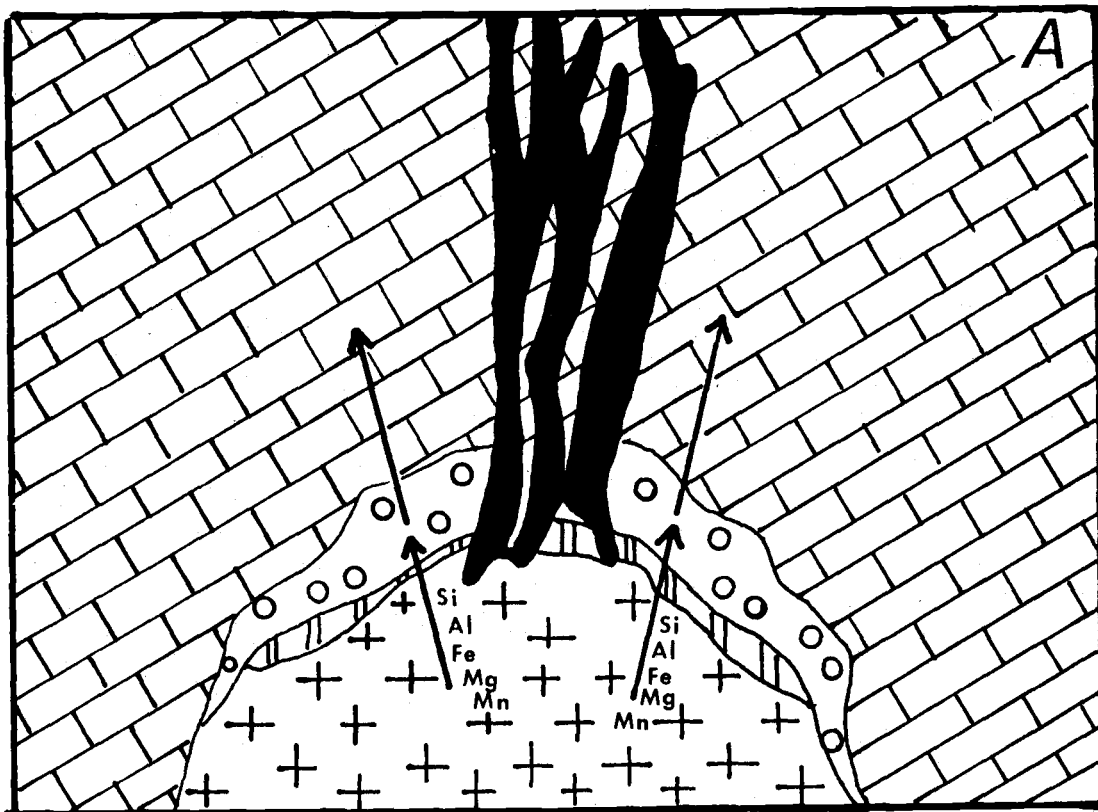


Figure 6.

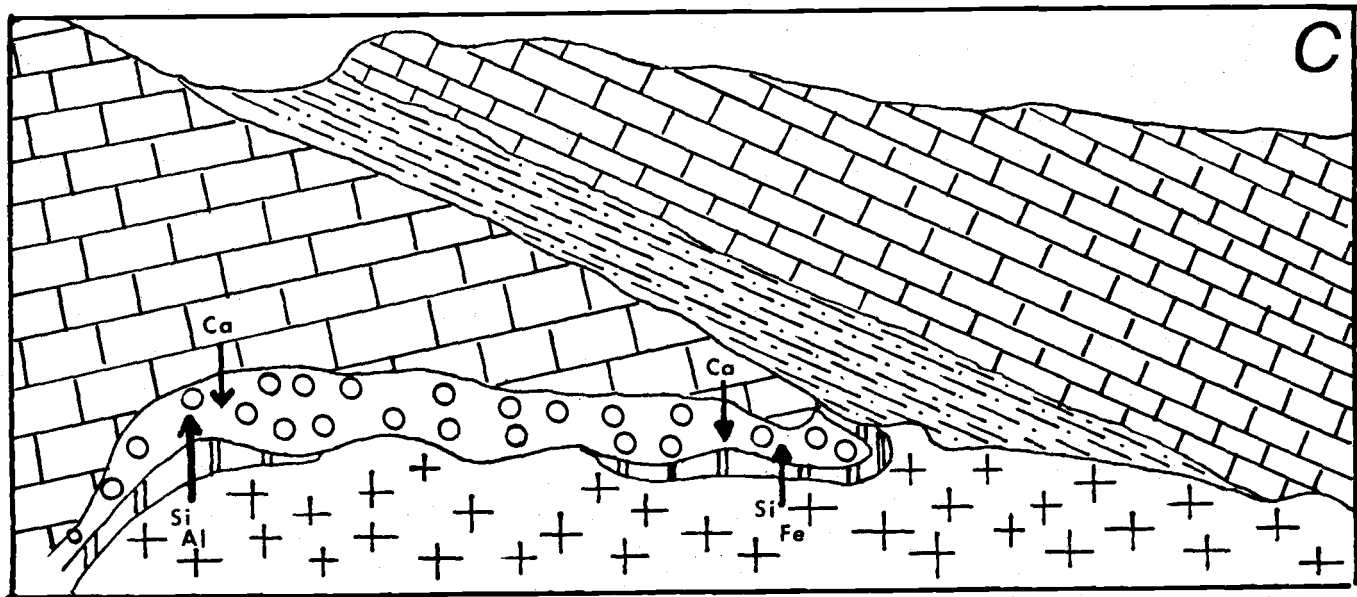


Figure 6 continued.

(modified from Zharikov, 1968).

The minerals which are characteristic of limy skarns include: garnet (of the grossuralite-andradite series), clinopyroxenes (of the diopside-hedenbergite-johannsenite series), epidote, wollastonite, rhodonite, vesuvianite, scapolite, and plagioclase and potassium feldspar.

The physiochemical factors which govern the formation of skarns, and which determine their mineral assemblages include temperature, pressure, oxygen and carbon dioxide fugacities, pH, carbonate equilibria, and the chemical activities of silicon, aluminum, iron, potassium, and sodium. These factors of the solution media causing skarn-type alteration evolve with time and with position in the host rock-skarn-intrusion system. The different diffusion rates of the mobile constituents, and the contrasting pH of the early and late stage fluids are among the effects of fluid evolution that principally control the mineral paragenesis of the limy skarns.

The diffusivity of aluminum is lower than that of calcium or silicon (Zharikov, 1968); therefore, the early reactions of bimetasomatism are dominated by lime and silica exchange. Because aluminum does not diffuse into the exoskarns in the early stages of skarn formation, garnet skarns are not generally formed at

this time. Later, however the activity of aluminum increases as the desilicification of the endoskarn becomes intense, particularly in the periskarns, and the progressive growth of garnet zones begins.

The iron concentration of the altering solutions increases with time and reaches a maximum in the terminal stages of skarn formation. The mineralogical expression of increasing concentrations of iron is the presence of andradite garnet, which characteristically has replaced pyroxene or garnet skarns (Zharikov, 1968).

Ores of the skarn deposits include iron, cobalt, molybdenite, scheelite, metallic sulfides, phlogopite, and minerals that contain the rare metals beryllium and tin. Depending on the mode of deposition, several specific ore assemblages are distinguished. Ores deposited during the early stages of skarn formation (early alkaline stage) are termed simultaneous; those deposited later (late alkaline stage) are termed companion; and those of the terminal or post-skarn (acid-leaching) stages are termed imposed ores. Examples of the occurrence of simultaneous ores are rare and are only of mineralogical interest (Zharikov, 1968). The genetic types of ore deposits and the types of metasomatic alteration associated with the ores of skarns are listed in Table 2.

COMPANION ORES

- 1) Magnetite
- 2) Cobaltite-magneite
- 3) Safflorite-glaucodote-arsenopyrite
- 4) Magnetite-chalcopyrite

IMPOSED ORES

- 1) In connection with quartz-feldspathic metasomatism:
 - A) Scheelite-molybdenic
 - B) Scheelite-sulfidic (often with SnO_2)
- 2) In connection with greisenization:
 - A) Scheelite-sulfidic
 - B) Rare metals
- 3) In connection with propylitization:
 - A) Polymetallic
 - B) Cupric
 - C) Polysulfidic
- 4) In connection with quartz-feldspathic metasomatism and berezitation:
 - A) Scheelite-sulfidic (occasionally with Au)
 - B) Chalcopyritic (often with Au)
 - C) Borosilicate

Table 2. Genetic types of limy skarn ore deposits (after Zharikov, 1968).

SEDIMENTARY ROCKS

Measured stratigraphic sections of unaltered sedimentary rocks in the northeast part of the Copper Chief Prospect are shown in cross-section and map drawings in Figure 7. They illustrate the relative abundance and thickness of the dominant rock types at the prospect (siltstone and limestone). Siltstone is more abundant than limestone and forms thicker beds. Quartzite, not shown in Figure 7, occurs at two locations: one in the northeast part of the prospect, and the other in the central part. Although the quartzites are a minor lithotype with regard to overall extent of outcrop, they may be the best marker horizons in the area for stratigraphic correlations.

At least two distinctive types of siltstones occur in the northeast part of the Copper Chief Prospect. The most abundant type is characteristically fissile and occurs as flaggy fragments; the rocks are calcareous and sparsely to moderately fossiliferous. These siltstones are pale red (10R 6/2) or grayish orange pink (10R 8/2) on fresh and weathered surfaces (Figure 8). The second type is non-fissile and breaks into angular blocks (Fig. 9). This type is dark gray or brown on fresh surfaces and weathers to yellowish or orangish brown (10 YR 6/6).

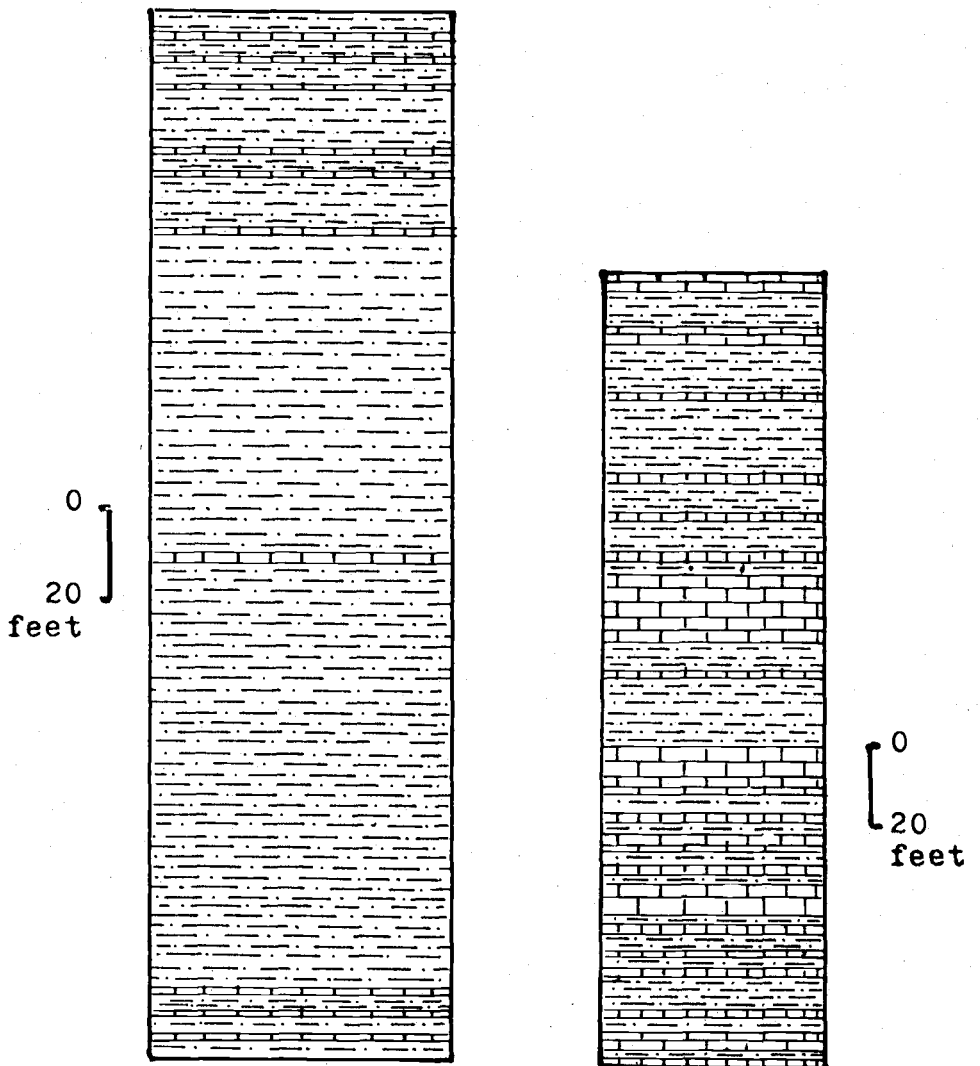
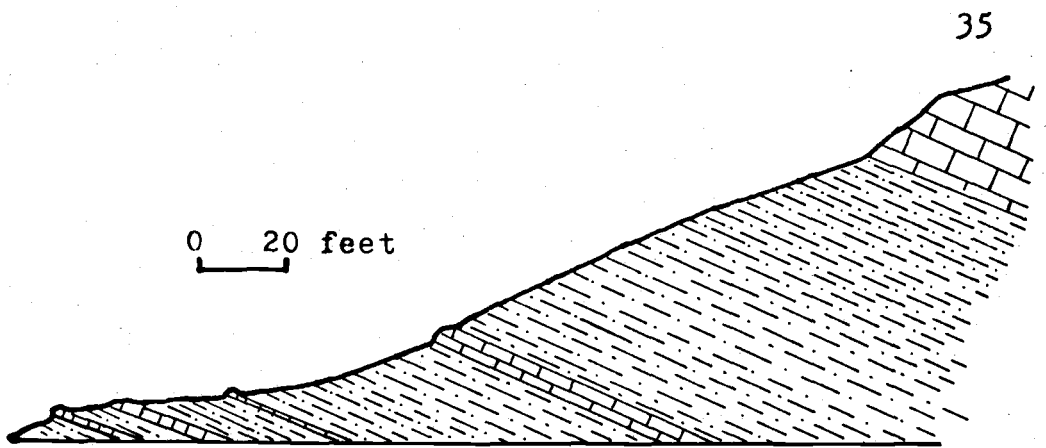


Figure 7. Measured stratigraphic sections of the Luning Formation in the northeast part of the Copper Chief Prospect.



Figure 8. Pink fissile siltstone of the Luning Formation. Also note limestone interbedded beneath the hammer.



Figure 9. Yellowish brown siltstone of the Luning Formation.

The siltstone beds vary from a few feet to several tens of feet in thickness and form recessive slopes which typically contain one or more thin rib-like interbeds of more resistant limestone.

The limestones of the Copper Chief Prospect are medium dark gray (4N4), brown to dark brown, grayish orange pink (5 YR 7/2), and pale yellowish brown (10 YR 6/2) in exposures of the northeast part of the prospect; and they are black, brown, blue, and mottled medium dusky red gray in the central and northwest parts. Thin wispy lenses of dark brown cherty material are present in many limestone beds (Fig. 10). The beds of limestone are massive and resistant to mechanical weathering. Examination of thin sections, acetate peels, and hand specimens has indicated that the limestones of the Copper Chief Prospect vary from lime packstones to lime wackestones. Bioclastic material is locally abundant and consists of complete and broken shell material. The limestone beds vary from several inches to more than twenty feet thick in the northeast section of the prospect. The thickest carbonate exposure, approximately four hundred feet thick, crops out in the northwest section of the prospect. However, most of the limestone beds range from a few inches to a few feet in thickness.

Fossils collected from the limestones and



Figure 10. Sandy lime packstone with wispy interbeds of cherty material.

siltstones include brachiopods, pelecypods, one ammonite, star-shaped crinoid columnals, spongiomorphs, corals, and sponges (Table 3). The fossil assemblage is similar to collections from the lower Luning Formation (Lower Norian in age; N.J. Silberling, written communication, 1980).

The occurrence of abundant fossil material is restricted to the exposures of the northeast part of the Copper Chief Prospect but one pelecypod and several fossil imprints were found in black limestone in the northwest part of the prospect (CCLS-85).

Quartzite and conglomerate form massive outcrops and angular colluvium. Quartzite is much more abundant than the conglomerate and the conglomerate occurs within the quartzite as irregular shaped interbeds. Clasts in the conglomerates consist of quartz and chert pebbles. The matrix of the conglomerates is fine-grained siliceous material, mainly quartz. Intermediate in texture between the fine-grained quartzites and the conglomerates are pebbly quartzites. The quartzites are light to dark gray and weather to reddish brown. Thin films and coarse blebs of manganese oxide(?) stain the surfaces of many quartzites. The conglomerates are white to pale tan (Fig. 11). The pebbly quartzites consist of dark grayish black and light gray subrounded pebbles in medium gray to black fine-grained

BRACHIPODA

Articulata

Terebratulida

Terebratulidae

plecochoncha

COELENTERATA

Hydroza

Spongiomorphida

Spongiomorphidae

spongiomorphia or hepastylus

MOLLUSKA

Pelecypodia

Trigonioidia

minetrigonia

Mytilacea

Pinnidae

trichites

PORIFERA

Calcispongea

Thalamida

uncertain

polytholosia

uncertain

ascosymplegma

Table 3. Fossil collection from the northeast section of the Copper Chief Prospect.



Figure 11. Chert pebble conglomerate of the Luning Formation.

matrix. As previously noted for the conglomerates, the pebbly quartzites also occur as irregular interbeds in quartzite.

The sedimentary and metasedimentary rocks of the Copper Chief Prospect were mapped as Luning Formation by Ferguson and Muller (1949). The fact that the siltstones are more abundant than the limestones suggests that the exposures are correlative with the middle Luning Formation as defined by Muller and Ferguson (1939). However the faunal assemblages are correlative with the lower Luning Formation which suggests lateral facies changes within the formation.

The sedimentary environment in which the siltstones, limestones, and quartzites of the Copper Chief were deposited was near shore, as indicated by the abundant pelecypod facies (Muller and Ferguson, 1936). Oldow (1978) has proposed shallow-marine to upper delta-plain environments of deposition for siliciclastic rocks of the middle Luning Formation in the northern Pilot Mountains.

INTRUSIVE ROCKS

More than 60 intrusive bodies were recognized during the field mapping. These include relatively large elongate stock-like masses and small linear sill and dike-like bodies (Plate 1, Fig. 12). The largest stock has a circumference of more than 11,000 feet and accounts for more than one-fifth of the mapped area. The intrusive bodies at the Copper Chief Prospect probably coalesce at depth to form a single pluton. Medium to coarse-grained plagioclase feldspar, amphibole, and biotite can be identified in specimens from fresh exposures. Honey-brown sphene is a common mineral that can be recognized in most samples of intrusive rock with the aid of a hand lens. The Copper Chief intrusive rocks are nearly structureless and lack linear features or xenoliths. However, joints are well developed in a few exposures. The intrusions have sharp contacts with their sedimentary host rocks. Sparse inch-scale veins parallel the contacts and extend limited distances into the hosts (Fig. 13).

Most exposures of fresh intrusive rock at the Copper Chief Prospect are light to medium gray in color. With increasing amounts of the ferromagnesian minerals their colors change from light to dark. Parts of the largest mapped intrusion (Plate 1) are reddish gray;



Figure 12. Distribution of intrusive bodies (black) at the Copper Chief Prospect.



Figure 13. Inch-scale veins of quartz monzodiorite (dark) in calc-silicate host rock.

and, where jointed dark red stains are present along joint surfaces (Fig. 14).

Intrusive rocks at scattered locations at the Copper Chief Prospect have been altered to endoskarn, periskarn, quartz-sericite, and carbonate mineral bearing assemblages (Table 4, Fig. 15). Both endoskarn and periskarn contain calc-silicate minerals. Periskarns have extremely high contents of potassium feldspar; whereas, endoskarns have approximately the same amounts of potassium feldspar as the unaltered intrusive rocks.

Quartz and sericite have pervasively replaced the groundmass and phenocrysts minerals at one sampled location (CCP-33). At another location (CCP-57) calcite has selectively replaced some groundmass mineral, presumably potassium feldspar; whereas phenocrysts of plagioclase feldspar and groundmass crystals of quartz have been little affected.

Outcrops of endoskarn and periskarn are white to light yellow brown and contain rare crystals of red brown garnet. The one exposure of quartz-sericite altered rock is toffee brown, quartz-veined, and stained with copper "carbonate". Samples of intrusive rock in which potassium feldspar has been selectively replaced by calcite were collected from exposures of pinkish gray quartz monzodiorite (Plate 1).



Figure 14. Red stained joints in pinkish gray intrusive rock.

ALTERATION STATE

<u>Unaltered</u>	<u>Endoskarn</u>	<u>Periskarn</u>	<u>Quartz-Sericite Alteration</u>
Pl-kfs-qz- bio-hbld-mt	Pl-kfs-qz- cpx-wo	Kfs-pl-wo-cpx- gar	Ser-qz-lim
CCP-21	CCP-30	9/20/78	CCP-33
CCP-38	TS-5	CCP-4	
CCP-40		CCP-39	
CCP-41		CCP-49	
CCP-54		CCP-51	
CCP-58		CCSR-4	
<u>Calcite Alteration</u>		<u>Veined (vein type)</u>	
<u>Pl-cal-qz</u>		CCP-6 (clay)	
CCP-57		CCP-11 (quartz)	
		CCP-18 (garnet)	
		CCP-22 (garnet)	

Table 4. Alteration state of the intrusive rock samples for which chemical and petrographic data were obtained.

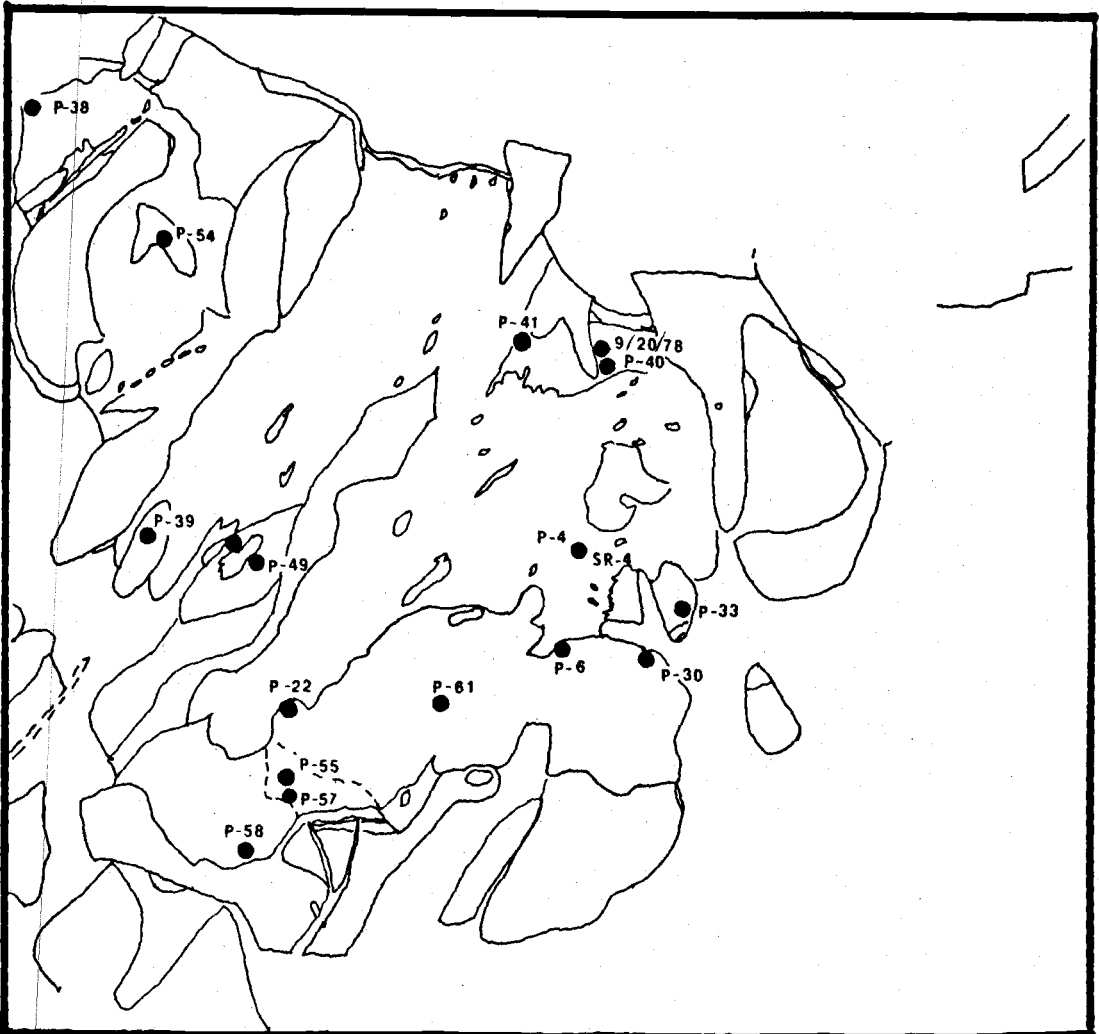


Figure 15. Locations of plutonic rock samples collected for petrographic and chemical analyses.

Exposures of unaltered and slightly altered intrusive rock are crosscut by several mineralogically distinct types of veins and veinlets that contain garnet, quartz, quartz-limonite, and clay.

Petrography

Intrusive rocks from thirteen locations were analyzed to determine their modal mineral abundances by the method of Chayes (1956) with approximately 1000 points counted per thin section. Potassium feldspar was stained with sodium cobaltinitrate (Bailey and Stevens, 1960) to differentiate it from quartz and fine-grained plagioclase feldspar. In addition, ten other thin sections of intrusive rock were examined for texture, mineralogy, and other characteristics such as veins. The modal abundances of the essential, varietal, accessory, and alteration minerals are listed in Table 5 and are plotted with respect to plagioclase feldspar content in Figure 16.

Unaltered Intrusive Rocks

The unaltered intrusive rocks contain more than 85 percent (by volume) of quartz and feldspar. The ferromagnesian minerals, amphibole and biotite, constitute about 10 percent of the unaltered rocks. The remaining 5 percent includes the accessory

	<u>9/20/78</u>	<u>CCP-6</u>	<u>CCP-30</u>	<u>CCP-33</u>	<u>CCP-38</u>	<u>CCP-39</u>	<u>CCP-41</u>	<u>CCP-51</u>	<u>CCP-54</u>	<u>CCP-55</u>	<u>CCP-58</u>	<u>CCP-61</u>	<u>IS-5</u>
Plagioclase	57.5	53.5	65.5		56.9	31.3	61.2	15.0	51.0	53.7	54.5	59.4	49.3
Potassium feldspar	29.7	22.0	7.1		16.3	52.3	19.9	58.9	23.3	20.8	21.0	18.7	24.4
Quartz	6.5	8.9	15.4	25.4	12.0	0.4	7.7	0.4	14.0	11.2	10.6	10.8	7.7
Hornblende		7.6			9.3		7.2		4.3	8.0	7.9	8.3	
Biotite		1.5			2.2		1.8		4.2	2.0	2.0		
Chlorite	tr.				tr.				0.2	0.4	0.4		
Sphene	0.9	0.2	0.3	0.1	0.7	0.3	0.7	0.2	1.0	0.6	0.8	1.0	0.1
Apatite	0.4	0.2	0.2	0.9	0.2		0.4	0.5	0.2	0.2	0.3	0.4	0.4
Opaque mineral(s)	1.4	1.2	0.1	8.0	2.4	0.9	1.2	0.2	0.8	2.8	1.5	1.0	3.8
Clinopyroxene	1.4		10.3		10.0			14.6					1.3
Epidote			0.4		0.6			0.9					3.1
Wollastonite	tr.		0.2		2.6								6.5
White Mica	2.0		0.2	65.7				1.1					1.9
Calcite			0.3		0.3			8.4					1.0
Clay mineral(s)		4.3											
Total	99.8	99.4	100	100.1	100	96.7	100.1	100.2	99.8	99.7	99.0	99.6	100.1
Points counted	1004	1070	1030	1034	1046	1028	1020	1134	1005	2021		1038	1034

Table 5. Modal analyses of samples of intrusive rock from the
Copper Chief Prospect.

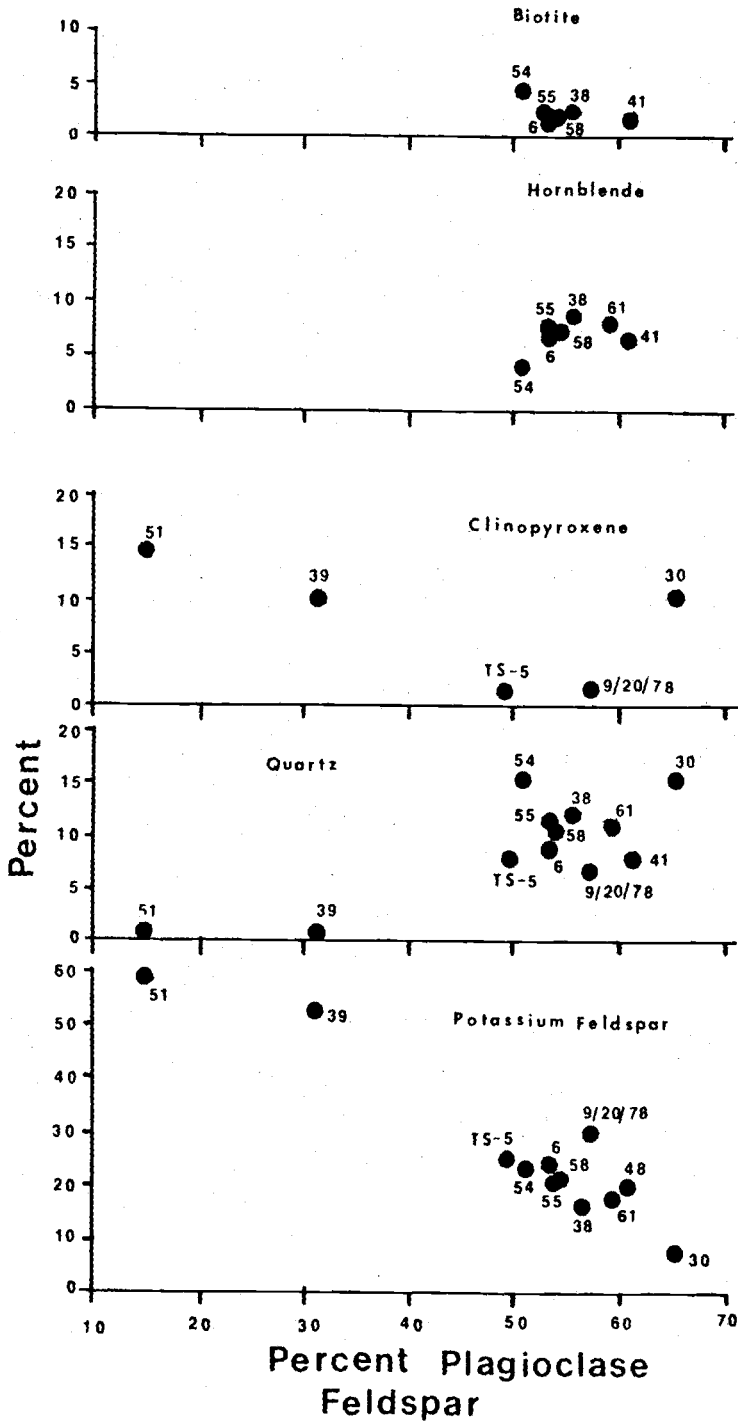


Figure 16. Modal percentages of minerals versus that of plagioclase feldspar in intrusive rocks of the Copper Chief Prospect.

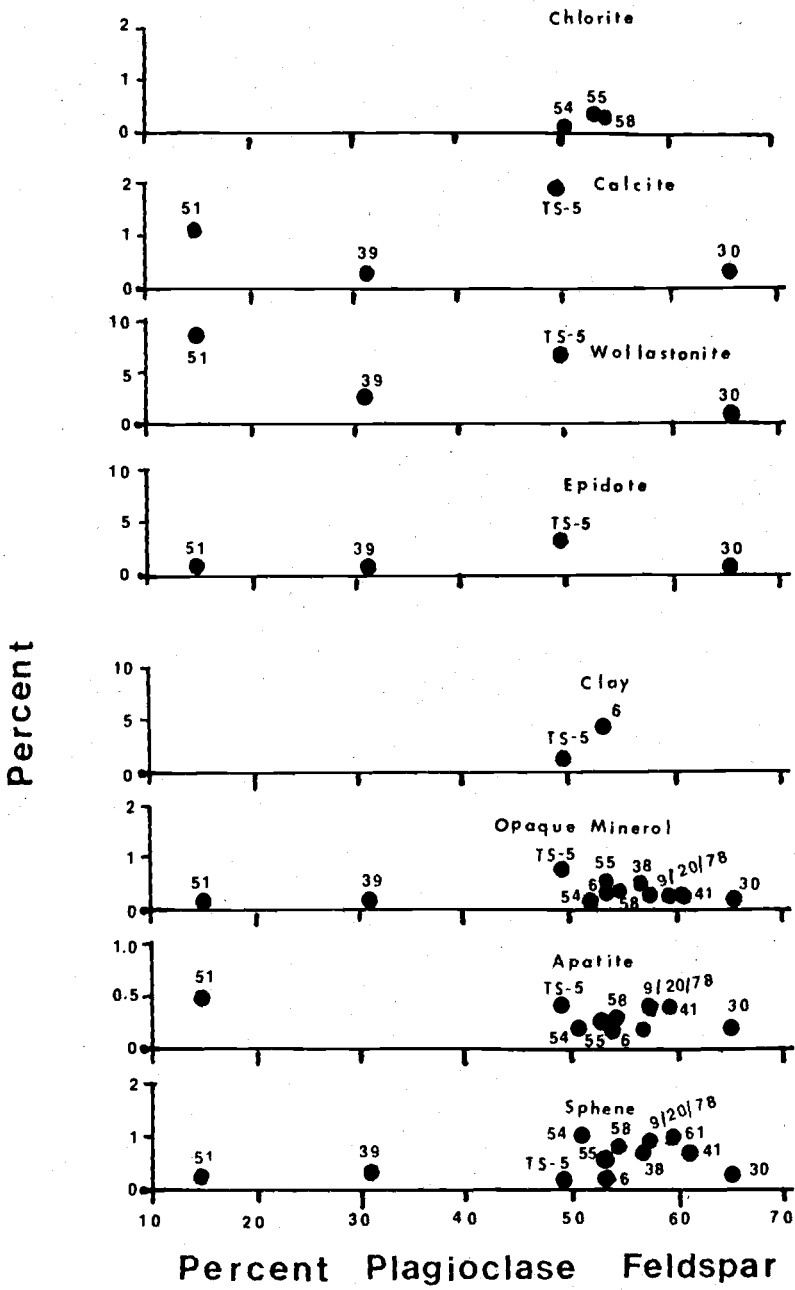


Figure 16 continued.

minerals (apatite, sphene, opaque oxides, and zircon) and clay and white mica. The clay and white mica are alteration minerals of plagioclase feldspar.

The texture of the unaltered intrusions is holocrystalline-hyaline (porphyritic) to seriate. Plagioclase feldspar, biotite, hornblende, and sphene are the phenocryst phases. The groundmass of porphyritic varieties and the finer grained minerals of seriate varieties include quartz, potassium feldspar, fine-grained equivalents of the phenocrysts, and the accessory minerals.

Quartz and potassium feldspar are almost exclusively confined to the groundmass of the samples of intrusive rock but a few phenocrysts also occur in the thin sections. Phenocrysts of potassium feldspar in sample CCP-58 have embroidered borders (Fig. 17). The groundmass textures of the rocks are largely controlled by the geometric relations between quartz and potassium feldspar. These two minerals occur in aplitic (Fig. 17), seriate, amoeboidal, and micropegmatitic (Fig. 18) intergrowths. Potassium feldspar is more abundant than quartz. Subhedral quartz is present as isolated crystals in a matrix of stubby potassium feldspar anhedral and subhedral.

Plagioclase feldspars are the most abundant and form the largest (up to 5 mm) crystals in the fresh

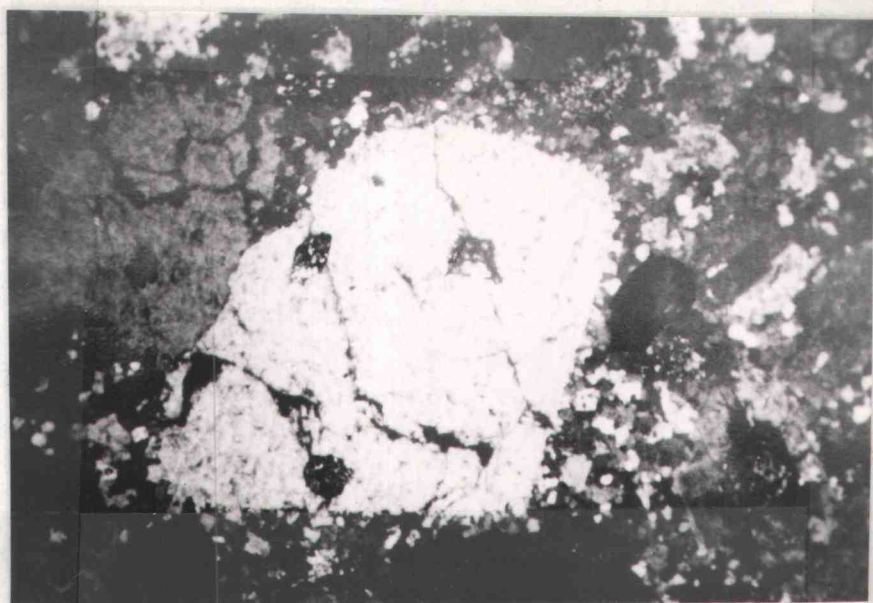


Figure 17. Crystals of potassium feldspar with embroidered borders in aplitic groundmass. The field of view is approximately three millimeters.



Figure 18. Micropegmatitic groundmass. Also note the selective replacement of one oscillatory zone in phenocrysts of plagioclase feldspar near the top center of the photograph. The field of view is approximately three millimeters.

intrusive rocks. The phenocrysts are subhedral to euhedral. Many phenocrysts have four or more oscillatory zones with preferential alteration of a single zone to clay (Fig. 18). Crystals of plagioclase feldspar are twinned according to the albite, carlsbad, and, rarely, pericline laws. Synnuesis twins (Vance, 1969) are relatively common and penetration and glide twins are also present in samples of unaltered intrusive rock (Fig. 19). The plagioclase feldspar of the groundmass is subhedral and has the same variety of twins as do the phenocrysts. The composition of the plagioclase feldspars, as determined by the Michael-Levy and combined carlsbad-albite methods (Kerr, 1959), is andesine and is in the range of An_{35} to An_{41} .

The crystals of hornblende are euhedral to subhedral. The hornblendes are strongly pleochroic from dark brown to olive drab green. Many crystals of hornblende contain abundant inclusions of the opaque minerals. Some crystals of hornblende have been replaced by sparse to moderate amounts of ragged anhedral chlorite.

Hexagonal platelets and cross-sectioned crystals of biotite are pleochroic from dark chocolate brown to straw yellow. Most of the biotite is interleaved with ragged patches of chlorite, and many crystals enclose opaque minerals.

Figure 19. Characteristics of twins and zones in crystals of plagioclase feldspar from samples of intrusive rocks:

- A) Selective alteration of one oscillatory zone in a pair of synnuesis twins
- B) Pericline twins
- C) Synnuesis twins and oscillatory zones
- D) Selective alteration of the calcic core of a crystal of plagioclase feldspar
- E) Penetration twins with NW-SE twin having oscillatory zones
- F) Glide twins.

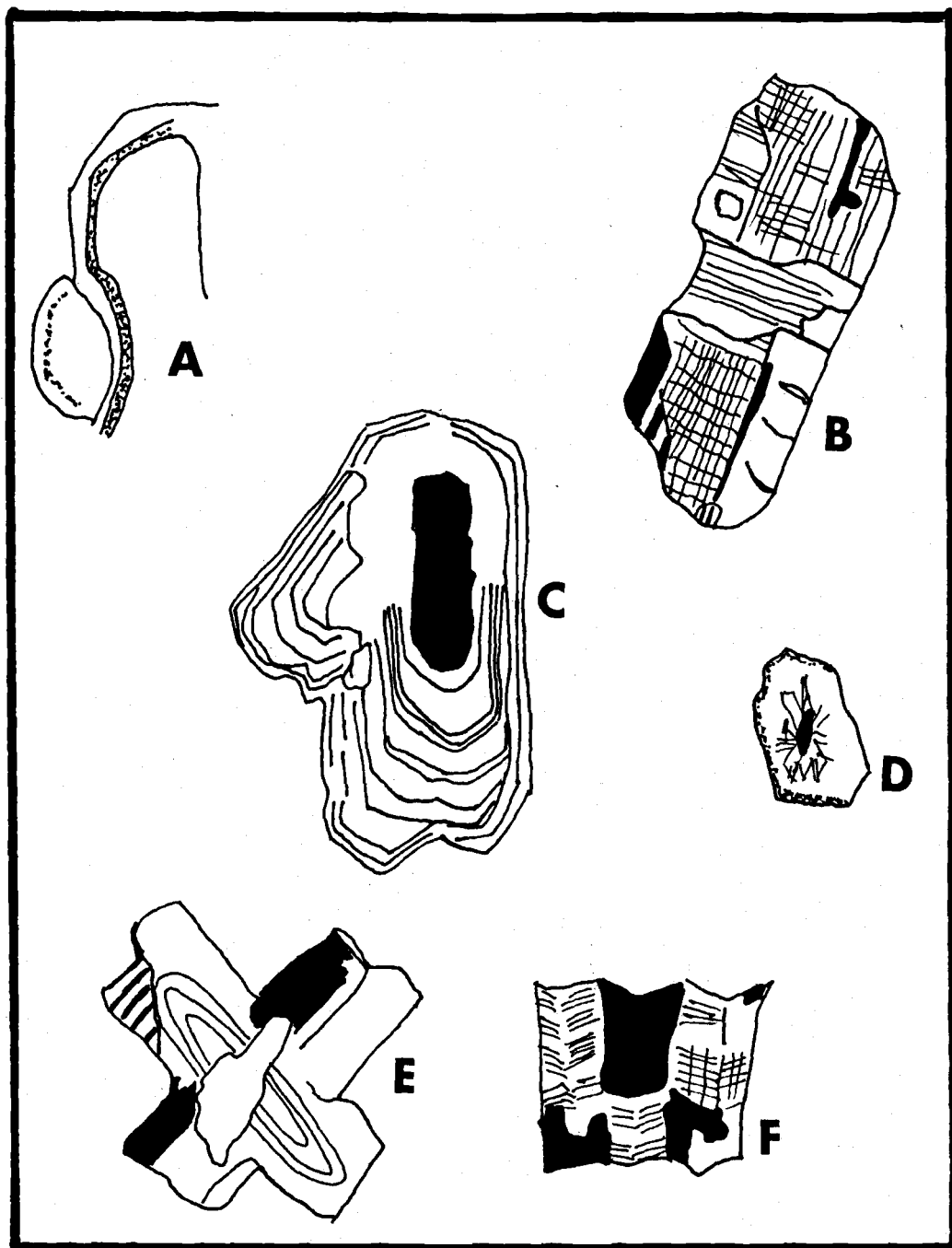


Figure 19.

The opaque minerals include magnetite and limonite. The crystals of magnetite are euhedral to subhedral both in the groundmass and where enclosed by the ferromagnesian minerals. The limonite is an oxidation product of magnetite and the ferromagnesian minerals.

Sphene is present as single crystals, crystal trains, dovetail twins, and penetration twins. The sphene is euhedral to subhedral and mostly larger than the minerals of the groundmass. Apatite forms rod-shaped and stout prismatic crystals. Zircon is a rare constituent of the intrusive rocks at the Copper Chief Prospect.

The quartz and feldspar constituents of the samples of intrusive rock from the Copper Chief Prospect have been recalculated to total 100 percent and plotted in Figure 20; also shown in the figure is the I.U.G.S. classification of plutonic rocks of intermediate to silicic composition (Streckeisen, 1976). The unaltered samples (Table 4) plot in the field of quartz monzodiorite.

Endoskarn and Periskarn

The total abundances of the essential minerals quartz and the feldspars, are nearly the same in the modal analyses of the calc-silicate altered intrusive

Figure 20. Ternary quartz-potassium feldspar-plagioclase feldspar plot of rocks from the Copper Chief Prospect.

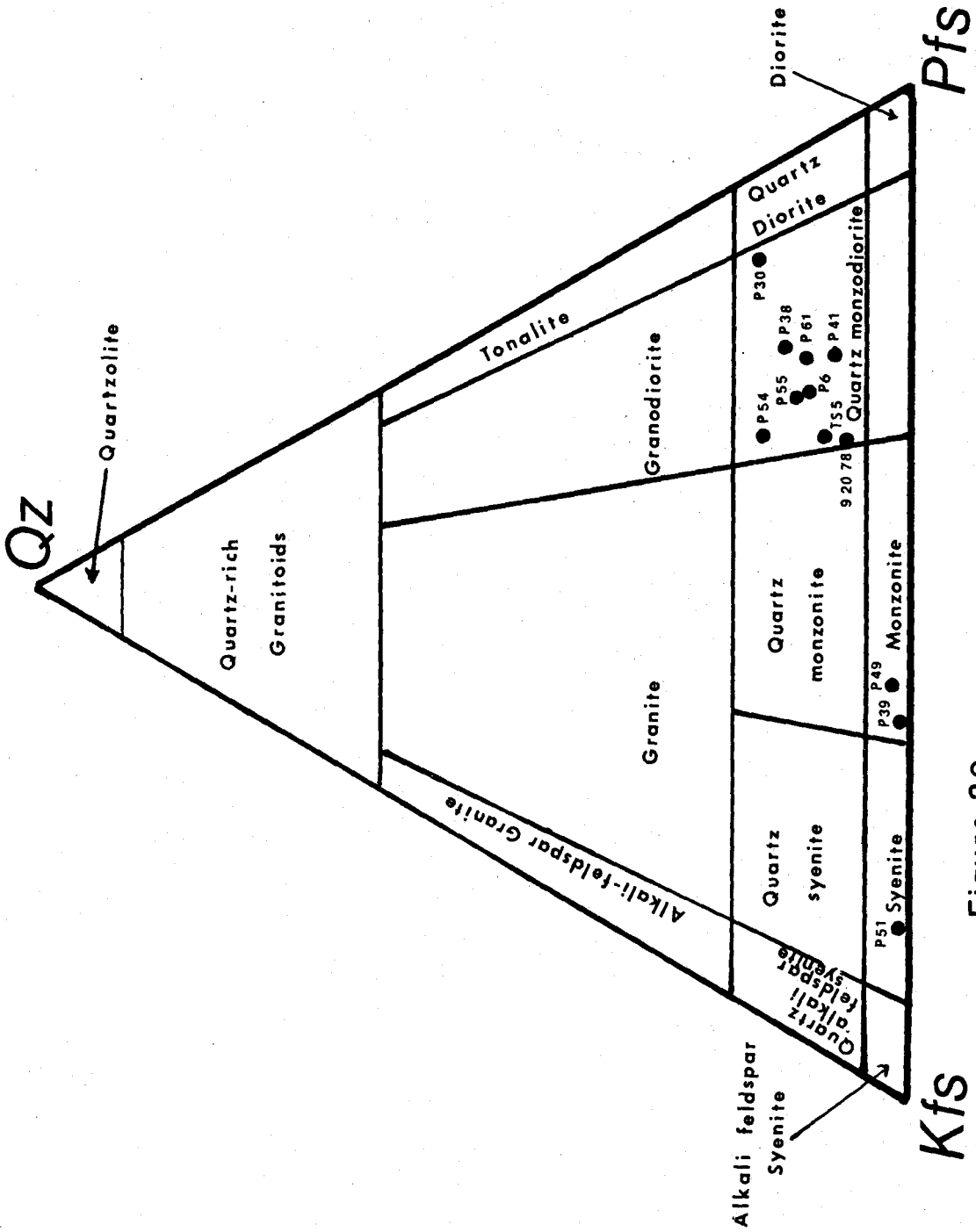


Figure 20.

rocks as in their unaltered equivalents. The samples of fresh intrusive rock and the endoskarns of low alkalinity have plagioclase feldspar as their major constituent, and have slightly more potassium feldspar than quartz. In contrast the highly alkaline endoskarns (periskarns) have potassium feldspar as their most abundant mineral phase. The quartz content of the periskarns is less than 1 percent, as compared with 6 to 14 percent quartz in fresh and endoskarned intrusive rocks. The ferromagnesian minerals, amphibole and biotite, present in the unaltered rocks are absent in samples of endoskarn and periskarn; instead, clinopyroxene, wollastonite, epidote, and garnet characterize the skarns that have replaced intrusive rocks.

The clinopyroxene is dull, colorless, and non-pleochroic in plane-polarized light. The extinction of elongate sections is inclined. The maximum interference colors are middle second order. The optic axis figures of suitably oriented sections are biaxial positive with large $2V$, and the dispersion is $r > v$. The crystal form of the clinopyroxenes is that of amphibole (Fig. 21) and more rarely that of biotite which suggests that the clinopyroxene is pseudomorphic after these minerals.

Crystals of wollastonite are clear, colorless,

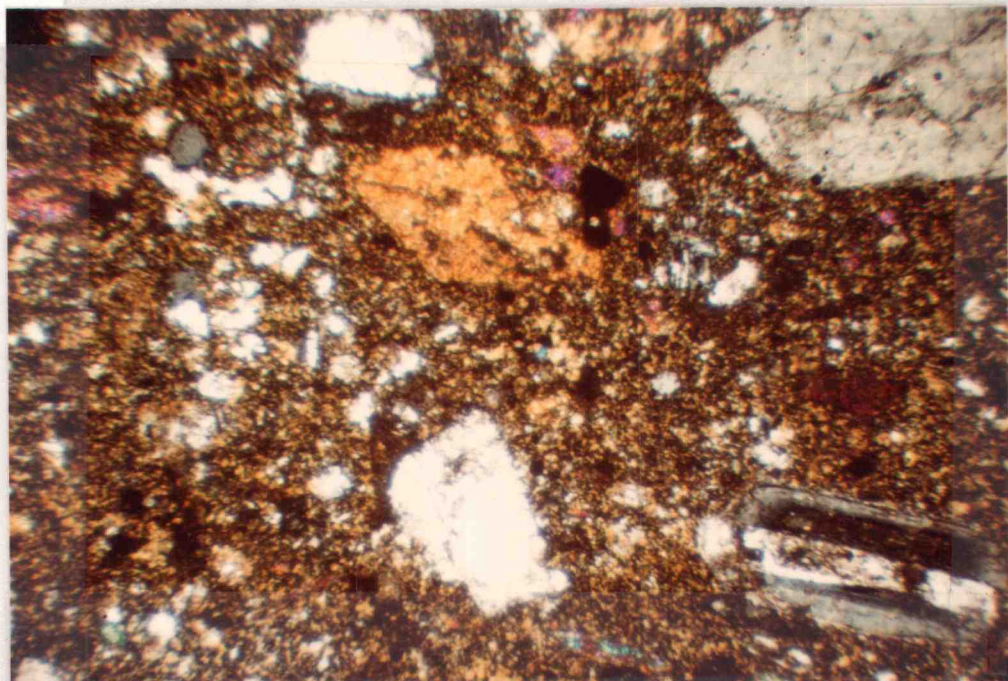


Figure 21. Pseudomorph of clinopyroxene after amphibole (top center) in a sample of periskarn from the Copper Chief Prospect. The field of view is approximately three millimeters.

and non-pleochroic in plane-polarized light. The maximum interference colors are of the lower first order (Fig. 22). The crystal form is skeletal to massive prismatic, and the extinction of prismatic sections is parallel. The interference figures are biaxial negative with small $2V$. Wollastonite grows freely as a replacement mineral that crosscuts several mineral species as well as occurring with crystals of clinopyroxene after amphibole and with remnant crystals of plagioclase feldspar. Its habit as a freely growing mineral species renders it distinguishable from the clinopyroxene in thin sections of periskarns.

The plagioclase feldspars of the endoskarns are the same as those of the unaltered intrusive rocks, whereas many crystals are replaced by potassium feldspar in the periskarns. The abundance of plagioclase feldspar in the periskarns is 20 to 45 percent lower than that of unaltered samples or endoskarns. Phenocrysts of plagioclase feldspar in the periskarns are euhedral to anhedral-skeletal or rounded. Fresh euhedra are located in close proximity to intensely altered anhedral. Potassium feldspar invades plagioclase feldspar along cleavage traces and fractures, and it corrodes directly across crystal faces. The phenocrysts that have been predominantly altered along planes and fractures are anhedral skeletal, whereas those that have been

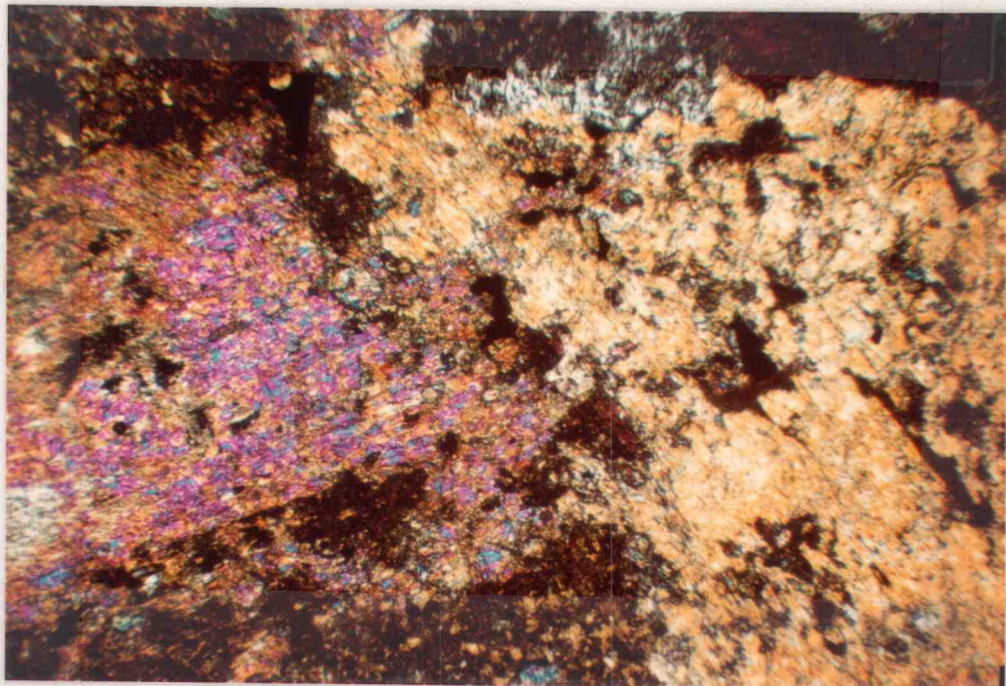


Figure 22. Crystals of wollastonite in a sample of periskarn from the Copper Chief Prospect. The field of view is approximately three millimeters.

predominantly corroded through crystal faces are anhedral rounded.

The groundmass of periskarns and endo karns is finer-grained and more anhedral than that of the unaltered intrusive rocks. The groundmass of periskarns is cryptocrystalline and consists of potassium feldspar with lesser quantities of apatite and sphene.

Epidote forms subhedral crystals, and occurs in veinlets with calcite. The calcite fills cavities and veinlets. Apatite, sphene, and zircon are present in subequal amounts in the samples of fresh and calc-silicate altered intrusive rocks; they have subhedral to euhedral crystal forms.

Garnet was observed in one thin section (CCP-48). The garnet is dull, colorless, and has high relief in plane-polarized light. The crystals are euhedral to subhedral, slightly anisotropic, and have sector and concentric zones.

The opaque minerals of most calc-silicate altered intrusive rocks are magnetite and limonite, but a sulfide phase (pyrite?) occurs in two thin sections (CCP-51 and TS-5).

The endoskarns plot in the field of quartz monzonite whereas the periskarns plot in the fields of monzonite and syenite on the Qz-Kfs-Pfs classification diagram given in Figure 20.

Quartz-Sericite Alteration

Finely foliated white micas (muscovite, paragonite) are termed "sericite" (Niggli, 1954; Deer and others, 1966). Sericite, quartz, and pyrite are the characteristic minerals of the phyllic assemblage of hydrothermal alteration (Burnham, 1962; Lowell and Guilbert, 1970; Brown, 1976; Drummond and Godwin, 1976). The replacement of significant quantities of the magmatic minerals by white mica is pervasive in the thin section of a rock sample collected from one location at the Copper Chief Prospect.

Sample CCP-33 is from the toffee-brown colored exposure of intrusive rock in the central part of the prospect. The rock is cut by numerous veinlets of quartz and is stained by supergene copper minerals. The thin section consists of sericite, quartz, clay, and limonite. The sericite occurs as felted polycrystalline mats in a groundmass of fine to medium-grained quartz and limonite. The preservation of the crystal form and of the selectively altered oscillatory zones of plagioclase feldspar replaced by sericite (Fig. 23) indicates the pseudomorphic nature of the mica. Quartz and limonite are the major constituents of the groundmass, although apatite and sphene occur in minor amounts. Veinlets of quartz cut the mats of sericite

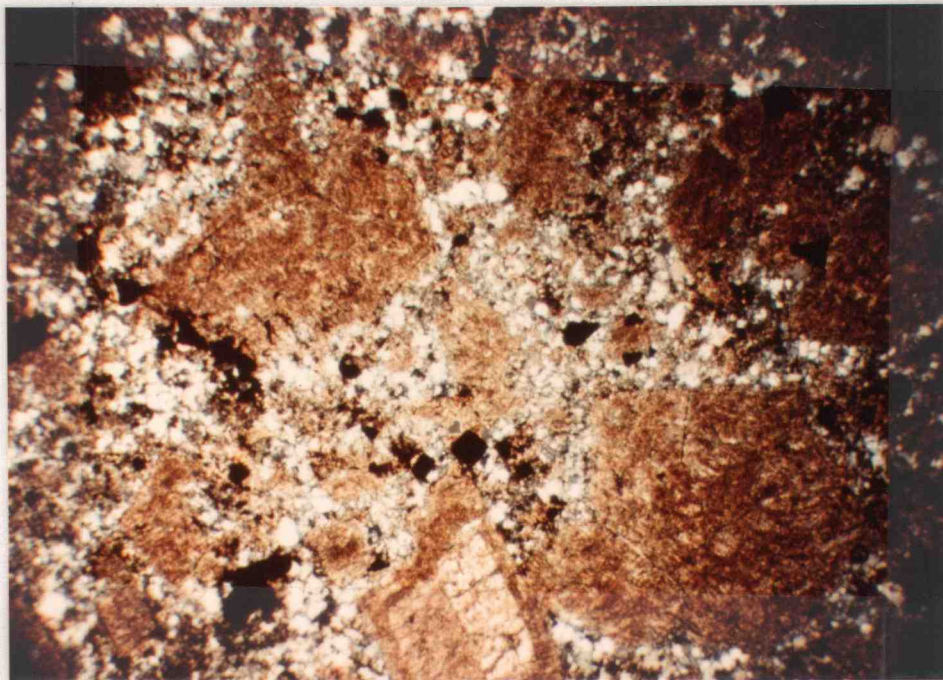


Figure 23. Quartz-sericite alteration of intrusive rock. Note the preservation of the crystal form of the plagioclase feldspar and of the selectively altered oscillatory zone of the crystal at bottom center. The field of view is approximately three millimeters.

and the groundmass. The quartz in the veinlets is coarser than the quartz in the groundmass. Both the quartz in the veinlets and that in the groundmass are subhedral to anhedral in form. The opaque minerals of this sample are heavily oxidized to limonite. The crystal form and appearance of the limonite in reflected light suggest that either magnetite or cubes of pyrite were the pre-oxidation parental minerals.

Calcite Alteration

Sample CCP-57 is the deepest red of the samples collected from the pinkish gray quartz monzodiorite (Plate 1). The mineralogy of the sample is similar to that of the unaltered intrusions, but the potassium feldspar and the ferromagnesian minerals are sparse to absent. Calcite occupies a groundmass position similar to that of potassium feldspar in the unaltered intrusives (Fig. 24). This textural relationship suggests that the calcite has formed by the selective replacement of the potassium feldspar. Plagioclase feldspars have been only incipiently altered to calcite or not at all. The crystals of plagioclase feldspar are stained by limonite along fractures and cleavage planes. Remnant ferromagnesian minerals are sparse in this thin section, but where present are non-pleochroic and have been replaced by a mineral aggregate composed

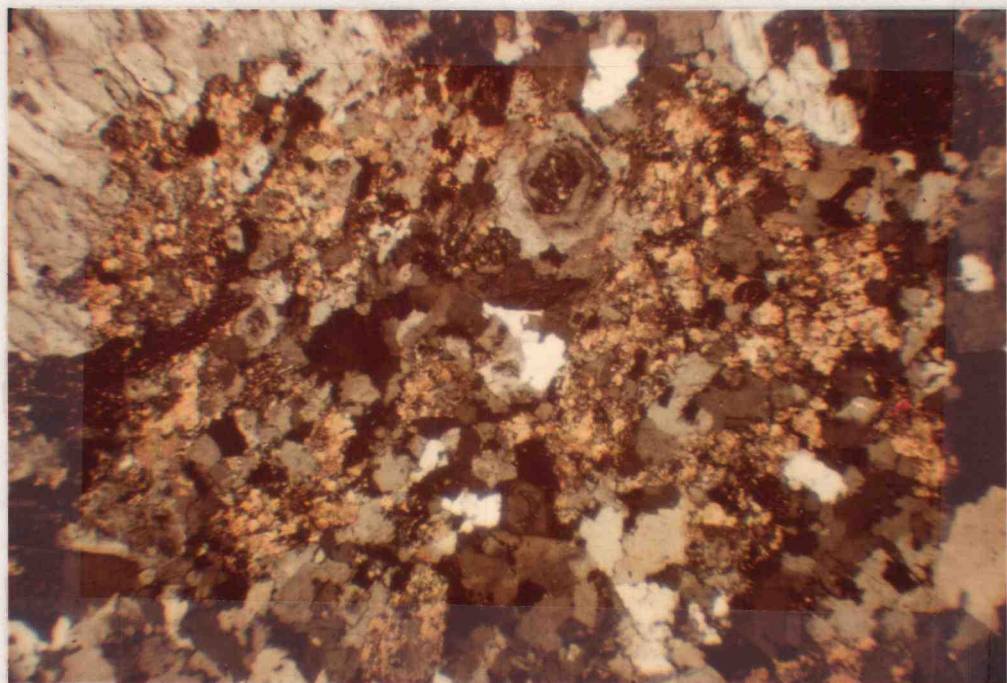


Figure 24. Quartz monzodiorite with secondary calcite in groundmass (brightly birefringent crystals). The field of view is approximately three millimeters.

of calcite, limonite, and clay(?). Quartz is present as subhedral to anhedral crystals partly enclosed in patches of calcite.

Veined Intrusive Rocks

Veins of clay, garnet, quartz (\pm limonite), and calcite-quartz-epidote cut fresh and altered intrusive rocks at the Copper Chief Prospect.

Veins of clay crisscross one another in sample CCP-6. They are less than 0.5 mm wide and are filled with acicular crystals of clay which are oriented nearly perpendicular to the clay walls.

Veins of garnet cut samples CCP-18 and CCP-22. Sample CCP-22 has one garnet vein which is slightly wider than 2.5 mm. The vein is bicolored in hand sample with red brown vein-wall garnet and pink vein-center garnet. In plane-polarized light the garnet is dull to clear, colorless, and has high relief. Between crossed polarizing filters the garnet is mostly isotropic but is slightly birefringent locally. Clinopyroxene has replaced amphibole in the selvages of the vein. Quartz is more abundant in the selvages than it is in the rock further away from the vein. The garnet in sample CCP-18 is present in plume-like veinlets that radiate from central veins. Clinopyroxenes after hornblende and biotite are more abundant, and the bleached selvages

are wider, in this sample than in CCP-22. Pleochroic hornblende has reaction rims of, and is partly enclosed in, ragged patches of clinopyroxene.

Parallel veinlets of quartz are present in sample CCP-11. The veins are 2.5 to 7.6 mm wide and are filled with quartz that displays comb texture near the walls of the veins but is granular in their centers. Exotic limonite (Blanchard, 1968) stains both the veins and the host intrusive rocks.

Petrochemistry

The percentages of major-oxide constituents in samples of three fresh and four altered intrusive rocks from the Copper Chief Prospect were determined by X-ray fluorescence and atomic absorption (Na_2O) spectrometry. Specific gravity was determined by Joly balance. The results of the analyses as well as those for CIPW normative mineral abundances (Washington, 1917), Niggli numbers (Barth, 1962), and selected oxide ratios calculated from the analyses are listed in Table 6. For comparison, the average major-oxide percentages of 33 plutonic rocks from the east Sierra Nevada Range (Bateman, 1961; Bateman and Chappell, 1979), average granodiorite (Le Maitre, 1976), and one analysis of quartz monzodiorite from the White Mountains Range (Sylvester and others, 1978) are also

Major Oxides

	COP-6	COP-22	COP-31	COP-38	COP-39	COP-40	COP-58	1	2	3
SiO ₂	66.2	61.6	61.8	64.2	62.9	63.8	65.3	66.1	57.0	52.1
TiO ₂	0.55	0.52	0.45	0.54	0.59	0.52	0.50	0.54	0.51	1.18
Al ₂ O ₃	15.9	16.1	12.1	17.4	16.6	16.7	16.8	15.73	15.42	17.0
Fe ₂ O ₃	0.77	2.18	2.90	2.51	1.39	3.14	2.51	1.38	1.63	8.86
FeO	1.29	1.68	1.16	1.93	1.16	1.36	1.26	2.73	2.00	
MnO	0.70	0.08	0.09	0.70	0.03	0.10	0.50	0.08	0.07	0.14
MgO	1.27	0.79	1.93	1.05	0.79	1.21	0.76	1.74	1.42	4.19
CaO	0.55	9.11	9.66	4.54	5.03	4.51	3.91	3.83	3.61	8.19
Na ₂ O	3.05	3.87	1.21	4.06	2.22	3.98	4.11	3.75	3.71	3.91
K ₂ O	3.58	3.25	3.08	2.96	7.93	3.05	3.15	2.73	3.57	2.52
P ₂ O ₅	0.20	0.20	0.15	0.21	0.24	0.21	0.19	0.18	0.17	0.78

Normative minerals

Qz	24.4	12.4	28.9	18.5	11.2	18.8	20.7	22.4		
Or	21.7	19.4	19.5	17.6	46.9	18.3	18.9	16.1		
Ab	26.5	33.1	11.0	34.5	19.0	34.2	35.3	31.7		
An	19.7	17.2	19.8	20.6	12.4	19.1	18.4	17.3		
Wo	0.91	9.23	10.5	0.27	4.73	0.93	0.00	0.00 (Di)		
En	3.25	3.37	5.14	2.63	1.99	3.06	1.92	0.00 (Wo)		
Fs	0.78	0.58	0.00	0.71	0.06	0.00	0.00	7.40 (Hy)		
Mt	1.15	3.19	2.32	3.66	2.04	3.25	2.81	2.00		
Hm	0.00	0.00	1.09	0.00	0.00	0.94	0.61	-		
Il	1.07	1.00	0.93	1.03	1.14	1.00	0.96	1.03		
Ap	0.49	0.48	0.38	0.50	0.58	0.50	0.46	0.42		
Cor	0.00	0.00	0.00	0.00	0.00	0.00	0.02	0.26		
Cal	0.00	0.00	0.00	0.00	0.00	0.00	0.00	0.19		

Niggli numbers

sl	290.34	217.63	251.54	255.65	251.30	258.22	280.63	267.26		
sl	41.10	33.58	29.07	40.81	39.11	39.93	42.63	37.47		
fm	14.56	15.16	20.41	16.65	10.78	17.03	13.63	24.21		
c	21.37	30.69	37.76	19.36	21.55	19.56	18.00	16.59		
slk	22.97	20.58	12.77	23.18	28.57	23.49	25.75	21.73		
tz	98.45	35.33	100.47	62.93	37.02	64.27	77.65	80.34		
k	0.44	0.36	0.63	0.32	0.70	0.34	0.34	0.32		
ng	0.57	0.47	0.57	0.37	0.44	0.43	0.36	0.43		

Specific gravity

	Sp. Gr.	2.72	2.69	2.72	2.70	2.68	2.67	2.67		
FeO ₃ /FeO	0.60	1.30	2.50	1.30	1.20	2.30	1.99	0.51	0.81	--
FeO/FeO+MgO	0.61	0.32	0.66	0.80	0.75	0.78	0.82	0.70	0.71	0.98
Normative Qz/Or	1.12	0.64	1.48	1.05	0.24	1.03	1.10	1.38		
Normative plagioclase	An ₆₃	An ₃₄	An ₆₄	An ₃₇	An ₃₉	An ₃₆	An ₃₄	An ₃₅		

Table 6. Chemical data for samples of intrusive rocks from the Copper Chief Prospect. See text for sources of data for the average of the east Sierra Nevada Range intrusions (1), the average granodiorite (2), and the quartz monzodiorite of the White Mountains Range (3).

listed in ^{Table} Figure 6.

With the exception of MnO the chemical compositions of the fresh intrusive rocks from the Copper Chief Prospect (CCP-38, 40, 58) agree moderately well with both the average granodiorite (Av. Gd.) and with the plutonic rocks of the east Sierra Nevada Range (ESN). The content of MnO in samples of two fresh intrusive rocks (CCP-38, 58) is up to ten times higher than those of the ESN plutonic rocks or the average granodiorite.

Iron is more oxidized in the samples from the Copper Chief Prospect than in the other intrusive rocks as indicated by higher $\text{Fe}_2\text{O}_3/\text{FeO}$ ratios. The ratios of total iron as FeO (FeO*) to iron plus magnesium oxide ($\text{FeO}^*/\text{FeO}^*+\text{MgO}$) and of $\text{K}_2\text{O}/\text{Na}_2\text{O}$ of the fresh intrusive rocks are similar to those of average granodiorite. The values are between those of the ESN intrusions and of the quartz monzodiorite of the White Mountains Range. The normative An contents of the plagioclase feldspars of the fresh intrusive rocks are close to that of the average granodiorite and are within the range of values of plagioclase feldspars determined petrographically.

Silica variation (Harker) diagrams that have been used to illustrate the chemical evolution of igneous rocks along the liquid line of descent (Bowen, 1928) may be useful in determining whether or not particular rocks belong to the same or different suites, and may

assist in the identity of anomalous samples in a suite (Ross, 1969). The major-oxide analyses of the samples of intrusive rock from the Copper Chief Prospect are shown on standard silica variation diagrams in Figure 25. The major-oxide trends of ESN plutonic rocks (Bateman, 1961; Crowder and Ross, 1973; and Bateman and Chappell, 1979) are also shown on these plots. Straight lines drawn through the points representing unaltered samples from the Copper Chief Prospect are parallel, or subparallel, to the linear trends of ESN intrusions (Fig. 25). The values of CaO, K₂O, FeO*, TiO₂, and P₂O₅ plot close to or on the ESN trends, whereas the values of Al₂O₃, MgO, and Na₂O plot significantly above or below them. The divergence of the latter three trends from those of the ESN may be due either to analytical error, or to chemical differences between the intrusive sample suites of the Copper Chief Prospect and those of the east Sierra Nevada Range. The intrusive rocks that are altered to quartz and sericite (CCP-33), and those veined by clay (CCP-6) or garnet (CCP-22) have higher CaO values than their unaltered equivalents. The sample of periskarn (CCP-39) is strongly enriched in K₂O. The periskarn, quartz-sericite altered rock, and clay-veined samples are all depleted in Na₂O. The sample altered to quartz-sericite is depleted in Al₂O₃ with respect to the other samples.

Figure 25. Silica variation diagram for intrusive rocks of the Copper Chief Prospect. The linear trends are:

----- intrusive rocks of the
east Sierra Nevada Range

———— unaltered intrusive rocks
of the Copper Chief Prospect.

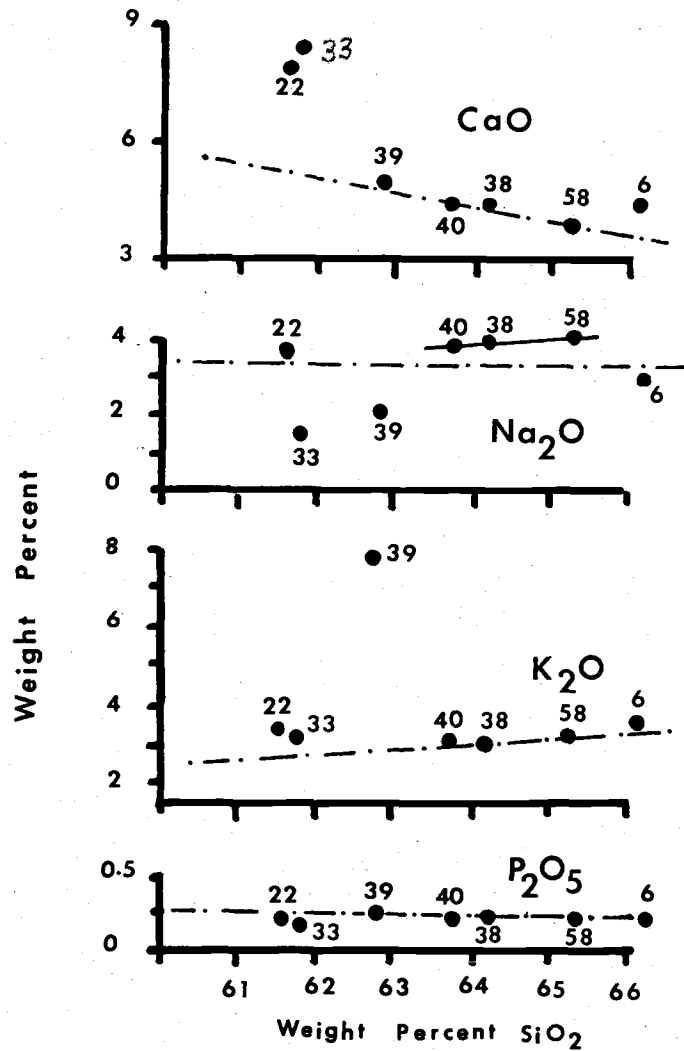
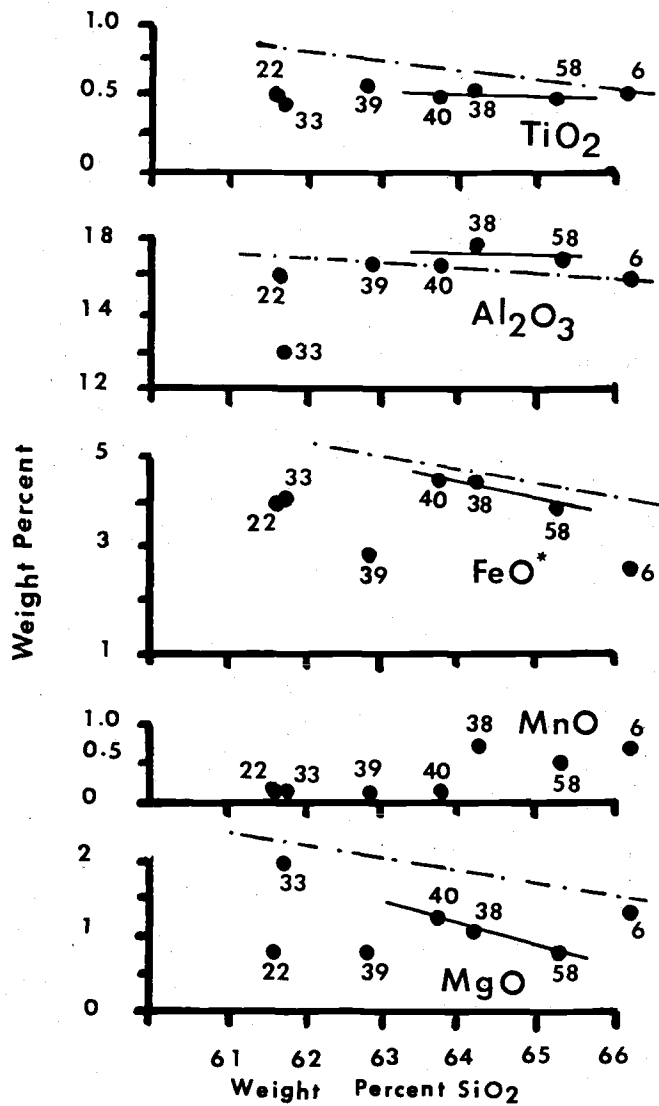


Figure 25.

Various ternary ratios of oxides and normative minerals were calculated from the analyses of the samples of intrusive rock from the Copper Chief Prospect. These ratios are shown on ternary plots in Figures 26 and 27. For comparison, the field of variation of the ESN intrusive rocks is included in both figures, and the fields of variation of 885 granodiorites and 135 adamellites (Le Maitre, 1976) are included in Figure 27. The analyses of fresh intrusive rocks from the Copper Chief Prospect plot in the field of granodiorite (Streckeisen, 1976) on the Qz-Pfs-Or ternary diagram (Fig. 26), and within the region defined by the analyses of ESN plutonic rocks (Reinhart and Ross, 1964; Bateman, 1965; and Ross, 1969). Sample CCP-39 plots in the field of quartz syenite which reflects its anomalously high modal content of potassium feldspar. The sample that is strongly altered to quartz-sericite (CCP-33) and the specimen displaying veins of clay (CCP-6) plot within the field of ESN plutonic rocks, but have higher normative quartz than their associated unaltered counterparts (CCP-38, 40, 58). The sample of quartz-sericite altered intrusive rock (CCP-33) plots in the granite field whereas the sample veined by garnet (CCP-22) plots in the field of quartz monzonite.

Because granitic rocks consist essentially of

Figure 26. Normative Qz-Or-Pfs ternary diagram for the intrusive rocks from the Copper Chief Prospect. The enclosed area is the field occupied by the plutonic rocks of the east Sierra Nevada Range.

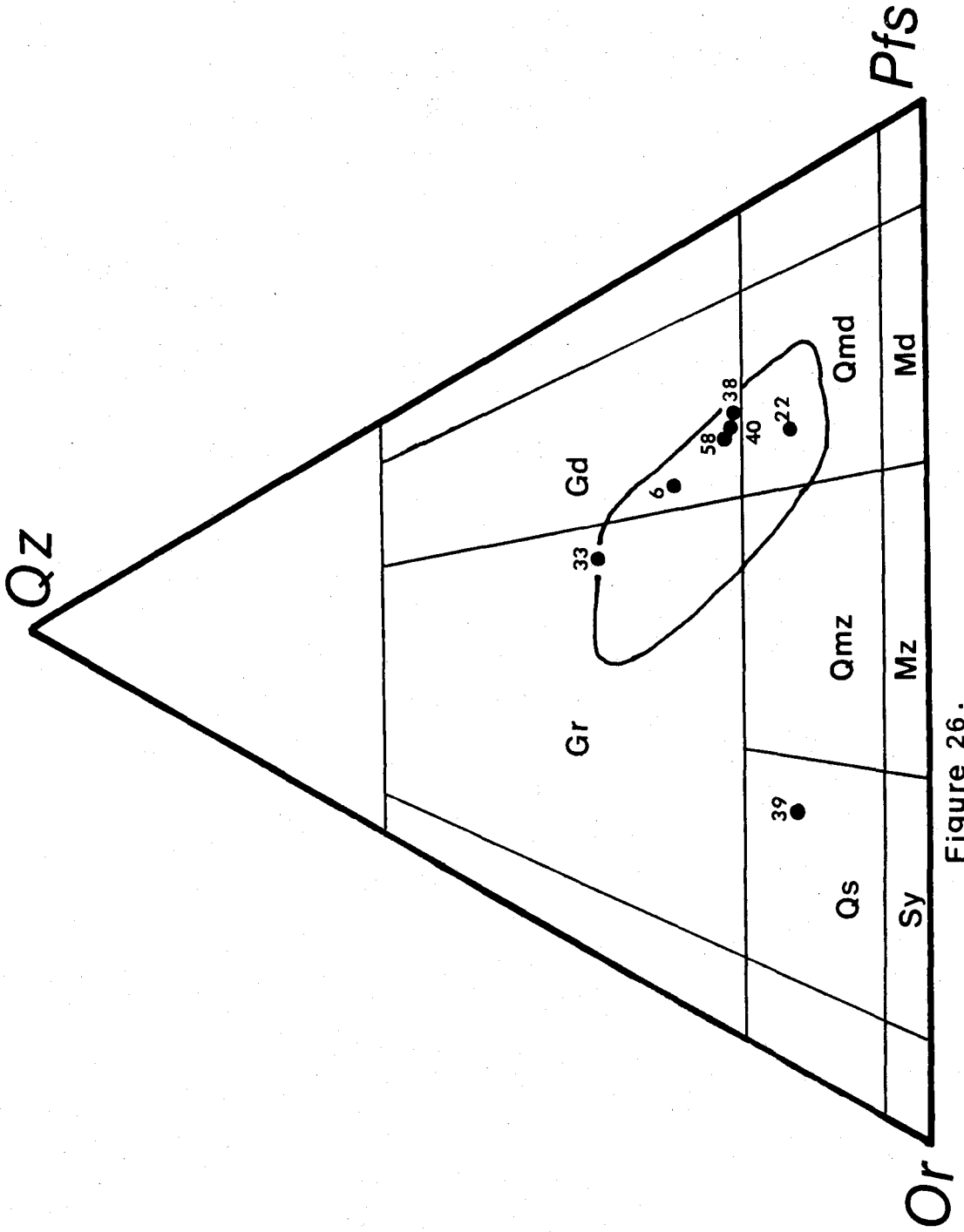


Figure 26.

Figure 27. Comparison of the normative Or-Ab-An contents of the intrusive rocks from the Copper Chief Prospect with the granodiorites and adamellites of the east Sierra Nevada Range and of world wide occurrences of these rock types (references are in text). The linear trend (x-x') is that of normative feldspars of the Mount Givens granodiorite (Bateman and Nokleberg, 1978).

----- granodiorites
..... adamellites
_____ plutonic rocks of the east
Sierra Nevada Range

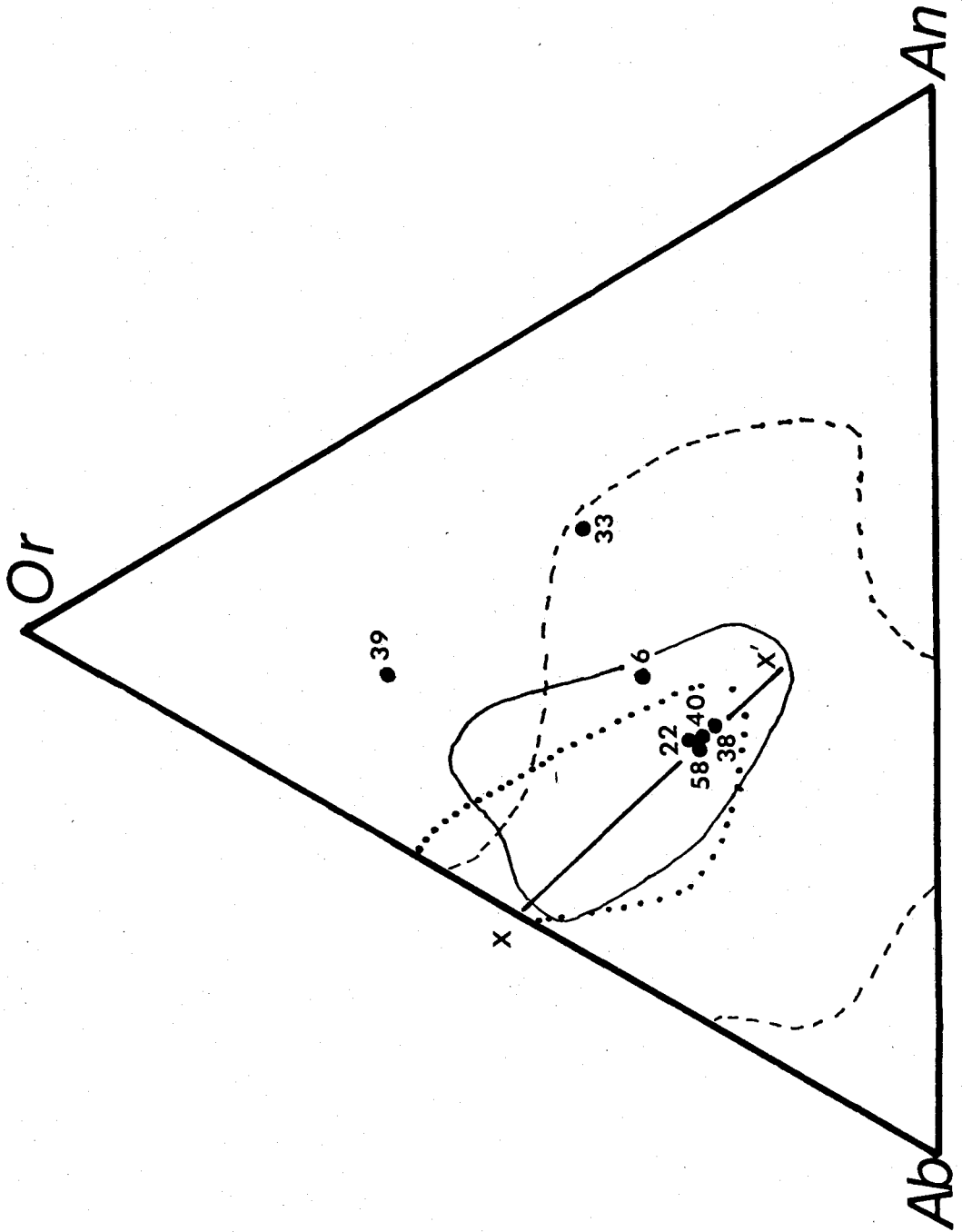
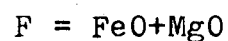
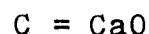
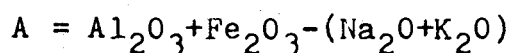
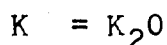
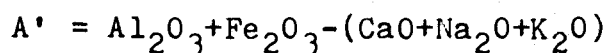


Figure 27.

quartz and feldspar, they can be approximated experimentally by mixtures of SiO_2 (Qz), $\text{CaAl}_2\text{Si}_2\text{O}_8$ (An), $\text{NaAlSi}_3\text{O}_8$ (Ab), and KAlSi_3O_8 (Or). The system Or-Ab-An has been studied by Franco and Schairer (1951), and has been used to determine the normative feldspars that would crystallize in equilibrium with a magma of granodioritic composition (Bateman and Nokleberg, 1978). The compositions of normative feldspars calculated from the chemical analyses of intrusive rock from the Copper Chief Prospect are shown in Figure 27. Also represented on the diagram are the fields of variation of granodiorite and adamellite (Le Maitre, 1976), the variation of ESN plutonic rocks, and a line drawn through the projections of normative feldspars calculated from analyses of the Mount Givens granodiorite of the Sierra Nevada Range (Bateman and Nokleberg, 1978). The plotted data show that the fresh intrusive rocks of the Copper Chief Prospect cluster tightly together, and that the garnet-veined sample lies near this cluster. These specimens and the sample of clay-veined intrusive rock (CCP-6) are contained within the field defined by the plutonic rocks of the east Sierra Nevada Range. The analyses of periskarn and quartz-sericite altered intrusive rock plot outside this region. The three samples of fresh intrusive rock and the one with the garnet vein

are near the line for normative feldspars of the Mount Givens granodiorite.

Ternary AKF and AFC diagrams have been used by metamorphic petrologists to evaluate chemical and mineralogical equilibrium in metamorphic rocks (Eskola, 1939; Turner, 1968). These diagrams have also been used to evaluate the chemical alteration of the copper porphyry deposits (e.g. Creasey, 1959; Field and others, 1975). The analyses of the intrusive rocks from the Copper Chief Prospect are plotted on A'KF and AFC diagrams in Figures 28 and 29. The apices of the two diagrams are calculated after the method of Hutchinson (1974) as follows:



Corrections for accessory and varietal minerals that have oxide components included in the A'KF and AFC calculations, but that do not occur within the two ternary diagrams have not been made.

The analyses of samples of unaltered intrusive rock from the Copper Chief Prospect and the average

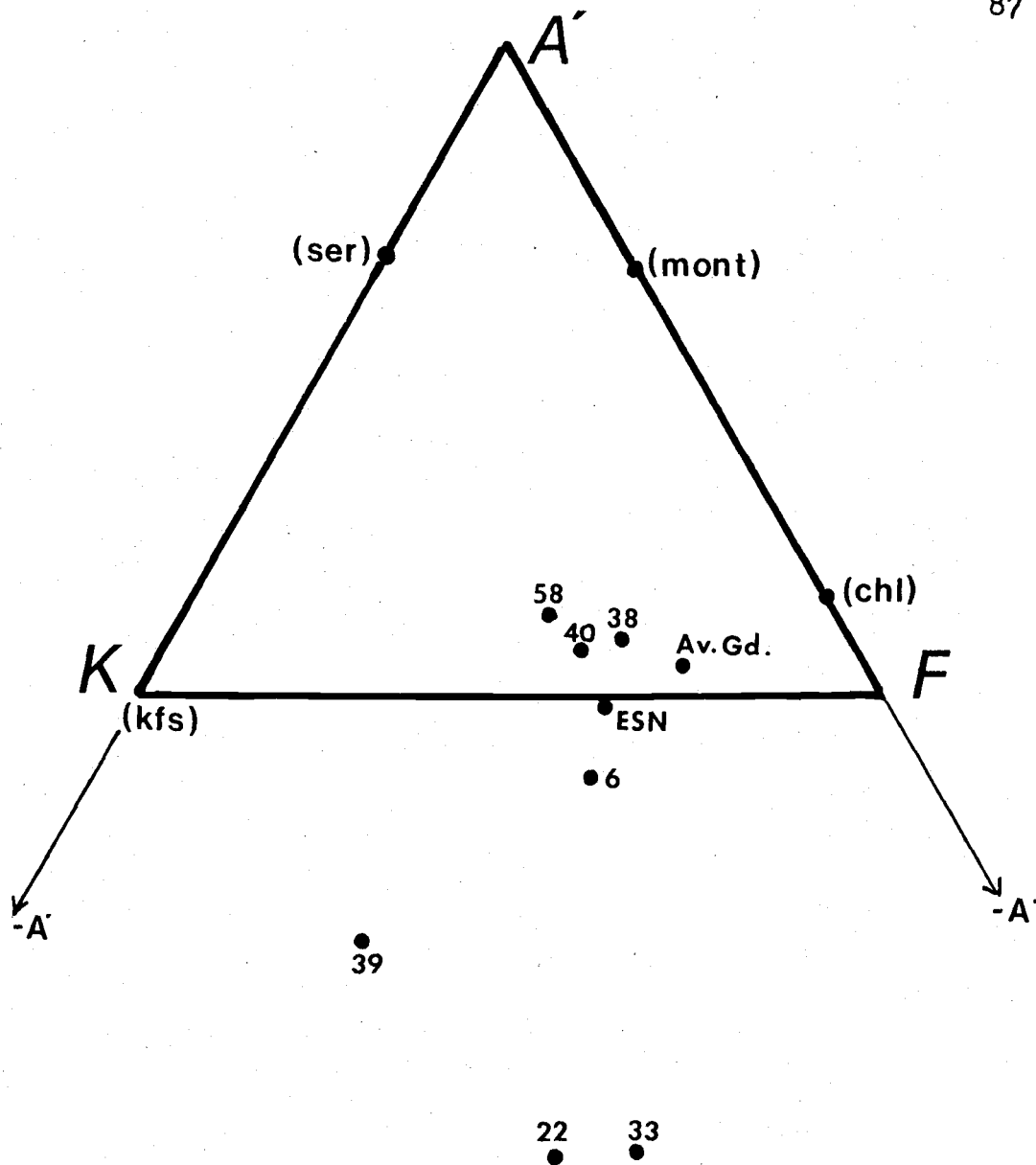


Figure 28. Ternary $A'KF$ diagram of plutonic rocks from the Copper Chief Prospect, the east Sierra Nevada Range (Bateman 1961; Bateman and Chappell, 1979), and the average granodiorite (Le Maitre, 1976).

Figure 29. Ternary ACF diagram for plutonic rocks of the Copper Chief Prospect, average granodiorite (Le Maitre, 1976), and the average of 33 samples of plutonic rock from the east Sierra Nevada Range (Bateman, 1961; Bateman and Chappell, 1979).

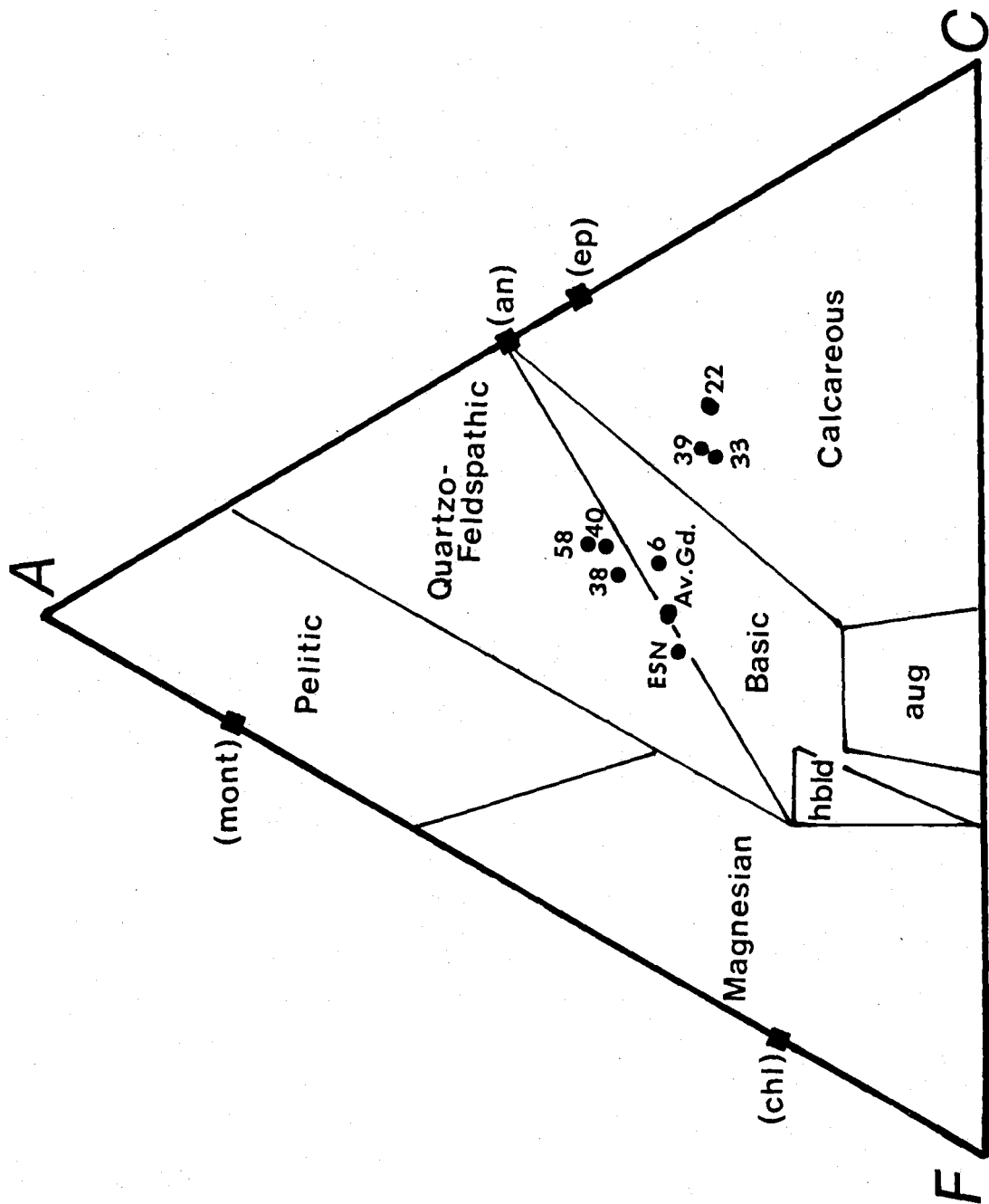


Figure 29.

granodiorite are the only ones that plot within the A'KF ternary diagram. The average of the ESN plutonic rocks and samples from the Copper Chief Prospect that are altered or veined have more Na_2O , K_2O , and CaO than the sum of Al_2O_3 and Fe_2O_3 . Therefore, because of their negative A' values, they plot below the KF join in Figure 28. The fact that the altered samples plot at large distances from their unaltered equivalents suggests that the process of alteration imposed pronounced changes in chemical composition.

All samples of intrusive rock from the Copper Chief Prospect, the average granodiorite, and the average of the ESN plutonic rock suite plot within the ACF diagram (Fig. 29). Since the chemical analyses of the quartz monzodiorite of the White Mountains Range did not include the oxidation state of iron, it cannot be compared to the other samples. Samples of unaltered intrusions from the Copper Chief Prospect, the average granodiorite, and the average of the ESN plutonic rock suite plot near the F-An join as would be expected of unaltered igneous intrusions of intermediate composition according to Ross (1969). The sample altered to quartz and sericite, the one veined by garnet, and the periskarn plot within the calcareous field, which suggests moderate additions of CaO with the alteration process.

METAMORPHIC AND METASOMATIC ROCKS

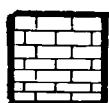
Metamorphic and metasomatic equivalents of limestone and siltstone are spatially related to intrusions, and are the dominant hosts to ore at the Copper Chief Prospect. The lithologies that were recognized by field and laboratory examination include hornfels, marble, and calc-silicate rock (Fig. 30).

All siltstone west of the Battles Well Fault Zone has recrystallized to form hornfels. Siliceous and calc-silicate hornfels are the most abundant metamorphic rocks at the Copper Chief Prospect, and are exposed throughout the central and northwest parts of the prospect.

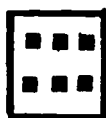
Calc-silicate rocks of at least three distinct types are present at the Copper Chief Prospect: garnetite, clinopyroxene-garnet rock, and wollastonite rock. The garnetite is the most abundant and widespread of the three types. It crops out throughout the central and northwest parts of the prospect, where it is subequal to marble in abundance. The clinopyroxene-garnet rocks are irregularly exposed in the northwest part of the prospect. Wollastonite has replaced limestone at three locations in the central part of the prospect near the north border of the

Figure 30. Distribution of metamorphic and metasomatic lithotypes at the Copper Chief Prospect.

Carbonate Protoliths



Marble, garnet-bearing marble (includes unaltered limestone)



Grandite garnetite



Clinopyroxene-garnet calc-silicate rock



End member garnetite
G- grossularite
A- andradite

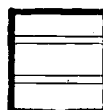


Wollastonite rock

Siltstone Protoliths



Siliceous hornfels, calcareous hornfels



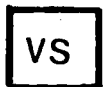
Clinopyroxene-garnet calc-silicate rock

After Intrusions



Endoskarn, periskarn

Other



Veins skarns

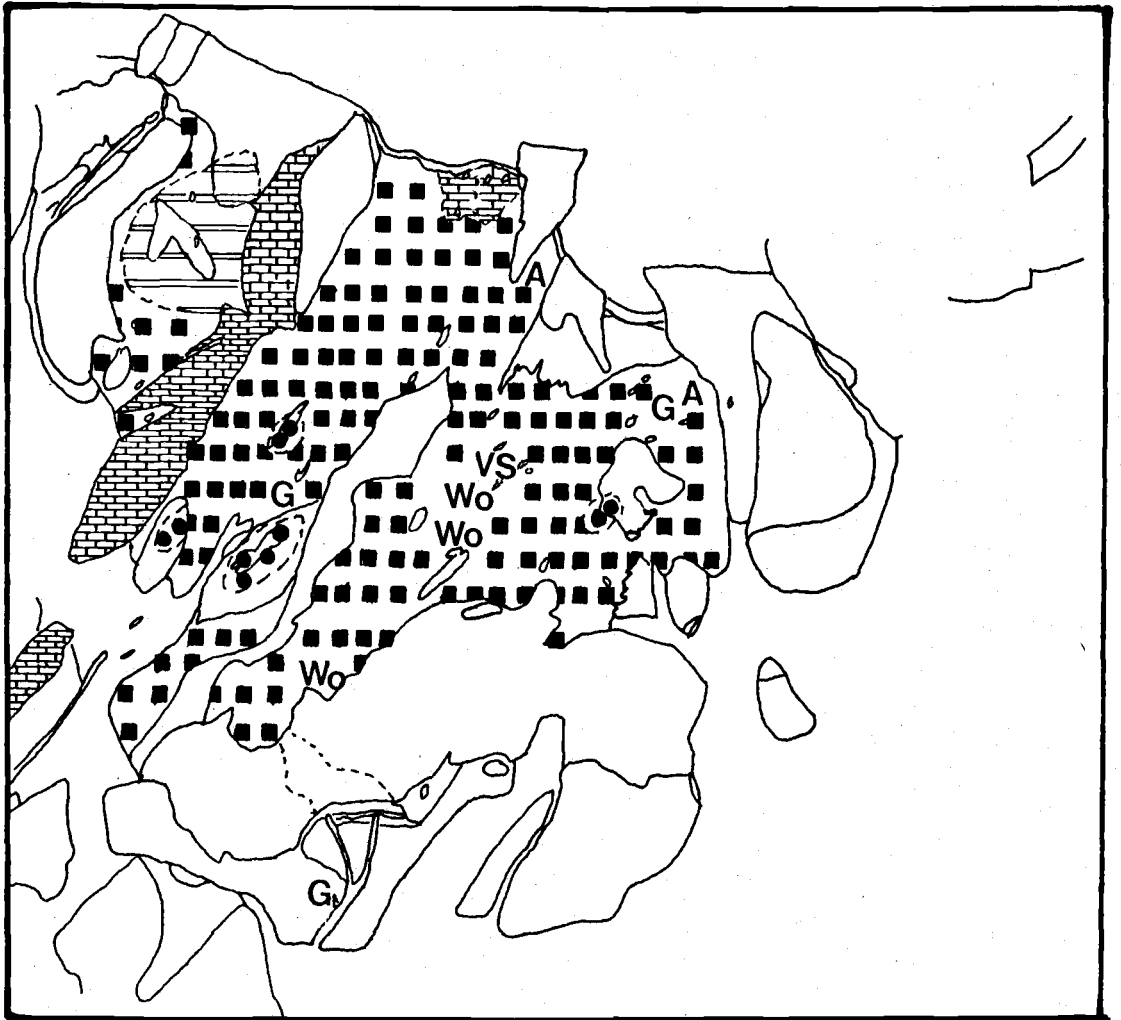


Figure 30.

largest intrusion.

Lithology

The hornfelses are hard, compact, and brittle; and they are easily broken by mechanical weathering. The fragmental material produced by weathering accumulates as talus and colluvium, which bury the underlying hornfels and adjacent lithologies. Outcrops of unbroken hornfels are less common than the colluvial deposits, but are found in the banks of drainages, on steep slopes, and on the crests of some ridges.

The siliceous hornfels consist entirely of microcrystalline minerals. Garnet and wollastonite porphyroblasts are relatively common in the calc-silicate hornfelses. The abundances of the constituent minerals determine the color of the hornfelses; siliceous hornfels is medium gray to white; calc-silicate hornfels in which garnet, clinopyroxene, or wollastonite are the predominant calc-silicate minerals are, respectively, light reddish to greenish brown, pale to medium forest green, and white. Many hornfelses are crosscut by veinlets, some of which have bleached selvages (Fig. 31).

The marbles of the Copper Chief Prospect are fine to coarse-grained granular with smooth to rough



Figure 31. Siliceous hornfels crosscut by veinlets, some of which have bleached selvages.

surfaces. Many marbles have relict internal structures. Whispy siliceous lenses, similar to the chert lenses in the unaltered limestones of the northeast part of the prospect are particularly evident. Most marbles consist exclusively of calcite, but some contain porphyroblasts of garnet or, rarely, epidote. The marbles are light grayish blue, light brown, dull red, and white.

Garnets of two distinct varieties are present as porphyroblasts in the marbles of the Copper Chief Prospect. One type consists of small (2-4 mm) crystals that have well-developed dodecahedral form. These garnets are transparent to translucent and are characterized by vitreous luster. The second type consists of rounded dodecahedrons with dull luster. They are opaque, milky to light brownish white; and they are embedded in marble of the same color as the crystals. These garnets are as large as 11 mm in diameter. The larger crystals form knots in marbles, and have internal concentric light and dark bands which can be seen on weathered surfaces and on cross-sectioned slabs.

The garnetites are hard, dense, and resistant to erosion. They vary from pale bottle green to dark reddish brown in color, but most are either light greenish brown or light brownish green. The colors

are probably influenced by the chemical composition of the constituent garnets. Two samples were analyzed by electron microprobe, and were found to consist of slightly andraditic grossularite (bottle green garnet; Fig. 32) and andradite of close to end member composition (dark reddish brown garnet; Fig. 33). Most of the garnets at the Copper Chief Prospect, however, are intermediate in composition between grossularite and andradite (grandites; Fig. 34). Clinopyroxene is a microcrystalline mineral in the calc-silicate rocks of the prospect. Its presence was suspected during the field work, but petrographic analyses were necessary to confirm this. Clinopyroxene-poor garnetites have uniform textures, color, and luster; whereas clinopyroxene-rich garnetites have mottled surfaces with subtle variations in color and luster that are coincident with the mottling. The crystal form and grain size of garnets in clinopyroxene-poor garnetites are rarely visible, but in clinopyroxene-bearing varieties, garnets frequently exhibit idioblastic form.

Clinopyroxene-garnet calc-silicate rocks have replaced both limestone and siltstone. These rocks are characterized by abundant groundmass clinopyroxene, and by the presence of sparse to abundant porphyroblastic garnet. They are overlain by knotted marble, and they



Figure 32. Photograph of grossularite garnetite from the Copper Chief Prospect.



Figure 33. Photograph of andradite garnetite from the Copper Chief Prospect.



Figure 34. Photograph of grandite garnetite from the Copper Chief Prospect.

are associated with rocks of the marble-garnetite-hornfels assemblage.

Limestone beds that have been replaced by clinopyroxene-garnet rock form resistant ledges and ribs. These resistant rocks consist of garnet porphyroblasts as large as 13 mm in diameter that are suspended in a clinopyroxene-rich groundmass. Many crystals of garnet have grown large enough to impinge on neighboring porphyroblasts (Fig. 35).

Other exposures of clinopyroxene-garnet rock presumably that formed from siltstone, resemble calc-silicate hornfels. These rocks are dominated by groundmass, porphyroblasts are present in sparse to moderate amounts. The porphyroblastic varieties contain ovoid garnets that occur as single crystals and as linear clots (Fig. 36).

The wollastonite rocks consist of light brownish gray, coarsely bladed crystals of wollastonite that are as much as 15 cm in longest dimension (Fig. 37). These rocks have replaced limestones; the exposures are small (typically five to ten feet long and one to two feet thick), and they are covered by alluvium on all sides.

Petrography

The metamorphic rocks at the Copper Chief Prospect consist predominantly of garnet, calcite, quartz,



Figure 35. Ideoblastic porphyroblasts of garnet in a groundmass of clinopyroxene and quartz.



Figure 36. Streaky garnet in clinopyroxene-rich groundmass.



Figure 37. Coarsely bladed wollastonite after limestone in the central part of the Copper Chief Prospect.

clinopyroxene, and wollastonite. Thin-sections of thirty-five samples of metamorphic rocks were examined. Locations are shown in Figure 38.

Crystals of andradite are honey yellow in thin sections. They are transparent in plane-polarized light. Most crystals are isotropic, although some are rimmed by thin birefringent zones (Fig. 39). Crystals of grossularite are clear (Fig. 40), translucent, frosted, and many are pitted with tiny crystals of clinopyroxene. Most are slightly anisotropic (first-order grays and yellows). The crystals of grossularite commonly display sector twins and concentric bands. The grandite garnetites have properties that are intermediate between the two end-member garnets. Slightly anisotropic crystals, or sectors within crystals, are particularly common in the grossularite-rich varieties. In andraditic varieties a slight yellow color is present in plane-polarized light.

Crystals of clinopyroxene are ideoblastic to xenoblastic. They occur as stout prisms with four and eight-sided cross-sections, and as ragged flakey crystals. The crystals vary from 0.01 to 0.1 mm in size and are birefringent in upper first and lower to middle second-order colors.

Calcite is present in marble, calc-silicate rocks, and calc-silicate hornfelses. It occurs as

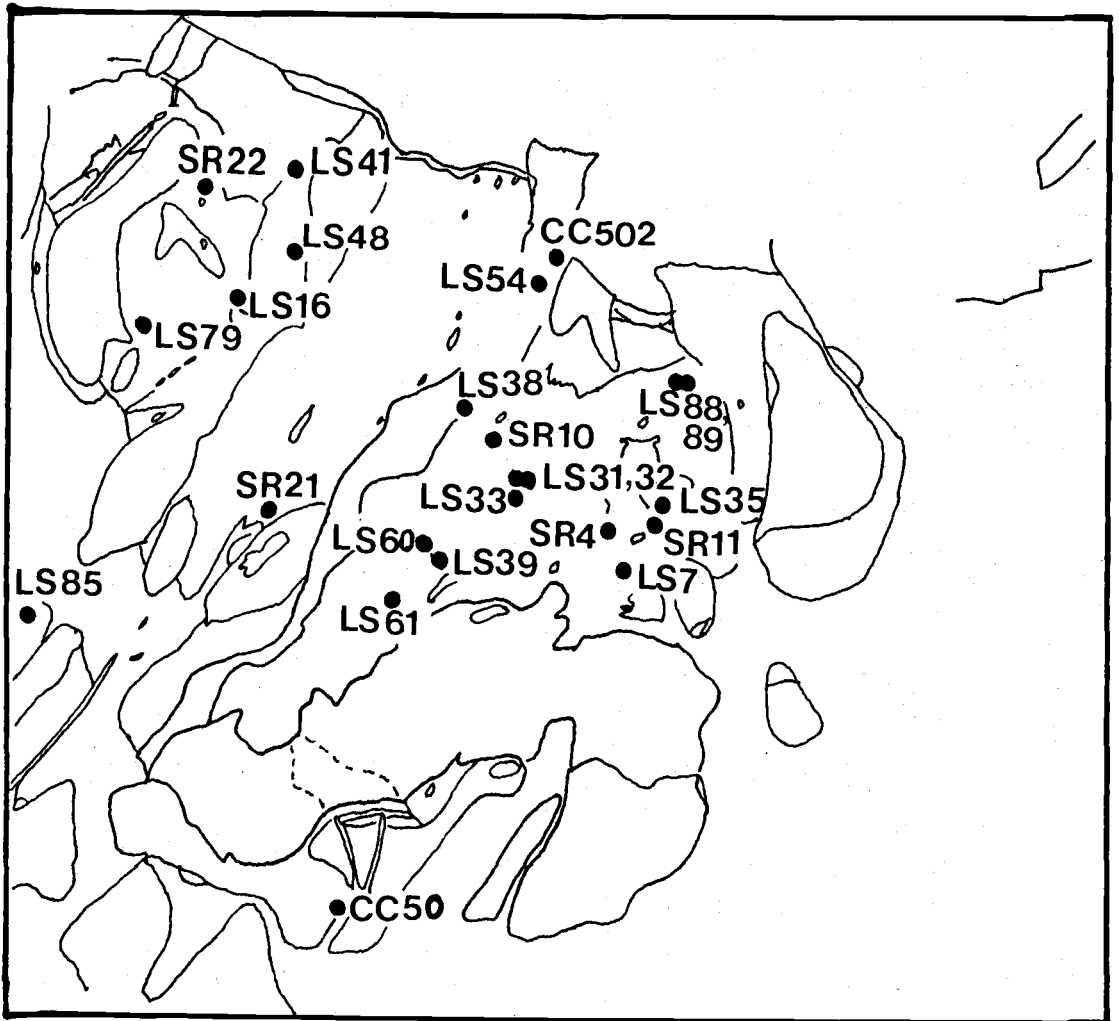


Figure 38. Locations of samples of metamorphic and metasomatic rock collected for petrographic and chemical analysis.

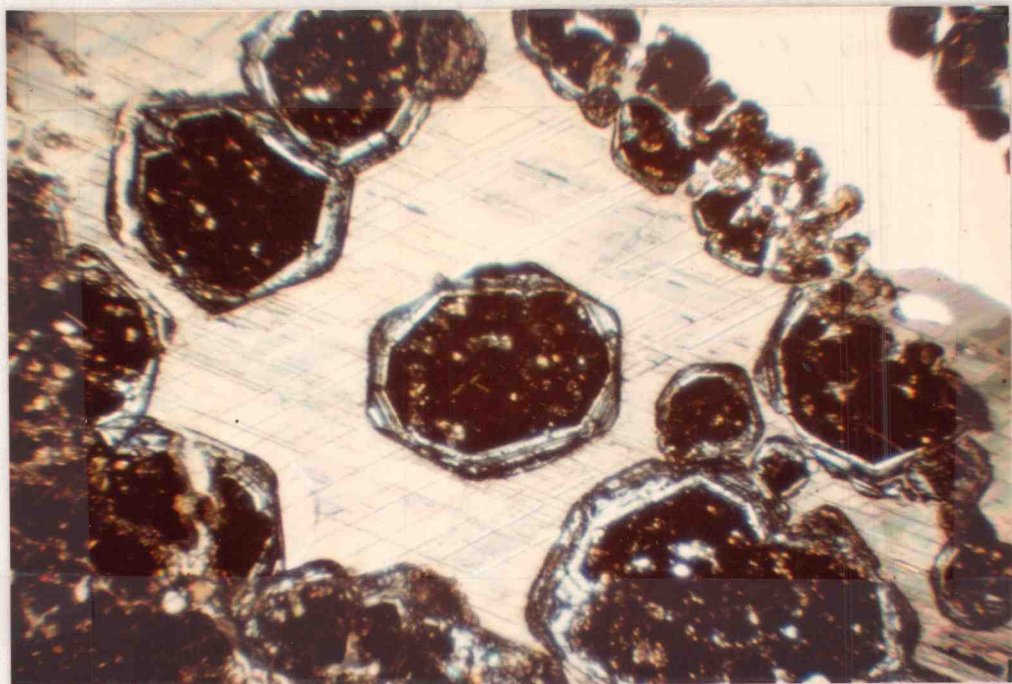


Figure 39. Crystals of andradite (black) and calcite. The calcite displays rhombic cleavage. The field of view is approximately three millimeters.

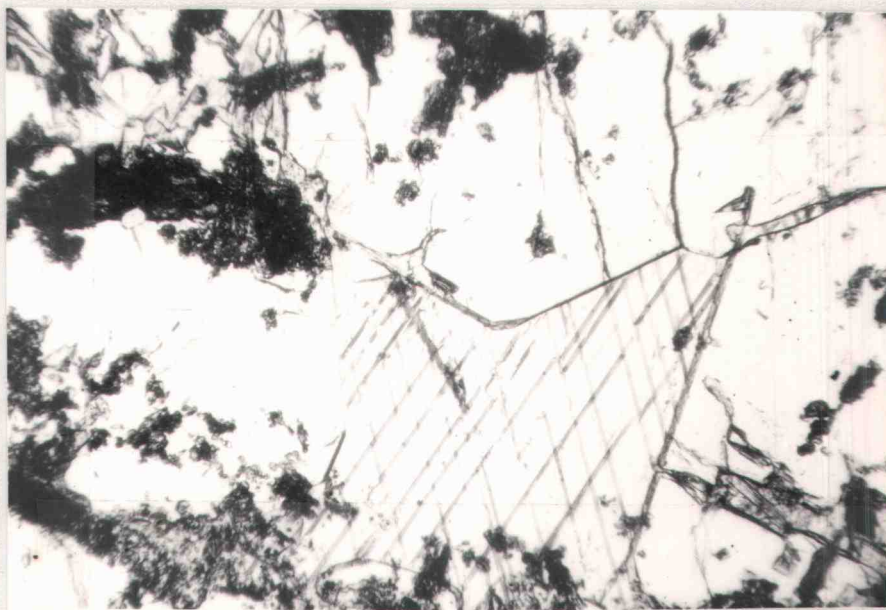


Figure 40. Crystals of grossularite. The field of view is approximately three millimeters.

microcrystalline intergrowths of monomineralic calcite and with the other minerals. It also is present as coarsely crystalline patches displaying prominent rhombic cleavage.

Quartz is present in thin sections as microcrystalline intergrowths with garnet, clinopyroxene, wollastonite, potassium feldspar, and calcite. It also forms overgrowths on garnet. The mineral fills veinlets, vugs, and other voids. The crystals of quartz are xenoblastic to idioblastic, and range from less than 0.01 mm to several millimeters in size.

Wollastonite is clear, transparent, and idioblastic to xenoblastic. It is birefringent in colors of the middle first-order. Cleavage is distinct in prismatic sections.

The hornfelses consist mainly of microgranular quartz. However, minerals such as clinopyroxene, potassium feldspar, garnet, wollastonite, and mica(?) are also common constituents of these rocks. Those that make up the hornfelses are uniformly fine-grained (0.01 to 0.1 mm) and granoblastic, although some hornfelses contain porphyroblasts of garnet and wollastonite. The garnets are idioblastic to subidioblastic and are up to 3 mm in diameter. Crystals of wollastonite are subidioblastic to xenoblastic. Coarse aggregates of clinopyroxene crystals observed in

one sample may have pseudomorphically replaced the shells of fossils. Quartz, potassium feldspar, and calcite fill the veinlets that crosscut the hornfelses. Fine-grained cubes of pyrite are disseminated throughout some hornfelses.

The marbles are equidimensional and xenoblastic in texture. They consist of crystals of calcite that vary from microcrystalline to coarsely crystalline in size. Porphyroblasts of garnet in the knotted marble are sieved by fine-grained xenoblastic calcite. The calcite is localized in concentric zones within the garnets.

The garnetites consist of varying proportions of garnet, clinopyroxene, calcite, and quartz. Because they constitute the predominant calc-silicate lithotype at the Copper Chief Prospect, modal analyses of four thin sections of garnetite were performed by the method of Chayes (1956). For comparison, one sample of clinopyroxene-garnet rock was also analysed (Table 7).

Grossularite and andradite garnetites consist of equigranular, dodecahedral crystals that are crudely layered or crustified. Most garnets in the grandite garnetites project idioblastic faces into adjoining crystals of calcite, or into aggregates of clinopyroxene, calcite, and quartz. However, where garnets impinge on other garnets, they are xenoblastic. Aggregates of

	<u>CCSR-22</u>	<u>CCLS-33</u>	<u>CCLS-54</u>	<u>CCLS-88</u>	<u>CCLS-89</u>
Garnet	44.2	61.2	82.3	69.9	89.4
Clinopyroxene	26.6	- -	8.4	19.1	6.5
Quartz	27.8	9.5	0.2	8.0	0.4
Calcite	1.4	27.2	8.2	3.3	3.3
Opaque mineral(s)	- -	2.1	1.0	trace	0.4
	<u> </u>				
Totals	100	100	100	100	100
Points counted	519	518	526	513	532

CCSR-22 Clinopyroxene-garnet rock

CCLS-33 Grandite garnetite with retrograde alteration features.

CCLS-54 Garnetite

CCLS-88 Veined garnetite

CCLS-89 Garnetite

Table 7. Modal analyses (in percent) of calc-silicate rocks from the Copper Chief Prospect.

clinopyroxene, calcite, and quartz crystals are irregularly distributed in the garnetites. Local accumulations of idioblastic to xenoblastic crystals of these minerals occur as diffuse lenses, streaks, and patches. Veinlets of calcite, quartz, and garnet cut the garnetites in parallel sets (Fig. 41), and as anastomosing networks; some veinlets contain metallic sulfides or limonite.

Retrograde metasomatic features were observed in one sample of garnetite (CCLS-33; Fig. 42). The retrograde minerals, calcite, quartz, and clinopyroxene fill voids in the garnetite or have corroded and replaced crystals of garnet. One void contained within the thin section, had the following sequence from the walls to the center of the void: 1) garnet, 2) garnet partly replaced by calcite, 3) garnet largely replaced by calcite, 4) calcite, 5) drusy and branching filamentary networks of feathery quartz, and 6) granular quartz. Because the transitional stages of the replacement of garnet by calcite have been preserved, calcite is easily recognized as being pseudomorphous after garnet. One crystal of clinopyroxene in this sample has the form of garnet but the middle-second order birefringence of clinopyroxene. Veinlets of calcite crosscut the sample, and therefore were filled penecontemporaneously with or

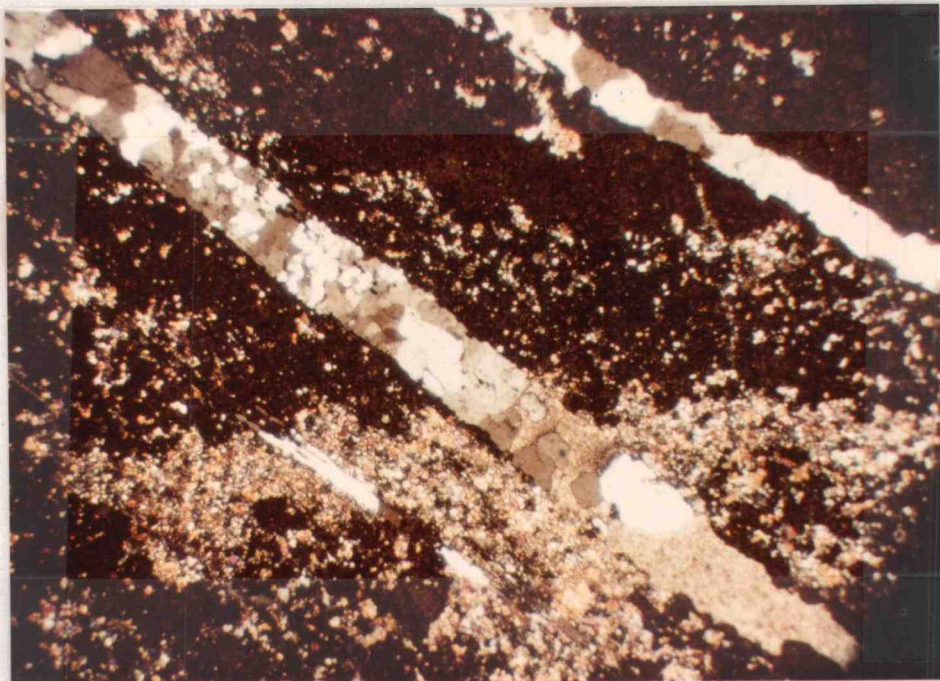


Figure 41. Parallel veinlets of quartz in garnetite. Note the irregular-shaped patches of clinopyroxene. The field of view is approximately three millimeters.

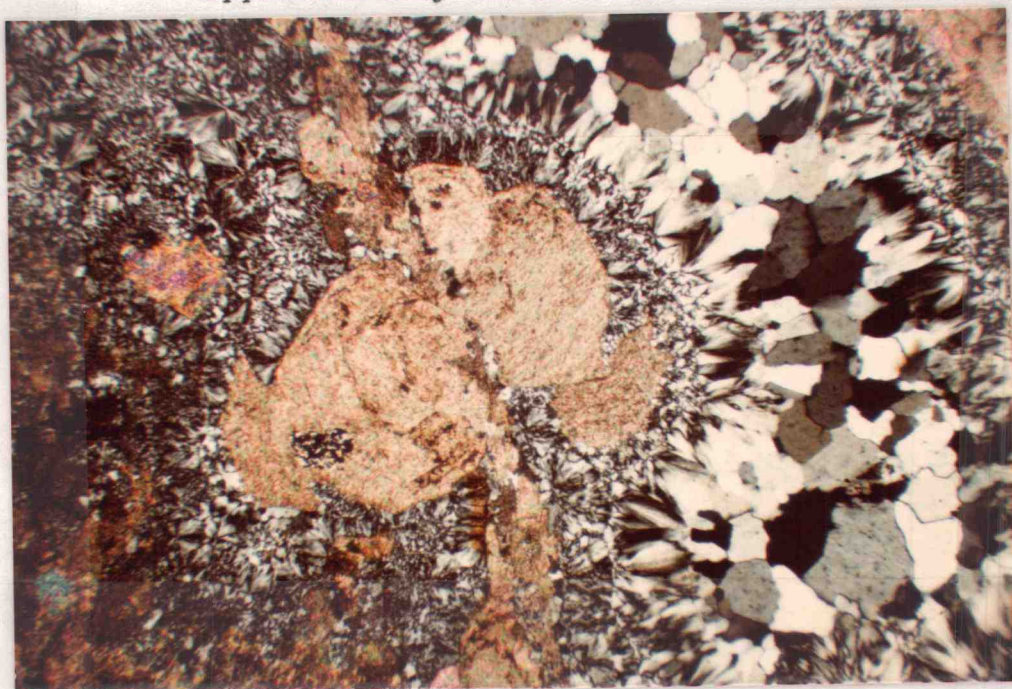


Figure 42. Retrograde mineralization of garnetite in sample CCLS-33. Note pseudomorphs of calcite after garnet (center).

after the replacement of the garnets.

The clinopyroxene-garnet rocks consist of microcrystalline clinopyroxene, quartz, plagioclase feldspar(?), and porphyroblastic garnet. The crystals of garnet have sieve textures caused by microcrystalline minerals contained as inclusions within the garnets (Fig. 43). The microcrystalline minerals are xenoblastic both in the groundmass and where they are included in garnets.

The wollastonite rocks consist predominantly of this mineral. Minor calcite and quartz are also present in the interstices between crystals of wollastonite.

Petrochemistry

The relative concentrations of the major oxides in samples of limestone and metacarbonate rocks collected from ten locations at the Copper Chief Prospect were determined by inductively coupled plasma and atomic absorption (SiO_2) spectroscopy. Because the totals of the major oxides for six of the samples were suspiciously low, reanalyses were requested and these gave higher totals. However, the six samples that had low total oxides in the original analyses remain low. The deficiencies in these samples are believed to be primarily in the

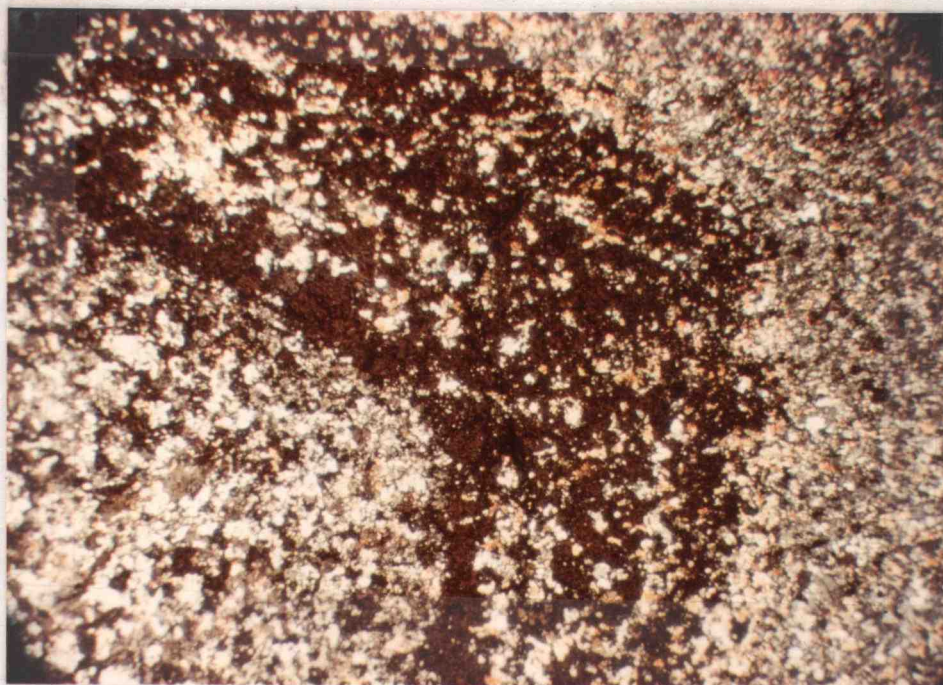


Figure 43. Sieved porphyroblast of garnet in clinopyroxene-garnet calc-silicate rock. The field of view is approximately three millimeters.

contents of SiO_2 and Al_2O_3 because: 1) the reanalyses provided increases of SiO_2 and Al_2O_3 that were not accompanied by changes in the other oxides, 2) analyses for several other elements not included in the original request were performed to determine if these might account for the deficiencies but none were found, and 3) only two of the samples contain greater than one percent of combined $\text{Cu}+\text{Zn}+\text{Mo}+\text{Au}+\text{Ag}+\text{WO}_3$ (Table 8), and none of these contain sufficient concentrations of these elements to bring the totals to 100 percent.

The metasomatic replacement of carbonate rocks by calc-silicates or skarn involves the addition of some substances and the removal of others. Accordingly, it is of interest to perform calculations to deduce the identity and amount of these substances added to or subtracted from the parental host with its conversion to a calc-silicate rock (Lindgren, 1924; Mackin, 1968). Gains and losses listed in Table 9 have been calculated from concentrations of the major oxides (reanalyses) and specific gravities (determined by Joly balance) for altered samples of the Copper Chief Prospect with respect to these data from sample CCLS-85 which is assumed to be representative of unaltered impure carbonate host rock. The gain (+) or loss (-) of each oxide component given in mg/cm^3 is determined

	<u>Cu</u>	<u>Zn</u>	<u>Mo</u>	<u>WO₃</u>	<u>Au</u>	<u>Ag</u>
CCLS-33	35800	470	5	45	6	122
CCLS-35	9500	4300	-1	8	-0.1	2
CCLS-41	210	90	91	5	-0.1	5
CCLS-48	100	35	1	5	-0.1	-1
CCLS-60	25	25	1	5	-0.1	-1
CCLS-74	35	30	19	30	-0.1	-1
CCLS-85	20	15	1	-5	-0.1	-1
CCLS-88	375	90	7	60	-0.1	1
CCLS-89	610	220	7	10	-0.1	-1

-0.1, -1, -5 = less than limit of detection

Table 8. Trace element concentrations (ppm) in samples of carbonate and metacarbonate host rocks from the Copper Chief Prospect for which major oxide analyses were obtained (see Table 9).

Table 9. Major oxide percentages and specific gravities of samples of carbonate and metacarbonate rocks from the Copper Chief Prospect, and with gains and losses calculated from these data (see text for elaboration of the calculations).

	<u>CCSR-22</u>			<u>CCIS-33</u>			<u>CCIS-35</u>		
	Wt. %	mg/cc	gains and losses mg/cc	Wt. %	mg/cc	gains and losses mg/cc	Wt. %	mg/cc	gains and losses mg/cc
SiO ₂	41.2	1300	+ 660	50.2	1720	+1080	43.3	1380	+ 740
Al ₂ O ₃	16.1	510	+ 320	1.4	50	- 140	5.5	180	- 10
FeO*	6.4	200	+ 140	9.9	340	+ 280	4.9	160	+ 100
MgO	3.1	100	+ 60	0.8	30	- 10	0.8	20	- 20
CaO	27.0	850	- 200	21.0	720	- 330	28.8	920	- 130
Na ₂ O	0.35	10	- 10	0.04	1	- 19	0.03	1	- 19
K ₂ O	0.22	6	- 14	0.05	2	- 18	0.04	1	- 19
CO ₂	0.2	10	- 760	6.5	220	- 550	9.5	300	- 470
H ₂ O	0.50	20	+ 10	1.5	50	+ 50	0.3	10	0
Totals	95.07		+ 206	91.39		+ 331	93.17		+ 152
Gains			1190			1400			840
Losses			984			1069			668
Specific Gravity	3.16			3.42			3.20		

	<u>CCIS-41</u>			<u>CCIS-48</u>			<u>CCIS-60</u>		
	Wt. %	mg/cc	gains and losses mg/cc	Wt. %	mg/cc	gains and losses mg/cc	Wt. %	mg/cc	gains and losses mg/cc
SiO ₂	38.5	1220	+ 580	48.6	1530	+ 890	39.8	1390	+ 750
Al ₂ O ₃	13.4	420	+ 230	0.25	10	- 180	8.9	310	+ 120
FeO*	2.8	90	+ 30	0.7	20	- 40	5.9	210	+ 150
MgO	2.4	80	+ 40	2.6	80	+ 40	3.5	120	+ 80
CaO	28.8	723	- 327	39.9	1261	+ 211	31.6	1100	+ 50
Na ₂ O	0.36	10	- 10	0.04	1	- 19	0.04	1	- 19
K ₂ O	1.8	60	+ 40	0.04	1	- 19	0.01	0	- 20
CO ₂	6.1	190	- 580	7.1	220	- 550	4.5	160	- 610
H ₂ O	0.7	20	+ 10	0.5	20	+ 10	0.1	3	- 7
Totals	94.86		+ 13	99.73		+ 343	94.35		+491
Gains			930			1151			1150
Losses			917			808			659
Specific Gravity	3.17			3.16			3.48		

Table 9.

	<u>CCIS-74</u>			<u>CCIS-85</u>			<u>CCIS-88</u>		
	Wt. %	mg/cc	gains and losses mg/cc	Wt. %	mg/cc	gains and losses mg/cc	Wt. %	mg/cc	gains and losses mg/cc
SiO ₂	40.6	1480	+ 840	22.8	640	---	48.7	1860	+1220
Al ₂ O ₃	17.8	650	+ 460	6.8	190	---	4.2	160	- 30
FeO*	2.2	80	+ 20	2.0	60	---	9.9	380	+ 320
MgO	0.69	30	- 10	1.5	40	---	1.8	70	+ 30
CaO	27.1	990	- 60	37.5	1050	---	23.5	900	- 150
Na ₂ O	0.31	10	- 10	0.62	20	---	0.03	1	- 19
K ₂ O	0.24	9	- 11	0.70	20	---	0.04	1	- 19
CO ₂	2.3	80	- 690	27.5	770	---	1.3	50	- 720
H ₂ O	0.4	10	0	0.2	10	---	0.2	10	0
Totals	91.64		+539	99.62		---	89.67		+633
Gains			1320			---			1570
Losses			781			---			937
Specific Gravity		3.65			2.81			3.82	

	<u>CCIS-89</u>		
	Wt. %	mg/cc	gains and losses mg/cc
SiO ₂	40.6	1360	+ 720
Al ₂ O ₃	11.0	370	+ 180
FeO*	7.5	250	+ 190
MgO	1.7	60	+ 20
CaO	30.6	1030	- 20
Na ₂ O	0.03	1	- 19
K ₂ O	0.04	1	- 19
CO ₂	0.6	20	- 750
H ₂ O	0.5	20	+ 10
Totals	92.57		+312
Gains			1120
Losses			808
Specific Gravity		3.35	

Table 9 continued.

from the relations:

gain or loss (mg/cm^3) = Spec. Grav. X % oxide X 10
for each altered sample relative to the unaltered host. The sample chosen to represent a protolith is an impure limestone (CCLS-85). It contains the largest amount of clastic debris (visual estimation of cut surfaces and acetate peels) of the samples of limestone obtained from the Copper Chief Prospect and thin lenses of chert are also common. This sample has relatively high contents of silica, alumina, and iron oxide, and simple contact metamorphism could produce a calc-silicate bearing marble from this protolith. Samples of altered limestone with substantially higher values of SiO_2 , Al_2O_3 , and FeO^* (total iron as FeO) are unlikely to have formed without the addition of materials from outside sources. The gains and losses calculated from the samples from the Copper Chief are illustrated in Figure 44. Although the values of SiO_2 for most samples are believed to be low, all samples show increases of more than $600 \text{ mg}/\text{cm}^3$ of silica. About one-half of the samples have more alumina than CCLS-85; the others have less. Gains in FeO^* and MgO are indicated for most samples, whereas losses are indicated for CaO , Na_2O , and K_2O . The contents of CaO in two of the samples (CCLS-41, 60) are greater than that of CCLS-85 which may suggest that they were derived from

Figure 44. Histogram showing gains and losses of metacarbonates from the Copper Chief Prospect.

- a. CCSR-22
- b. CCLS-33
- c. CCLS-35
- d. CCLS-41
- e. CCLS-48
- f. CCLS-60
- g. CCLS-74
- h. CCLS-88
- i. CCLS-89

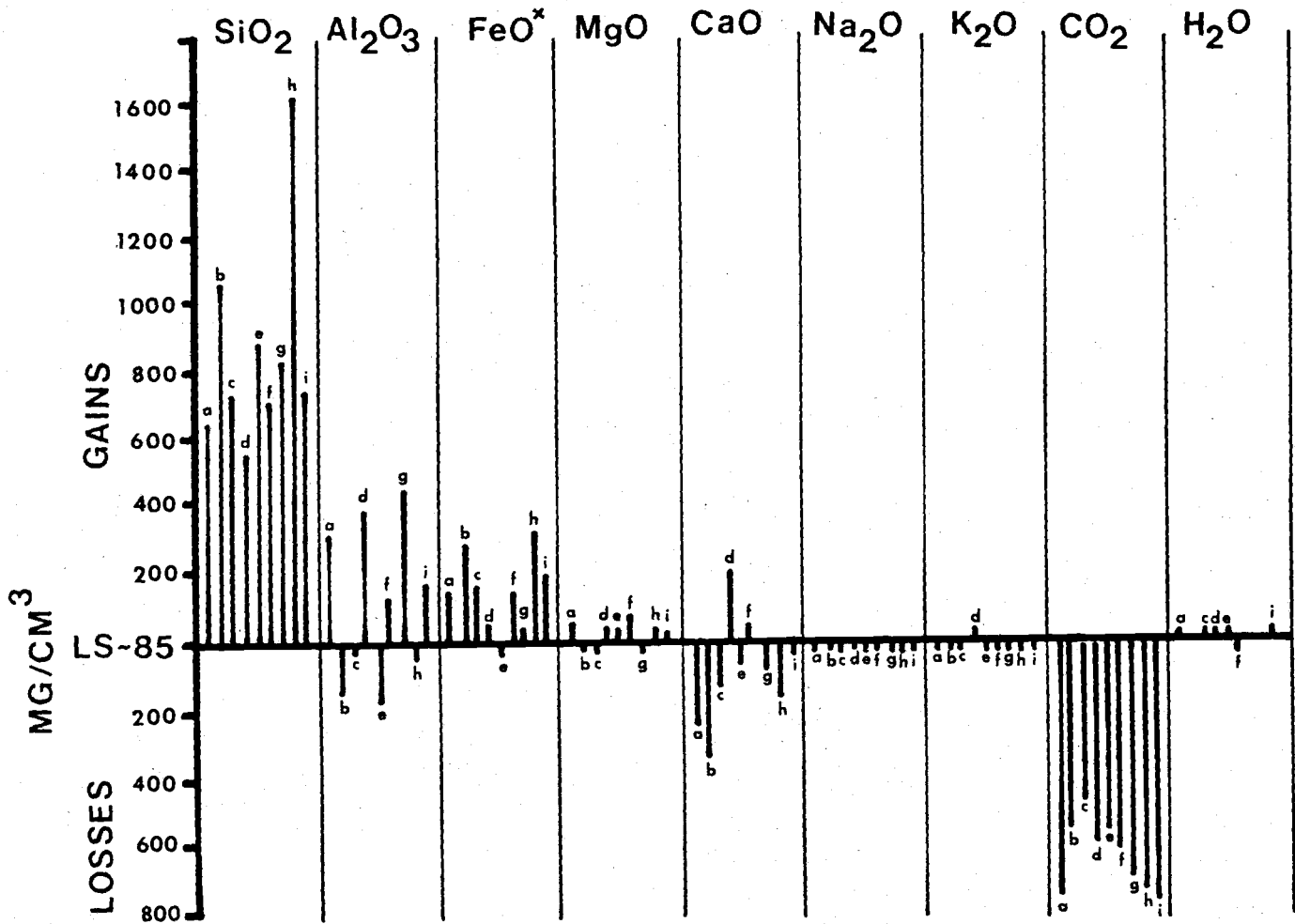


Figure 44.

a "cleaner" limestone than the assumed protolith. All samples show large losses of CO_2 .

Ratios of the major oxides have been calculated and are plotted on ACF diagrams (Fig. 45) according to the method of Hutchison (1974). All iron is assumed to be ferric because the predominant calc-silicate mineral in the samples is grandite garnet in which iron occupies trivalent sites. The specimens plot within the field of calcareous rocks (Fyfe and others, 1958). The mineral species that were determined by modal analyses of the samples are compatible with either the hornblende or pyroxene hornfels facies. Analyses were not attempted of rocks whose protoliths were compositionally dissimilar to the impure carbonate used herein as the reference standard and the mineral phases that are stable in the calcareous field of the hornblende hornfels facies are the same as those of the pyroxene hornfels facies. Nevertheless, the presence of pyroxene in the calc-silicate hornfels, and the presence of nearly monomineralic wollastonite after beds of limestone may suggest that the metamorphism and metasomatism occurred under the higher temperature conditions characteristic of the pyroxene hornfels facies.

Figure 45. Ternary ACF plots of samples of carbonate and metacarbonate rock from the Copper Chief Prospect.

- A. Compositional fields of Fyfe and others (1958)
- B. Albite-epidote hornfels facies
- C. Hornblende hornfels facies
- D. Pyroxene hornfels facies

22 - CCSR-22
33 - CCLS-33
35 - CCLS-35
41 - CCLS-41
48 - CCLS-48
60 - CCLS-60
74 - CCLS-74
88 - CCLS-88
89 - CCLS-89

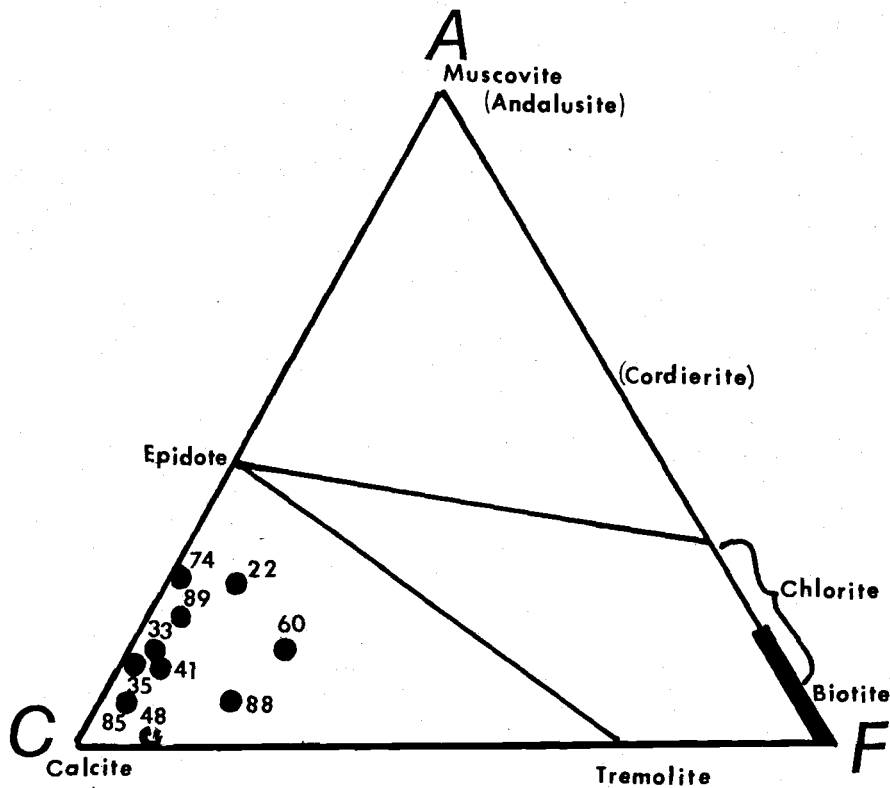
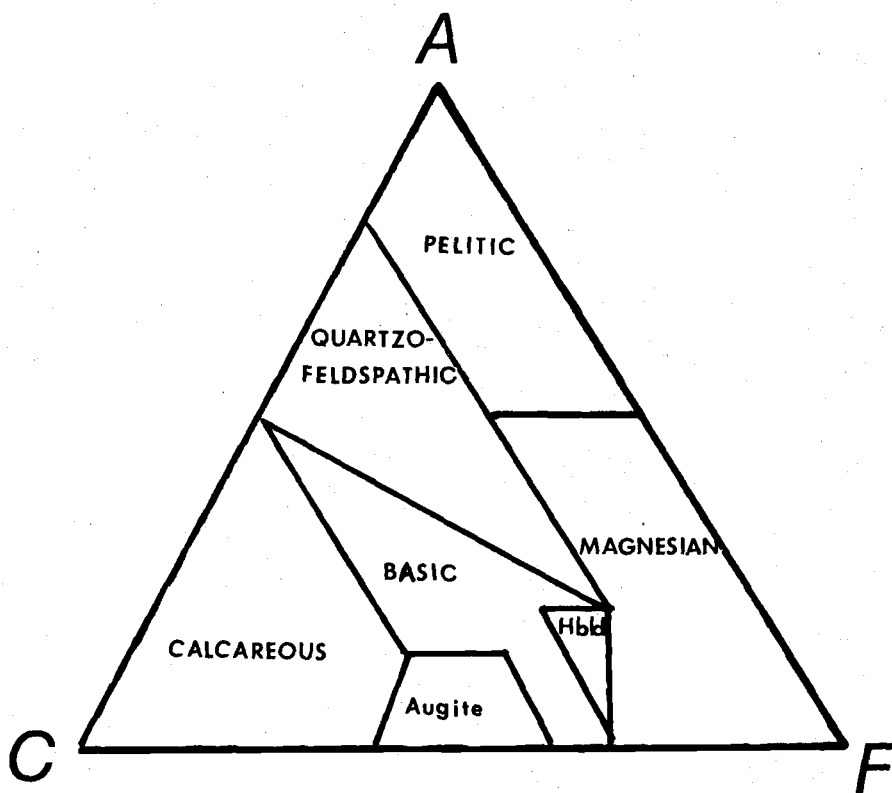


Figure 45.

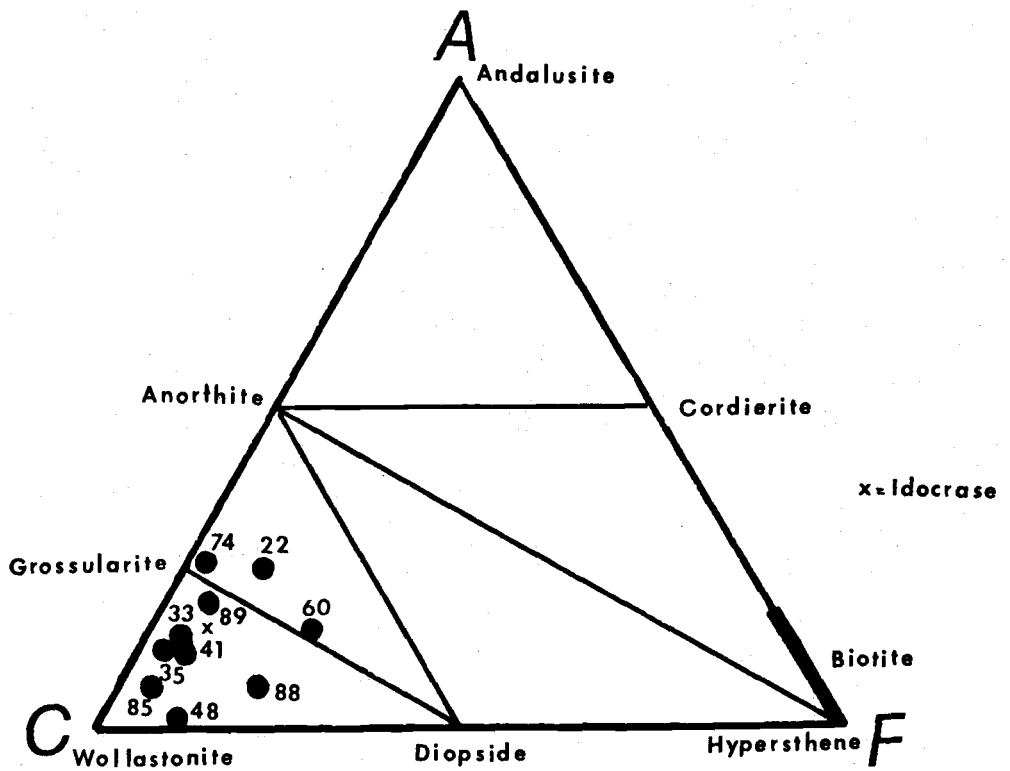
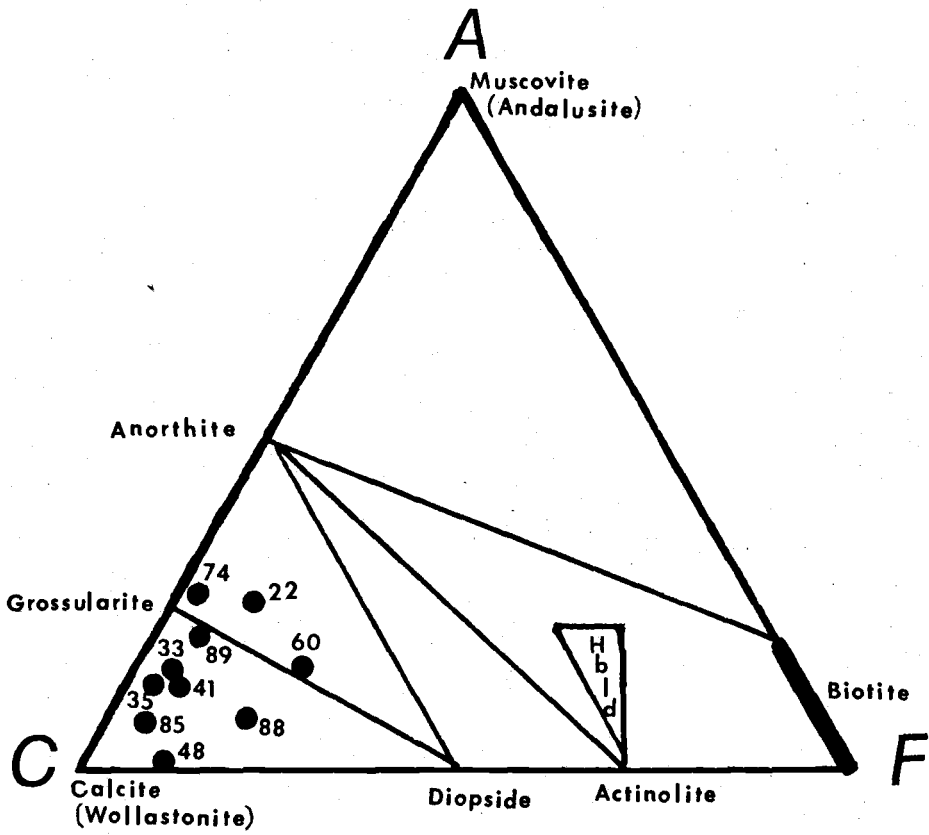


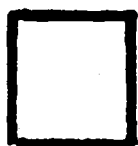
Figure 45.

VOLCANIC ROCKS

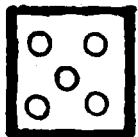
The exposures of quartz monzodiorite, sedimentary rocks of the Luning Formation, and the metamorphic and metasomatic rocks formed by the interactions between the intrusions and their hosts at the Copper Chief Prospect constitute a window in overlying volcanic flows and tuffs of Tertiary age (Fig. 46). Although the relatively great thickness and large areal extent of the volcanic rocks precluded detailed stratigraphic analysis, it was possible to distinguish several volcanic rock units in the mapped area. The units are based on field criteria supplemented by limited petrographic and chemical analyses. They include a minimum of two pyroclastic flows, one lava flow, and three units of undetermined origin.

The volcanic rocks are divided into an upper group and a lower group. The upper volcanic strata cap the plateau immediately north of the Copper Chief Prospect. A window of pre-Tertiary rocks is exposed on the relatively steep slopes below the plateau. The lower volcanic rocks and alluvium of Quaternary age overlie the pre-Tertiary rocks from the point where the slopes flatten to the south border of the prospect (Fig. 46B).

Figure 46. A. Geologic setting of the Copper Chief Prospect. Drawn from aerial photograph.
 B. Highly schematic cross-section of the Copper Chief Prospect showing generalized locations of major rock types.

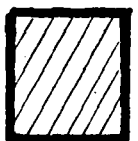


Quaternary alluvium. Includes some Tertiary volcanic rocks and exposures of the Luning Formation along the right edge of Figure 46A.



Tertiary volcanic rocks

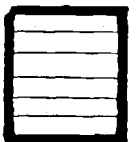
a. dacitic andesites



b. other volcanic rocks



Quartz monzodiorite



Triassic Luning Formation

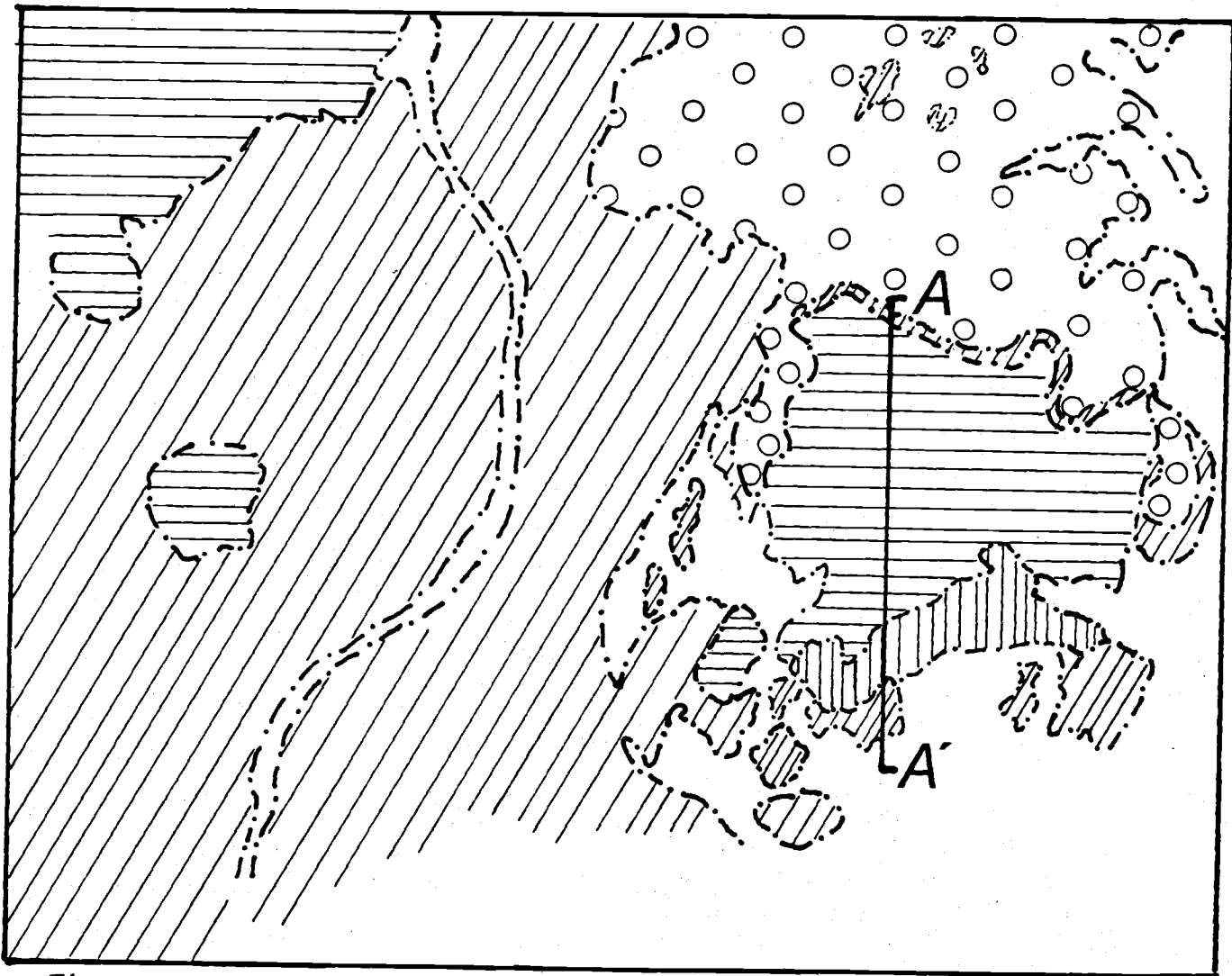


Figure 46 A.

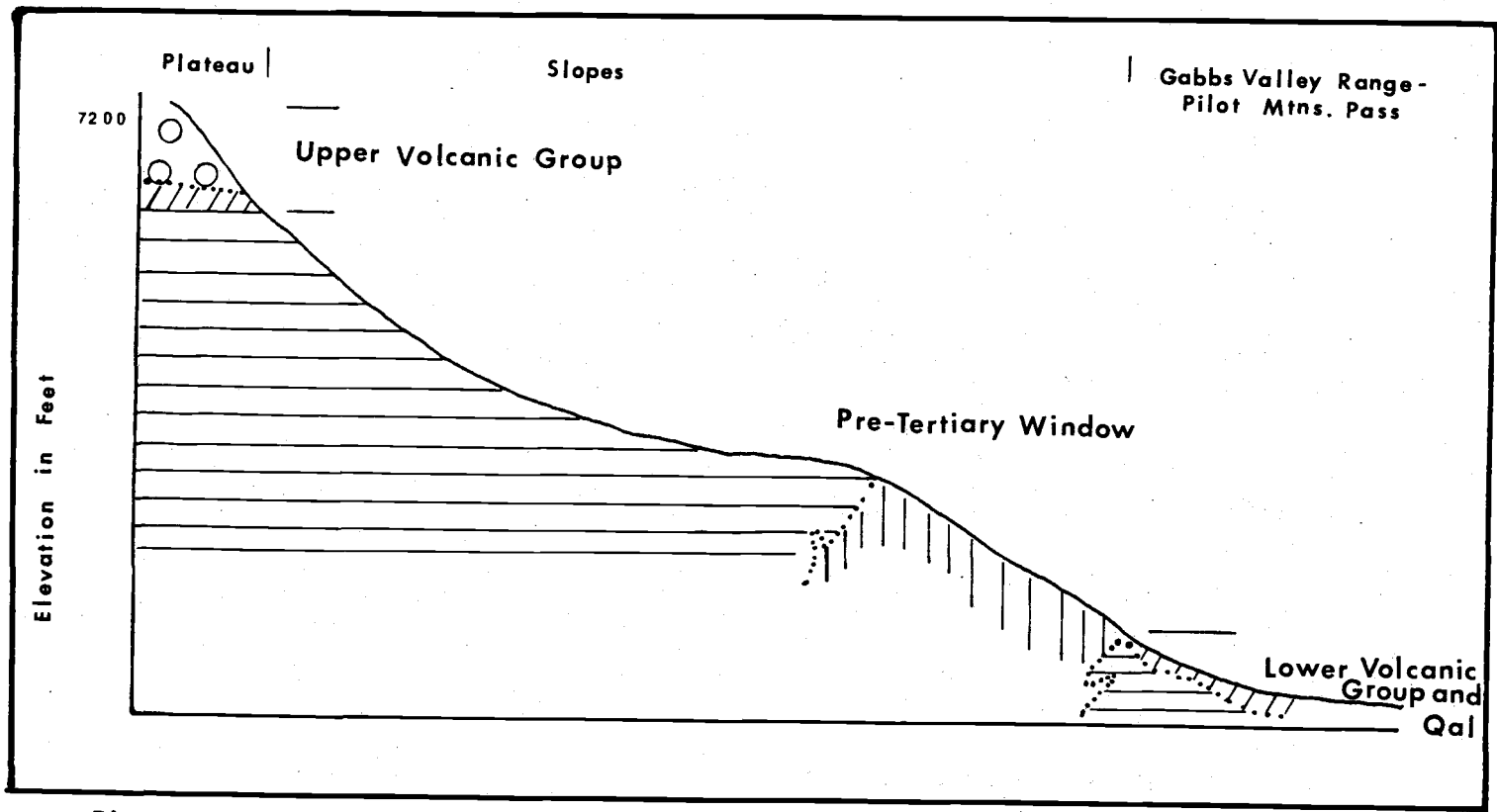


Figure 46B.

Lower Volcanic Group

The lower group of volcanic rocks consists of three units: a basal pyroclastic flow unit, a middle unit of aphanitic porphyritic volcanic rocks, and an upper unit characterized by phenocrysts of hornblende and plagioclase feldspar (Fig. 47).

The basal pyroclastic unit rests non-conformably on quartz monzodiorite (Fig. 48). The unit is characterized by the presence of lithic fragments, pumice lapilli, and phenocrysts of quartz up to two to three millimeters in size. The rocks of this unit are crystal vitric tuffs according to the compositional classification of Cook (1965). The lithic fragments consist of crystals of plagioclase feldspar in an aphanitic groundmass. Petrographically, these pyroclastic rocks contain rounded and broken crystals of quartz and potassium feldspar, devitrified glass shards and pumice fragments, lithic fragments, and an opaque mineral (Fig. 49). Sparse crystals of biotite have been partly replaced by chlorite. Chemical analyses of two splits of one sample of this tuff are given in Table 10. The rocks are rhyolites according to the classifications of Streckeisen (1979) and Middlemost (1980). The IUGS classification of volcanic rocks (Streckeisen, 1979) is compared to the analyses in

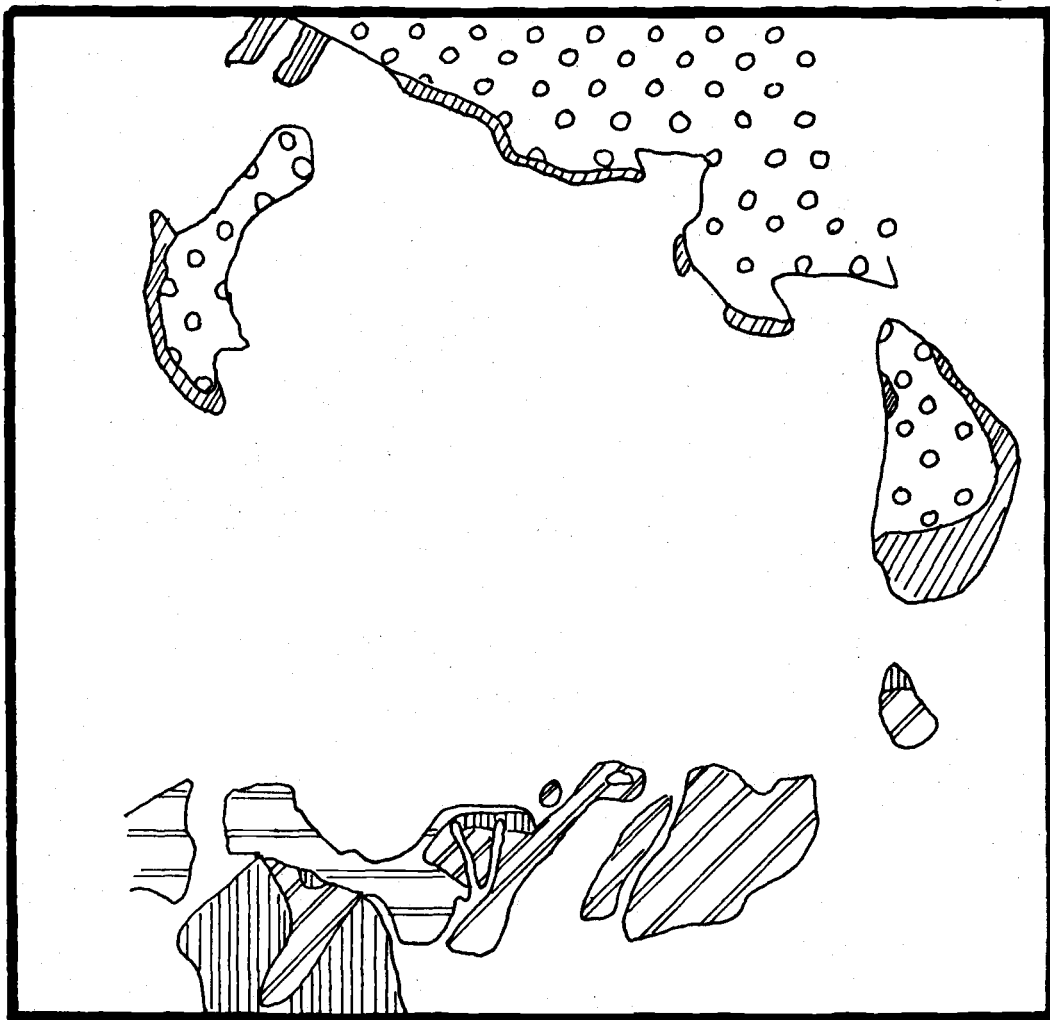


Figure 47. Distribution of volcanic rocks at the Copper Chief Prospect.

Upper Volcanic Group



Upper unit



Middle unit



Lower unit

Lower Volcanic Group



Upper unit



Middle unit



Lower unit



Figure 48. Quartz monzodiorite (left) non-conformably overlain by pyroclastic tuff (right).



Figure 49. Photomicrograph of basal pyroclastic unit of lower volcanic group. The field of view is approximately three millimeters.

	<u>CCVT-2A¹</u>	<u>CCVT-2b²</u>	<u>CCV-9</u>
SiO ₂	76.7	78.3	62.8
TiO ₂	0.16	0.19	0.60
Al ₂ O ₃	12.1	12.2	16.9
Fe ₂ O ₃ *	1.58	1.58	5.42
MgO	0.30	0.28	1.43
MnO	0.01	0.22	0.11
CaO	0.83	0.80	4.91
Na ₂ O	1.86	- -	4.46
K ₂ O	5.16	5.17	2.13
P ₂ O ₅	0.02	0.02	0.29
	<hr/>	<hr/>	<hr/>
Totals	98.7	98.8	99.1

1,2 Two splits of sample CCVT-2, the basal pyroclastic unit of the lower volcanic group.

CCV-9 is the upper unit of the upper volcanic group.

Fe₂O₃* is total iron reported as Fe₂O₃.

Table 10. Chemical analyses and normative mineralogy of volcanic rocks from the Copper Chief Prospect.

	<u>CCVT-2a</u>	<u>CCVT-2b</u>	<u>CCV-9</u>
Qz	44.2	44.8	16.1
Or	30.9	30.4	12.8
Ab	16.0	15.7	38.2
An	4.04	3.82	20.1
Wo	0.00	0.00	1.13
En	0.76	0.69	3.61
Fs	1.00	1.32	3.51
Mt	0.81	0.79	2.79
Il	0.31	0.36	1.15
Ap	0.05	0.05	0.70
Cor	1.91	2.15	0.00
Totals	99.99	100.1	100.1
$\frac{(K_2O+Na_2O)}{(CaO+K_2O+Na_2O)}$	0.89	0.90	0.57

Table 10 continued.

Figure 50.

The middle unit consists of rocks that contain small phenocrysts of feldspar (less than 1 mm) in a light colored groundmass. In thin section, rectangular crystals of plagioclase feldspar are accompanied by lath-shaped feldspar microlites (Fig. 51). In addition to feldspar, rocks of this unit contain very fine-grained (less than 0.01 mm) granular glass, sparse crystals of hornblende, and an opaque mineral.

Overlying the middle unit are volcanic rocks that contain abundant phenocrysts of hornblende. The dark colored hornblende and white feldspar crystals are in a groundmass that varies from lavender to lavender brown in color. Locally these rocks contain very fine-grained lithic fragments. The lithic fragments are as large as 3 cm, and consist of vesicular volcanic rocks. The groundmass includes microlites of plagioclase feldspar, granular glass, and an opaque mineral (Fig. 52). The pyroclastic origin of the basal unit is evidenced by the presence of pumice lapilli, glass shards, and rounded and broken phenocrysts; the lack of sorting in this unit suggests that it was deposited from an ash flow. The upper two units of the lower volcanic group, however, may have been deposited either from an ash flow or from a lava flow. They

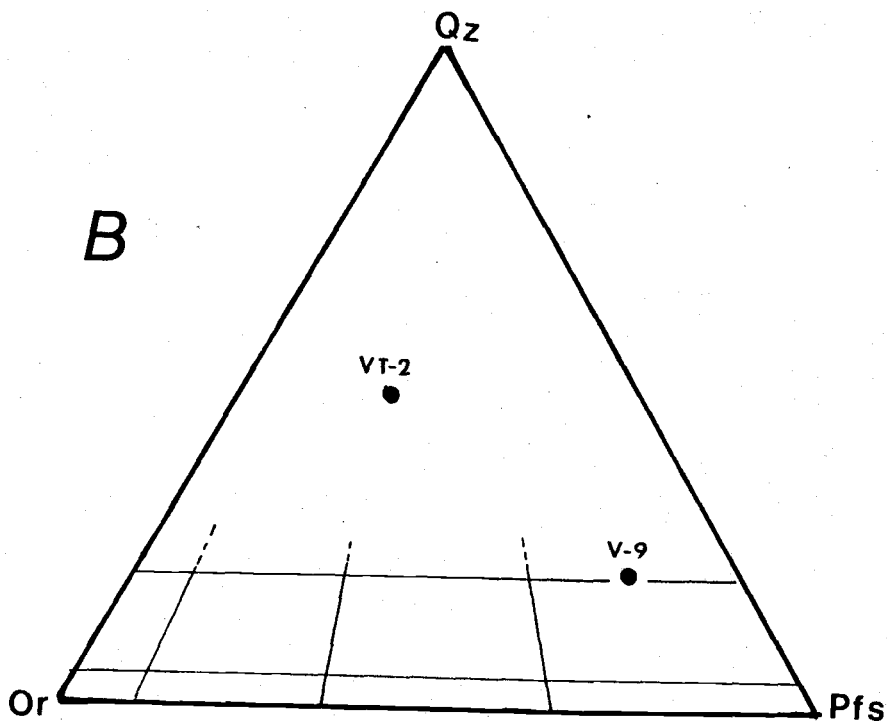
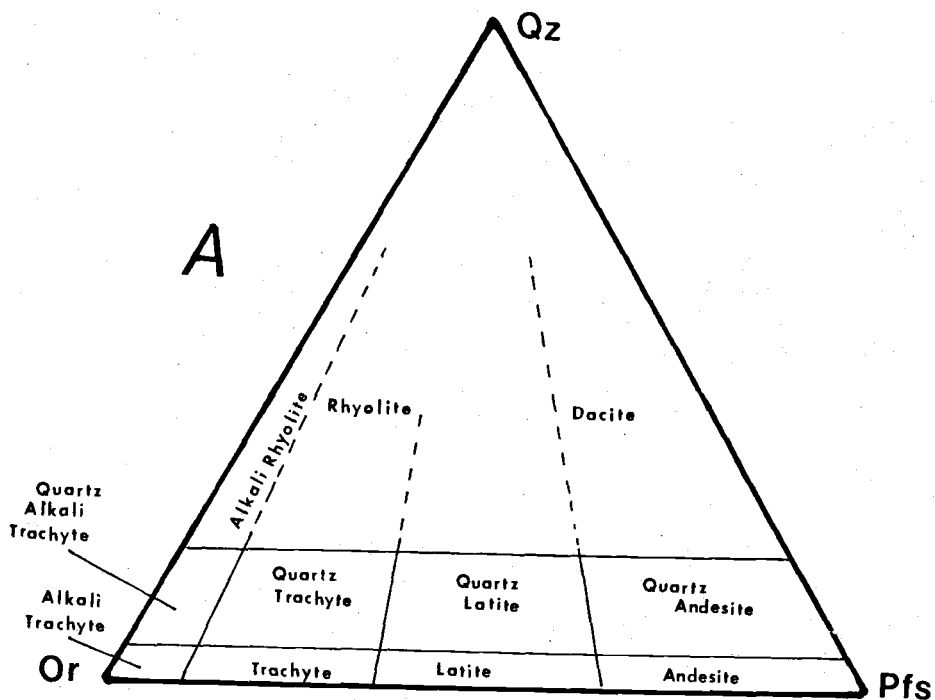


Figure 50. Ternary Qz-Or-Pfs plot of: A) IUGS classification of volcanic rocks of silicic to intermediate composition; and B. volcanic rock samples from the Copper Chief Prospect.

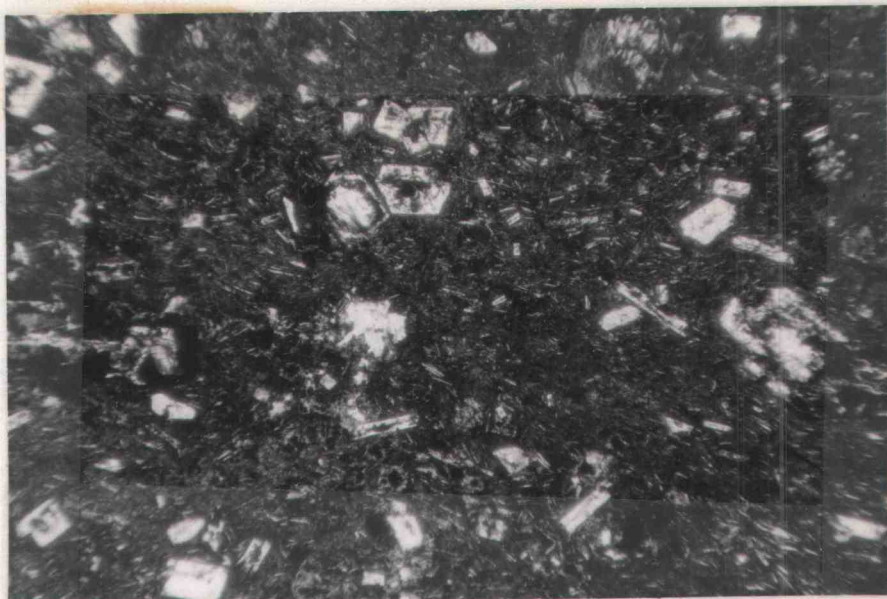


Figure 51. Photomicrograph of the middle unit of the lower volcanic group. The field of view is approximately three millimeters.

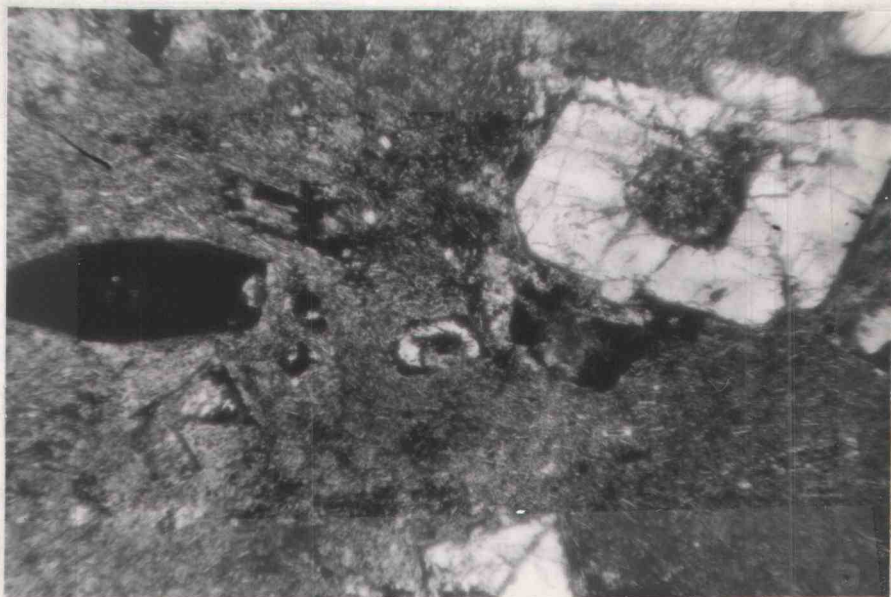


Figure 52. Photomicrograph of the upper unit of the lower volcanic group. The field of view is approximately three millimeters.

may represent separate events, or may have been formed by the same event. Although these two units were subdivided on the basis of field criteria, thin section examinations of both lithologies have indicated similar mineral assemblages and textures.

Upper Volcanic Group

The upper volcanic group also consists of three units: a lower unit rich in phenocrysts of hornblende and feldspar, a middle pyroclastic unit, and an upper lava flow.

The lower unit is included with the middle unit on the geologic map (Plate 1) and in Figure 47. The contact between these two units was not observed. The lower unit consists of light gray and lavender volcanic lithologies which are speckled by phenocrysts of dark colored hornblende and white feldspar. Because of similar lithologies, mineralogies, and textures, these rocks may be part of the same flow as the upper unit(s) of the lower volcanic group.

The middle unit is a leucocratic potassium feldspar and quartz crystal vitric tuff. It contains dark and light colored lithic fragments. Pumice lapilli are locally abundant. The groundmass consists of arcuate polygonal shards of glass, granular ash, and an opaque mineral (Fig. 53). Devitrification of glass shards and

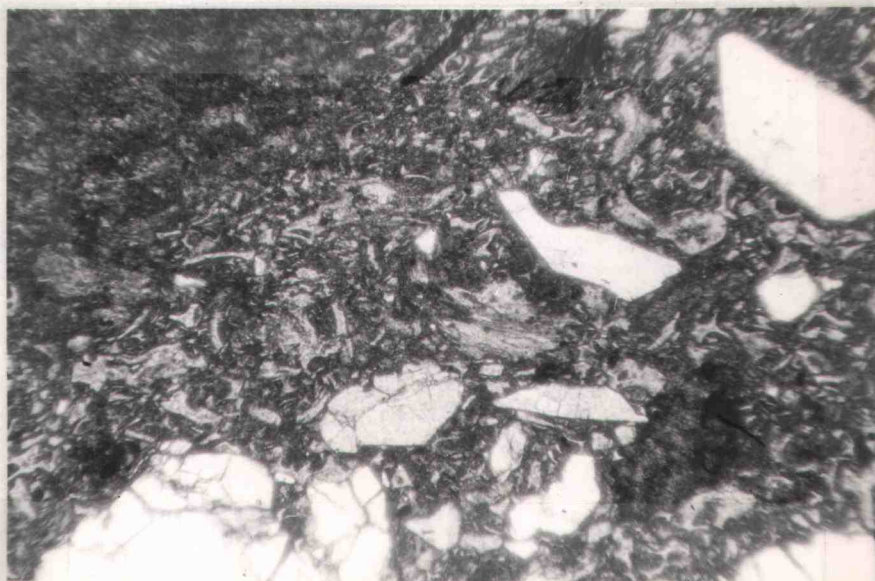


Figure 53. Photomicrograph of the middle unit of the upper volcanic group. The field of view is approximately three millimeters.

pumice lapilli is minor in these rocks as contrasted to the lower volcanic group. The crystals of quartz and potassium feldspar are rounded and some are embayed. Sparse ragged anhedral and subhedral crystals of biotite are present. The occurrence of pumice lapilli and glass shards, and the unsorted nature of the rocks suggest that they were deposited from a pyroclastic ash flow.

The upper unit caps the volcanic section and the plateau immediately north of the Copper Chief Prospect. It grades upward from platy medium gray (weathering to brown) to massive black outcrops. The platy fractures at the base of the flow may have been controlled by the orientation of collapsed vesicles. A flow foot breccia is present at one location in the basal part of the unit. Thin sections of this unit display a remarkably uniform mineralogy and texture. The rocks consist predominantly of lath-shaped crystals of plagioclase feldspar and dark colored volcanic glass. The feldspars are aligned to form a trachytic, or flow, texture (Fig. 54). A fine-grained opaque mineral was also observed in the thin sections. The abundances of normative quartz, orthoclase, and plagioclase calculated from a chemical analysis of this unit plot near the line that divides dacite from quartz andesite according to the classification of Middlemost (1980).

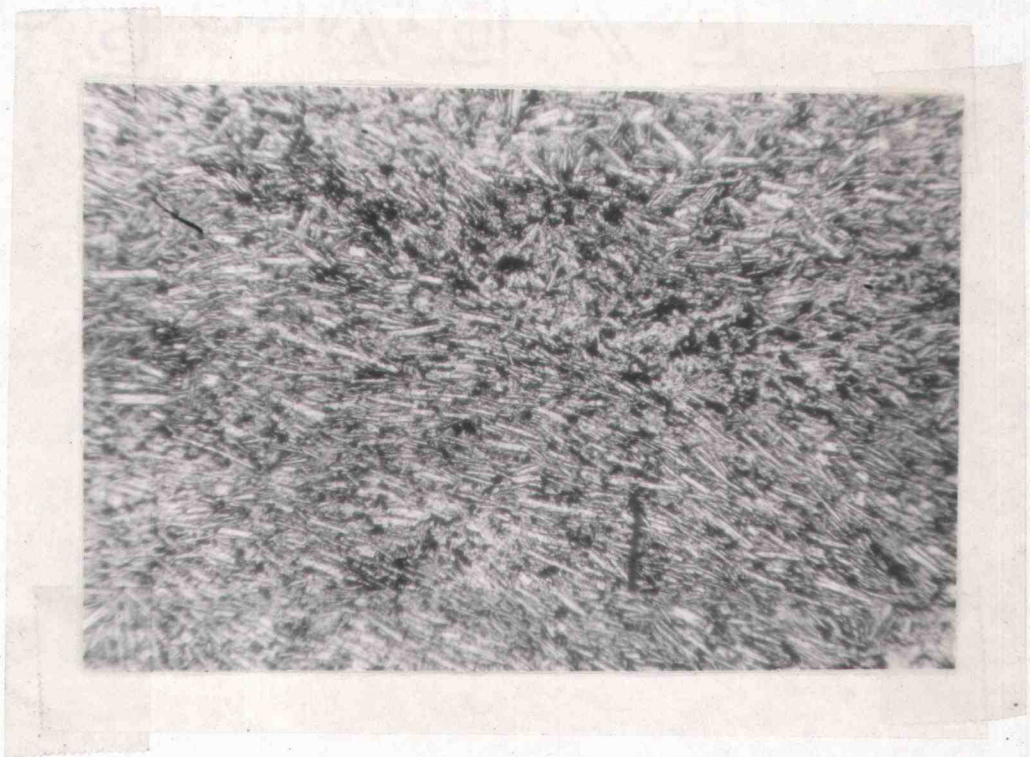


Figure 54. Photomicrograph of the upper unit of the upper volcanic group. The field of view is approximately three millimeters.

ECONOMIC GEOLOGY

The Copper Chief Prospect is a limy skarn deposit of the scheelite-sulfide subtype according to the classification of Zharikov (1968). The ore minerals were deposited during the late stages of skarn formation, and by the replacement of calc-silicate rocks and marbles by retrograde minerals after the skarns had formed.

Numerous small excavations pock the surface of the Copper Chief Prospect. Most of these shafts, inclined shafts, and adits have only been developed to depths of a few feet. However, some were extended to considerably greater depths, although most of these workings are now largely inaccessible.

Mineralogy

Tungsten ore has been mined from one shaft and associated slit trenches at the Copper Chief Prospect. The ore mineral is scheelite (CaWO_4). It is commonly associated with powellite (CaMoO_4). These two minerals are the end-members of a solid solution series, and are distinguished by their characteristic fluorescence colors when viewed in ultra-violet light. The scheelite occurs as disseminated millimeter-scale grains and as centimeter-scale platelets in

clinopyroxene-rich garnetite. The larger grains may have precipitated with garnet in veinlets (Fig. 55A). The distribution of powellite is the same as that of scheelite, but the mineral is less abundant. Textural relations between the two minerals suggest that powellite has exsolved from, or replaced, the scheelite.

Chalcopyrite is present in sparse amounts at several waste dumps. The mineral occurs in veinlets and as blebs in the interstices of andradite garnetite, and as pod-shaped nodules in calc-silicate rocks and marble. The nodules are often enclosed in crusts or diffuse "fogs" of blue or green supergene minerals (Fig. 55B&C).

Pyrite is present in diamond drill core samples of marble, hornfels, calc-silicate rocks, and quartz monzodiorite. It occurs as millimeter sized cubes which are disseminated throughout the samples or are localized along veinlets. Limonite has formed by the pseudomorphic replacement of pyrite in surface exposures of marble, hornfels, calc-silicate rock, skarn, and quartz monzodiorite. The pyrite and limonite that are contained in veinlets are commonly enclosed in drusy quartz.

The most abundant and widespread of the ore minerals at the Copper Chief Prospect are blue and

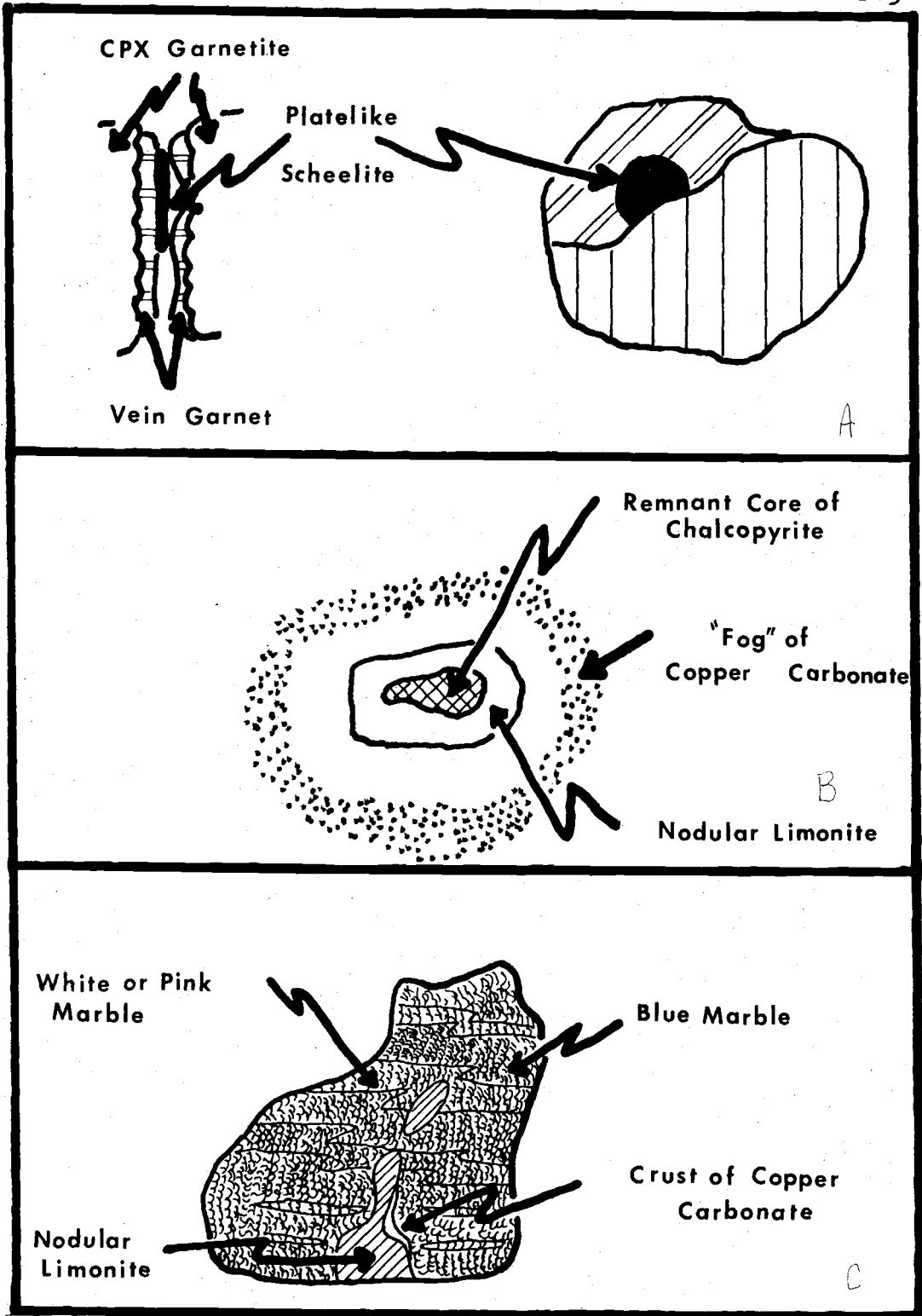


Figure 55. Textural relations of ore minerals.

green carbonates, sulfates, and silicates of copper. These minerals have formed by the supergene oxidation of chalcopyrite, and possibly chalcocite, by solutions carrying sulfuric acid. The acid was produced by the decomposition of pyrite to limonite by interactions with waters of the near surface environment.

Hand-picked stockpiles of the supergene copper minerals are present on waste dumps throughout the central and northwest sections of the prospect. These secondary minerals occur as fogs around nodules of pitchy limonite; as smeary, amorphous encrustations on calc-silicate rocks, hornfels, and marble; as a cement-like component of fault gouge; and as discrete crystals associated with andradite garnetite.

White, amorphous and botryoidal crusts of hemimorphite (calamine) are present on samples of skarn and copper "carbonate". Blocky, black chalcocite was found in trace amounts at two locations in the central part of the prospect. Yellowish-orange wulfenite was found in a sample of quartz monzodiorite on one waste dump.

Veins of bull quartz cut metasedimentary rock and quartz monzodiorite at several locations within the area of the Copper Chief Prospect. The veins range from a few inches to more than a yard in width. A quartz vein at one location grades into garnetite.

Textural relations suggest that this vein formed by the retrograde replacement of the garnetite by quartz and calcite. The replacement of the garnetite was accompanied by the precipitation of sulfide minerals. Limonites after pyrite and chalcopryrite are locally abundant within the vein and garnetite immediately adjacent to it.

Trace Element Chemistry

Rock chip samples from 213 locations within the Copper Chief Prospect were analyzed to determine the abundances of Cu, Zn, Mo, WO_3 , Au, and Ag. The analytical results are summarized in Table 11. The highest concentrations for each of these elements are in specimens of carbonate and metacarbonate rocks and veins of quartz.

The abundances of trace elements in lithologic units have been shown, in many cases, to follow log-normal rather than normal distribution laws (Ahrens, 1957) If the concentrations of these elements are plotted against sample frequencies, populations of samples with normal distributions define bell-shaped curves in histograms with arithmetic ordinates, whereas those with log-normal distributions define skewed curves with logarithmic ordinates (Fig. 56). These curves are converted to straight lines by

<u>HYDRIFELS</u>			<u>CARBONATE AND METACARBONATE ROCKS</u>				<u>WASTE DUMPS</u>			
	<u>min.</u>	<u>max.</u>	<u>min.</u>	<u>max.</u>	<u>background threshold</u>		<u>min.</u>	<u>max.</u>		
Cu	30	330	Cu	10	35800	85	35	Cu	290	36200
Zn	20	1900	Zn	15	48200	85	120	Zn	150	11800
Mo	1	39	Mo	<1	185			Mo	<1	262
WO ₃	<5	10	WO ₃	<5	125			WO ₃	10	1100
Ag	<1	2	Ag	<1	122	<1	3	Ag	<1	365
Au	<0.1		Au	<0.1	6			Au	<0.1	0.4
		17 Samples			88 Samples					15 Samples
<u>VOLCANIC ROCKS</u>			<u>PLUTONIC ROCKS</u>				<u>QUARTZ VEINS</u>			
	<u>min.</u>	<u>max.</u>				<u>background</u>	<u>Threshold</u>			
Cu	10	50	Cu	15	7900	120	250	Cu	60	8600
Zn	20	85	Zn	15	12400	45	80	Zn	70	23500
Mo	1	8	Mo	<1	17			Mo	1	296
WO ₃	<5	15	WO ₃	<5	30			WO ₃	10	160
Ag	<1	1	Ag	<1	12			Ag	<1	330
Au	<0.1		Au	<0.1				Au	<0.1	1.2
		13 Samples			56 Samples					10 Samples

Table 11. Maximum and minimum concentrations of trace elements in rocks of the Copper Chief Prospect.

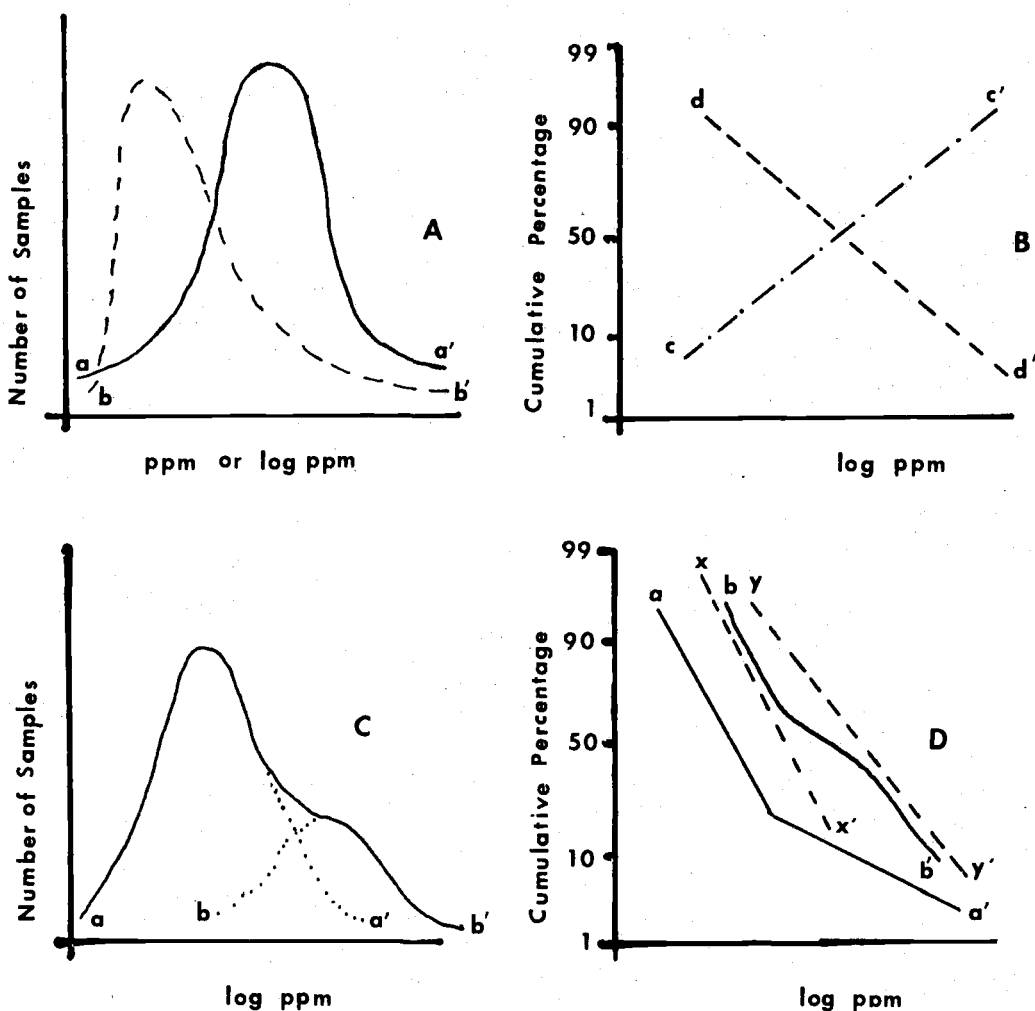


Figure 56. Plots of trace element distributions.

- Normal distribution (a-a', arithmetic ordinate). Log-normal distribution (b-b', logarithmic ordinate)
- Log-probability plots with cumulative frequency calculated from low to high values (c-c') and from high to low values (d-d').
- Data set consisting of two populations with different geometric means.
- Log-probability plots of a population that includes an excessive number of samples with high values (a-a') and of a data set (b-b') consisting of two populations (x-x' and y-y').

replacing sample frequency by cumulate frequency in probability units (Tennant and White, 1959; LePeltier, 1969; and Sinclair, 1977). The shapes of curves in histograms and probability plots can be affected by the inclusion of excessively large numbers of samples with high, or low, values in a population, or by the presence of more than one population of samples in a set of data (Fig. 56). The statistical parameters that can be read directly from log-probability plots include the geometric mean (background) and the standard deviation of the population, and the value (threshold) above which samples are considered to contain anomalously high concentrations of the metals.

The abundances of copper and zinc in samples of carbonate, metacarbonate, and plutonic rocks from the Copper Chief Prospect are shown in histograms and log-probability plots in Figures 57 and 58. An excessively large number of samples with anomalously high metal concentrations is clearly indicated for the carbonate and metacarbonate suite of samples. In contrast, the plutonic rocks exhibit nearly log-normal behavior with only a weakly defined anomalous population. These chemical distributions agree well with field observations; the copper and zinc minerals are more abundant in carbonate and metacarbonate rocks and less abundant in plutonic rocks of the Copper Chief.

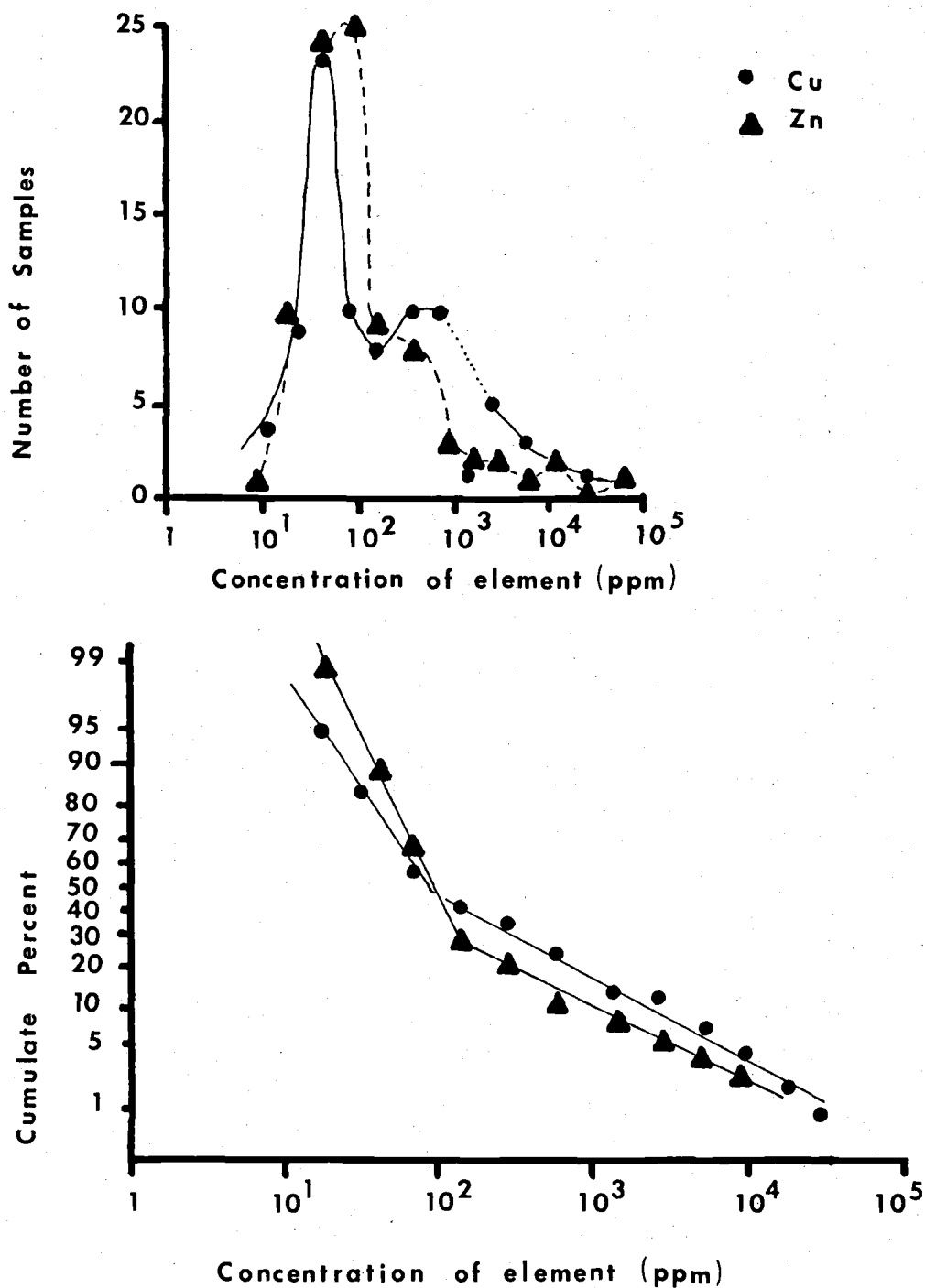


Figure 57. Histogram and log-probability plots of copper and zinc concentrations in samples of carbonate and metacarbonate rocks from the Copper Chief Prospect.

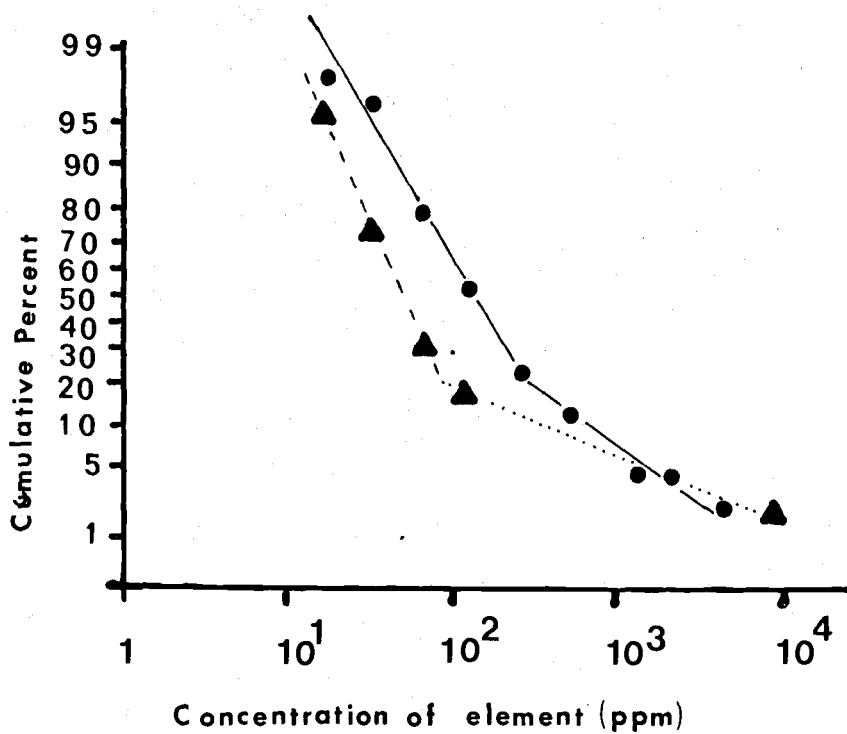
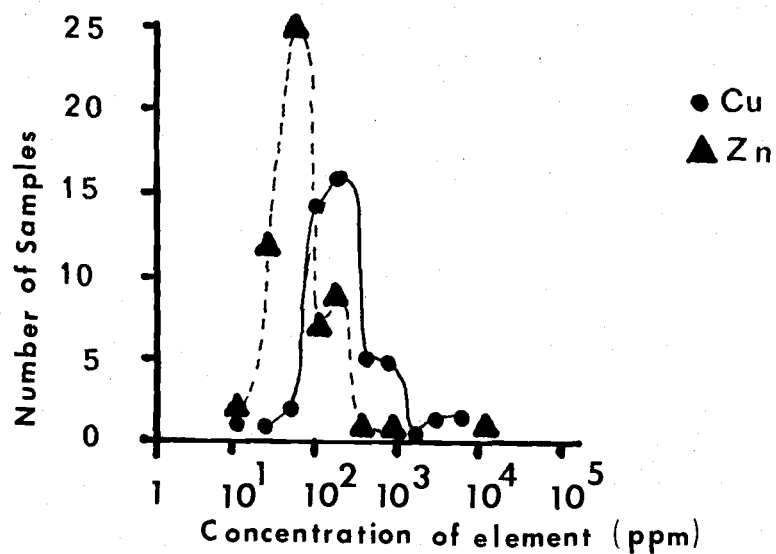


Figure 58. Histogram and log-probability plots of copper and zinc concentrations in samples of plutonic rocks from the Copper Chief Prospect.

STRUCTURE

The attitudes of sedimentary and relict bedding in unaltered and altered units of the Luning Formation in the northwest and central sections of the Copper Chief Prospect are shown in stereographic projections (Fig. 59) and in map view (Fig. 60). Limestones, marbles, calc-silicate rocks, and quartzites in the west-central part of the prospect strike about N. 30-40° E. and dip moderately steeply to the west. The sedimentary and metasedimentary rocks of the northwest section and the north-central part of the prospect also strike mostly N. 30-40° E., but dip steeply (60-90°) to both the east and the west. Relict bedding in the exposures of metasedimentary rocks of the east-central part of the prospect strikes from N. 60° E. to N. 80° E. and dips (1) at steep angles (70-90° W.) near the overlying ridge-capping volcanic rocks, and (2) at shallow angles (20-40° W.) near the largest body of quartz monzodiorite. The changes of attitudes between these four structural domains are abrupt and occur in a zone that parallels the main north-south access road to the property (Plate 1). This zone is the locus of many high and low-angle faults. The faults and associated disruption of bedding attitudes may have occurred (1) entirely prior to plutonism and thereby providing channels

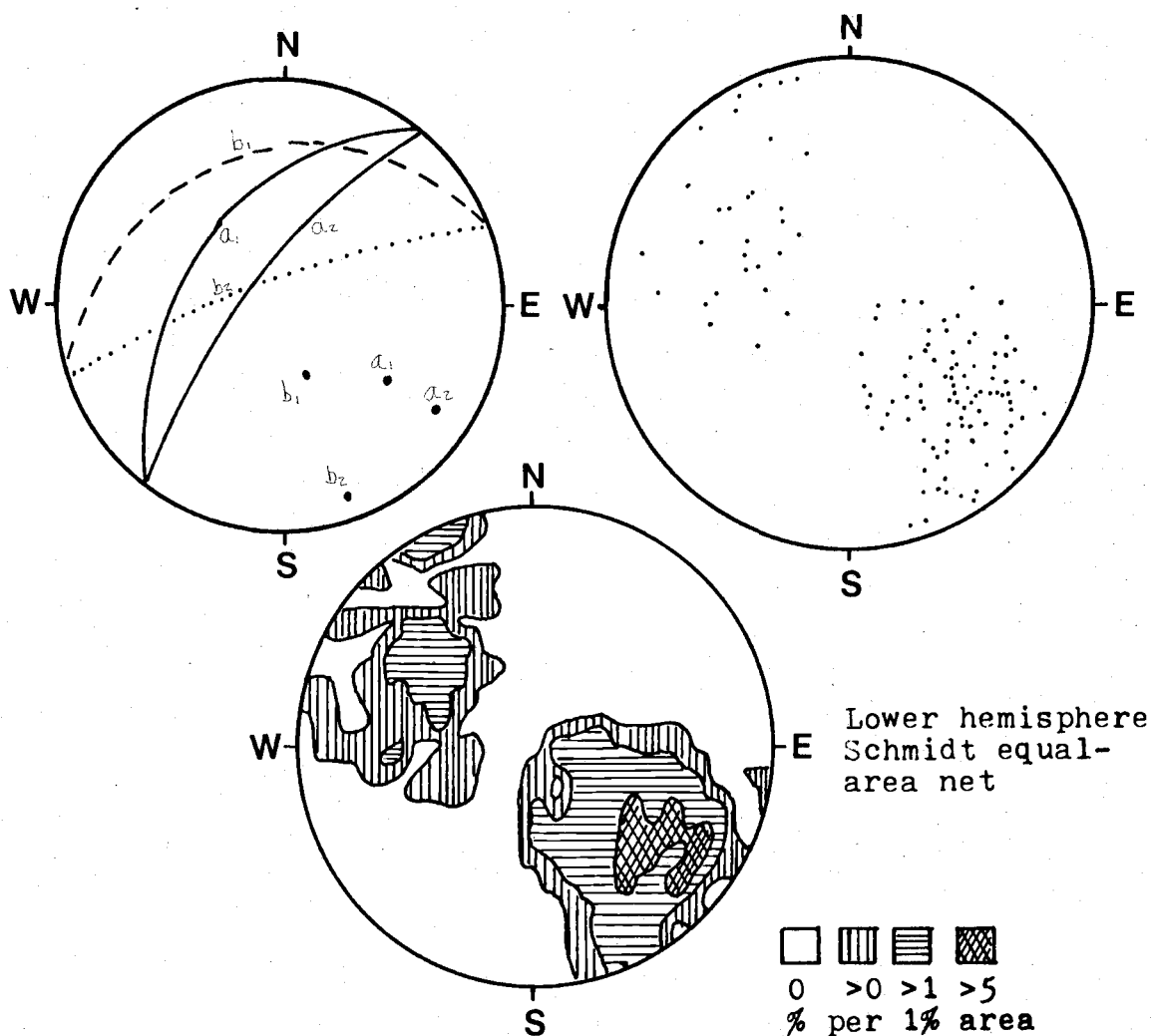


Figure 59. Stereographic projections of sedimentary and relict sedimentary bedding data from exposures of the Luning in the northwest and central sections of the Copper Chief Prospect.

- A. Representative bedding attitudes of the structural domains discussed in text
- a_1 west-central section
 a_2 north-central and northwest sections
 b_1 northeast-central section
 b_2 southeast-central section
- B. Poles to planes of sedimentary and relict bedding (115 locations)
- C. Contoured plot of poles to planes of bedding.

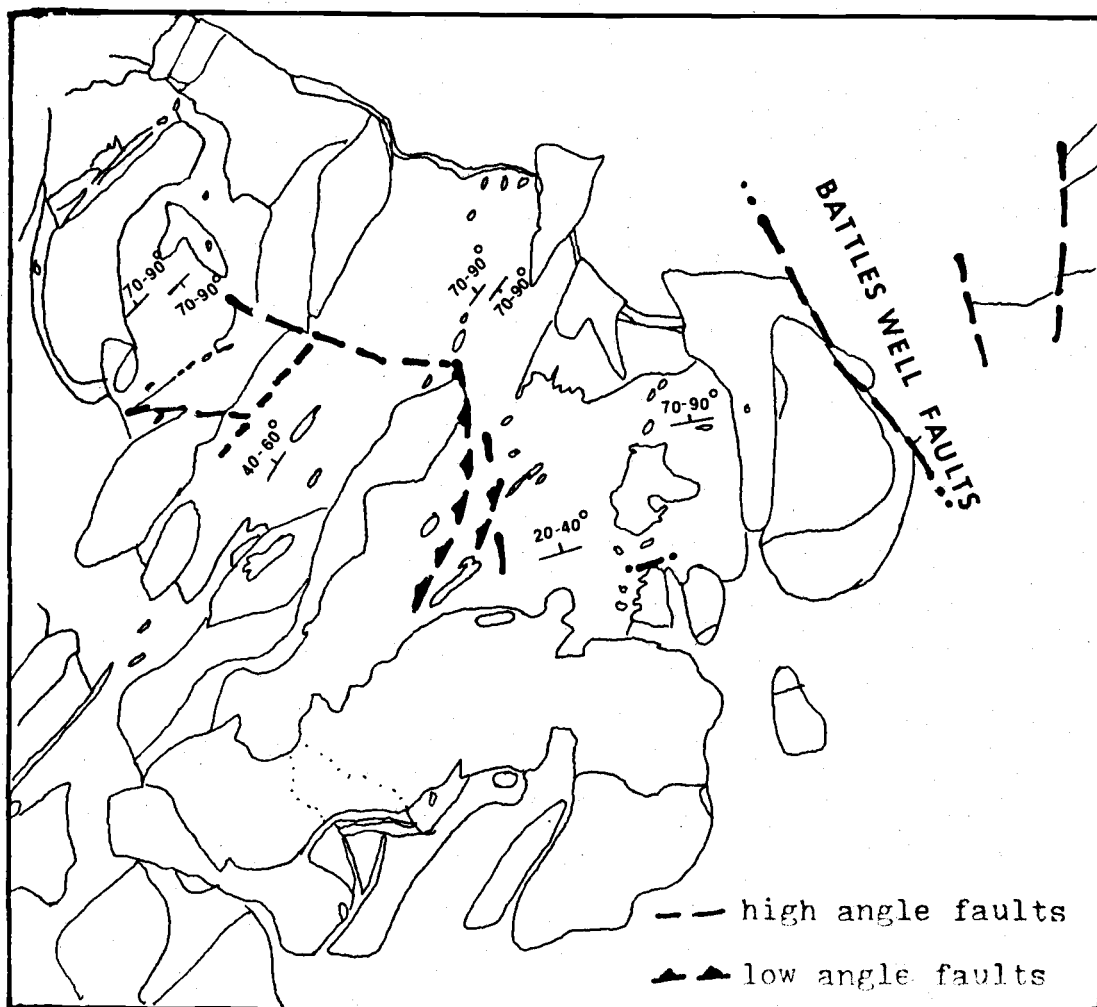


Figure 60. Highly schematic map view of the Copper Chief Prospect showing structural features.

for the intrusion of magma, (2) in response to magmatism, or (3) by a combination of pre-intrusive and syn-intrusive processes possibly modified by post-hydrothermal stage tectonism.

High and low-angle faults in the central and northwest parts of the Copper Chief Prospect trend to the north, northeast, and east-west. The faults represent more than one period of structural activity. A fault in the central part of the prospect contains fragments of garnetite breccia in a healed gouge of white marble and the displacement clearly postdates the formation of the garnets. Other faults are filled with quartz and, therefore, were active prior to the formation of the quartz veins during the retrograde stages of skarn formation.

Exposures of the limestones, shales, and quartzites of the Luning Formation in the northeast section of the Copper Chief Prospect are separated from those of the other sections by northwest and north-northwest trending faults. These faults constitute a part of the Battles Well Strand of the Walker Lane. Right lateral strike-displacement has occurred on these faults. They are visible on aerial photographs as linear drainages that cut across the sedimentary rocks of the Luning Formation and the overlying volcanic rocks of Tertiary age. Abrupt terminations of sedimentary bedding

coincide with lineations that are readily observed on these photographs.

GEOLOGIC SUMMARY

The geologic record at the Copper Chief Prospect begins in the Triassic Period with the deposition and lithification of the sedimentary rocks of the Luning Formation. These shales, limestones, and orthoquartzites were deposited in the near-shore to upper delta-plain environments of the Cordilleran arc-trench setting. Subsequent to lithification, the sedimentary rocks were invaded by magma of intermediate composition. The shales were converted to hornfels, and limestones to marble, by contact metamorphism in the thermal halos of the intrusions. Fluids emanating from the intrusions, either at the level of emplacement or at depth, carried mobile components that reacted with the inert components of the plutonic rocks and their hosts to form calc-silicate and ore minerals. The plutonic, metamorphic, and unaltered sedimentary rocks were uplifted and eroded following the formation of the skarn. Lava flows and pyroclastic rocks were deposited on this erosional surface during Tertiary time. Strike-slip faults of the Walker Lane Fault System cut the Tertiary and pre-Tertiary rocks.

Fossiliferous limestones are almost entirely restricted to the exposures of the northeast section of the Copper Chief Prospect. One exception is a

fossil-bearing exposure of limestone between the northwest and central sections of the prospect (CCLS-85). Fossils collected from the northeast part of the prospect are similar to those reported by the U.S. Geological Survey from the lower member of the Luning Formation. The strata that contain the fossils are comprised predominantly of shale with lesser amounts of interbedded limestone. The lithologic characteristics suggest a middle Luning age according to the tripartite division of the formation by Muller and Ferguson (1939). The apparent contradiction in age between evidence based on fossil assemblages and that based on lithology may reflect lateral changes of facies between the areas of deposition of the type section and those exposed at the Copper Chief Prospect. Because the fossil-bearing strata are physically separated by faults from the sedimentary rocks that have been intruded by the plutonic bodies, direct correlation of stratigraphic units is impossible. However, the similarity of the lithologic units and their relative abundances suggest that the strata in these two areas may represent the same part of the Luning Formation.

The magma that invaded the Luning Formation was quartz monzodioritic (modal analyses) to granodioritic (chemical analyses) in composition. The molten material

solidified to form sills, dikes, and stocks. Emplacement of the magma appears to have been controlled by the wedging aside of the sedimentary layers; but pre-existing zones of weakness, such as faults, may have provided channels for the intrusion of magma. The unaltered exposures of the intrusions consist predominantly of phenocrysts of plagioclase feldspar in a groundmass of potassium feldspar and quartz. The ferromagnesian minerals consist of hornblende and biotite, and accessory minerals include magnetite, sphene, and apatite that are present in trace amounts. Variations in the chemical data for intrusive rocks plotted on binary Harker diagrams and on ternary diagrams exhibit similarities to those of igneous rocks of the east Sierra Nevada Range, and it should be noted that the Copper Chief Prospect lies within the boundaries of the Sierra Nevada Batholith. The alteration of the intrusions during the stage of skarn formation resulted in two varieties of endoskarms:

- 1) low alkalinity endoskarn characterized by the presence of epidote, calcite, and crystals of clinopyroxene that have replaced hornblende; and
- 2) high alkalinity endoskarn (periskarn) characterized by large amounts of potassium feldspar (up to 60 percent by volume), wollastonite, garnet, epidote, and crystals of clinopyroxene that have replaced

hornblende. Another variety of alteration that may have occurred during the formation of the skarns is characterized by a red discoloration caused by the mobilization of iron, part of which has stained the normally gray rocks, associated with the hydrothermal destruction of the ferromagnesian minerals. The red stains are most evident along joint surfaces. The discolored rocks also contain abundant calcite in the groundmasses. Intrusive rocks at one location have been altered to an assemblage of quartz and sericite accompanied by fogs of copper "carbonate" and cubes of limonite after pyrite.

Chemical reactions between the carbonate strata at the Copper Chief Prospect and the metasomatizing hydrothermal fluids, which were laden with mobile constituents, resulted in the formation of a variety of calc-silicate minerals. The most abundant of these are garnetites. The garnetites range in composition from grossularite to andradite, but most have compositions between these two end-members (grandites). The end member garnetites form small, isolated bodies at a few scattered locations, whereas the grandite garnetites are present throughout the central and northwest parts of the prospect. The garnetites contain variable proportions of clinopyroxene, calcite, and quartz. Nearly monomineralic rocks that consist of

wollastonite with trace amounts of calcite and quartz are present at three locations within the prospect.

These may represent high temperature pods or remnants formed during the early stages of metasomatism.

Porphyroblastic garnets contained in a microcrystalline groundmass of quartz and clinopyroxene are interbedded with clinopyroxene-garnet calc-silicate hornfels in the northwest part of the prospect.

The mineral assemblages of the calc-silicate rocks from the Copper Chief Prospect are compatible with either the hornblende or pyroxene hornfels facies of contact metamorphism. The minerals of the endoskarns (particularly clinopyroxene, garnet, and wollastonite) and the presence of nearly monomineralic zones of wollastonite in the exoskarns suggest higher temperatures (600 to 800° C; Turner, 1968; Zharikov, 1968) characteristic of the pyroxene hornfels facies.

The Copper Chief Prospect is a contact metasomatic deposit formed by a scheelite-sulfide skarn. The scheelite occurs in a clinopyroxene-rich garnetite as disseminated grains and locally as single crystals and polycrystalline aggregates associated with garnet in veinlets that crosscut the garnetite. The sulfides are associated with andradite garnetite, marble, and veins of quartz. The quartz veins crosscut or replace, calc-silicate rocks, marble, and

quartz monzodiorite. The sulfides have been oxidized by supergene processes and now only remnants of the original ore minerals remain in surface exposures. The original hypogene minerals consisted of chalcopyrite, pyrite, and chalcocite, and these have been largely altered to a supergene assemblage consisting predominantly of malachite, azurite, and limonite.

The volcanic rocks that overlie the Luning Formation and the intrusions into this formation consist of the following sequence from bottom to top: 1) quartz and potassium feldspar phenocryst-bearing tuff; 2) hornblende and plagioclase feldspar-bearing volcanic rock; 3) quartz and potassium feldspar tuff; and 4) dacitic andesite with micro-trachytic textures. Possible feeder dikes consisting of a finely crystalline medium brown colored lithology containing phenocrysts of plagioclase feldspar crosscut the metasedimentary rocks at two locations.

Faults of the Battles Well Strand of the Walker Lane cross the northeast corner of the mapped area. They separate the mineralized and metamorphosed sedimentary rocks from unaltered strata. These faults also cut, and displace, the volcanic rocks that overlie the local basement complex of mineralized sedimentary, intrusive, and metamorphic rocks.

BIBLIOGRAPHY

- Ahrens, L. H., 1954, The lognormal distribution of the elements: *Geochim. et Cosmochim. Acta*, v. 5, p. 49-73; v. 5, p. 121-131.
- Albers, J. P., 1967, Belt of sigmoidal bending and right lateral faulting in the western Great Basin: *Geol. Soc. America Bull.*, v. 78, p. 143-156.
- Anderson, G. H., 1937, Precambrian stratigraphy in the northern Inyo Range, California (abs.): *Geol. Soc. America Proc.* 1936, p. 61-62.
- Bailey, E. H.; and Stevens, R. E., 1960, Selective staining of K-feldspar and plagioclase on rock slabs and thin sections: *Amer. Mineral.*, v. 45, p. 1020-1025.
- Barth, T. F. W., 1962, *Theoretical Petrology*: New York, John Wiley & Sons, 416 p.
- Bateman, P. C., 1961, Granitic formations in the east-central Sierra Nevada near Bishop, California: *Geol. Soc. America Bull.*, v. 72, p. 1521-1538.
- _____, 1965, Geology and tungsten mineralization of the Mount Givens granodiorite, Sierra Nevada, California: *U. S. Geol. Survey Prof. Paper* 470, 208 p.
- _____; and Chappell, B. W., 1979, Crystallization, fractionation, and solidification of the Tuolumne Intrusive Series, Yosemite National Park, California: *Geol. Soc. America Bull.*, v. 90, pt. I, p. 465-482.
- _____; and Nokleberg, W. J., 1978, Solidification of the Mount Givens granodiorite, Sierra Nevada, California: *Jour. Geol.*, v. 86,

p. 563-579.

- Blanchard, Roland, 1968, Interpretation of leached outcrops: Nev. Bur. Mines Bull. 66, 196 p.
- Bowen, N. L., 1928, The evolution of the igneous rocks: Princeton, Princeton Univ. Press, 332 p.
- Brown, A. S., 1976, Morphology and classification: Canadian Inst. Mining, Spec. Vol. 15, p. 44-51.
- Burnham, C. W., 1962, Facies and types of hydrothermal alteration: Econ. Geology, v. 57, p. 768-784.
- Chayes, Felix, 1956, Petrographic modal analysis: an elementary statistical appraisal: New York, John Wiley & Sons, 113 p.
- Clark, C. W., 1922, Geology and ore deposits of the Santa Fe District, Mineral County, Nevada: Calif. Univ. Geol. Sci. Bull. 14, p. 1-74.
- Cook, E. F., 1965, Stratigraphy of Tertiary volcanic rocks in eastern Nevada: Nev. Bur. Mines Rept. 11, 66 p.
- Creasey, S. C., 1959, Some phase relations in the hydrothermally altered rocks of porphyry copper deposit: Econ Geology, v. 54, p. 351-373.
- Crowder, D. F.; McKee, E. H.; Ross, D. C.; and Krauskopf, K. B., 1973, Granitic rocks of the White Mountains area, California: age and regional significance: Geol. Soc. America Bull., v. 84, p. 285-296.
- _____ ; and Ross, 1973, Petrography of some granitic bodies in the northern White Mountains California-Nevada: U.S. Geol. Survey Prof. Paper 775, 28 p.

- Curtis, G. H.; Evernden, J. F.; and Lipson, J., 1958, age determinations of some granitic rocks in California by the potassium-argon method: Calif. Div. Mines Spec. Rept. 54, 14 p.
- Deer, W. A.; Howie, R. A.; Zussman, J., 1966, An introduction to the rock forming minerals: New York, John Wiley & Sons, 528 p.
- Donath, F. A., 1962, Analysis of Basin-Range structure: Geol. Soc. America Bull., v. 73, p. 1-15.
- Drummond, A. D.; and Godwin, C. I., 1976, Hypogene mineralization - an empirical evaluation of alteration zoning: Canadian Inst. Mining Spec. Vol. 15, p. 52-63.
- Ekren, E. B.; Buckman, R. C.; Carr, W. J.; Dixon, G. L.; and Quinlivna, W. D., 1976, East-trending structural lineaments in central Nevada: U.S. Geol. Survey Prof. Paper 986, 16 p.
- Emmons, S. F., 1870, Geology of the Toyabe Range, Nevada: U.S. Geol. Expln. 40th Parallel Rept., v. 3, p. 320-348.
- Eskola, P., 1939, Die metamorphen gesteine: in Die enstehung der gesteine, Barth, T. F. W.; Correns, C. W.; and Eskola, P., eds., Berlin, Springer, p. 263-407.
- Evernden, J. F.; and Kistler, R. W., 1970, Chronology of emplacement of Mesozoic batholithic complexes in California and western Nevada: U.S. Geol. Survey Prof. Paper 623, 42 p.
- Ferguson, H. G., 1924, Geology and ore deposits of the Manhattan District, Nevada: U.S. Geol. Survey Bull. 723, 163 p.

Ferguson, H. G.; and Cathcart, S. H., 1924, Major structural features of some western Nevada ranges: Wash. Acad. Sci. Jour., v. 14, p. 376-379.

_____ ; and Muller, S. W., 1949, Structural geology of the Hawthorne and Tonopah quadrangles, Nevada: U.S. Geol. Survey Prof. Paper 216, 53 p.

Field, C. W.; Briskey, J. A.; Henricksen, T. A.; Jones, M. B.; Schmuck, R. A.; and Bruce, W. R., 1975 Chemical trends in Mesozoic plutons associated with porphyry-type metallization of the Pacific Northwest: Amer. Inst. Mining Metall. Pet. Engineers, Preprint 75-L-359 25 p.

Franco, R. R.; and Schairer, J. F., 1951, Liquidus temperatures in mixtures of the feldspars of soda potash, and lime: Jour. Geology, v. 59, p. 259-267.

Frischman, David, 1976, Geologic map of the Copper Chief Prospect: Continental Oil Co. Map (unpubl.).

Fyfe, W. S.; Turner, F. J.; and Verhoogen, J., 1958, Metamorphic reactions and metamorphic facies: Geol. Soc. America Mem. 73, 259 p.

Gianella, v. p.; and Callaghan, Eugene, 1934, The earthquake of Dec. 20, 1932, at Cedar Mountain, Nevada, and its bearing on the genesis of Basin-Range structure: Jour. Geology, v. 42, p. 1-22.

Gilbert, G. K., 1874, Preliminary geological report, expedition of 1872: U.S. Geol. Survey, W. 100th Meridian Prog. Rept.(Wheeler), p. 48-52.

_____, 1875, Report of the geology of portions of Nevada, Utah, and Arizona examined in the

years 1871 and 1872 U.S. Geog., Geol. Explor. Survey, W. 100th Meridian Prog. Rept. (Wheeler), v. 3, p. 17-187.

Gilluly, James, 1970, Crustal deformation in the western United States: in Johnson, H.; and Smith, B. L., eds., The megatectonics of continents and oceans: New Brunswick, Rutgers Univ. Press, p. 47-73.

Greensfelder, R. W., 1965, The $P_g - P_n$ method of determining depth of focus with applications to Nevada earthquakes: Seismol. Soc. America Bull., v. 55, p. 391-403.

Gumber, F. J.; and Scholz, C. H., 1971, Microseismicity and tectonics of the Nevada seismic zone: Seismol. Soc. America Bull., v. 61, p. 1413-1432.

Hamilton, Warren; and Meyers, W. B., 1966, Cenozoic tectonics of the western United States: Rev. Geophys., v. 4, p. 509-549.

Hess, F. L., 1919, Tactite - the product of contact metamorphism: Amer. Jour. Sci., v. 48, p. 377-378.

Hill, J. M., 1915, Some mining districts in northeastern California and northwestern Nevada: U.S. Geol. Survey Bull. 594, p. 1-74.

Hutchison, C. S., 1974, Laboratory handbook of petrographic techniques: New York, John Wiley & Sons, p. 374-437.

Jerome, S. E.; and Cook, D. R., 1967, Relation of some metal mining districts in the western United States to regional tectonic environments and igneous activity: Nev. Bur. Mines Bull. 69, 35 p.

- Kerr, P. F., 1959, Optical mineralogy: New York, McGraw-Hill Book Co., 442 p.
- Kistler, R. W.; Bateman, P. C.; and Brannock, W. W., 1965, Isotopic ages of minerals from granitic rocks of the central Sierra Nevada and Inyo Mountains, California: Geol. Soc. America Bull., v. 76, p 155-164.
- _____ ; Evernden, J. F.; and Shaw, H. R., 1971, Sierra Nevada plutonic cycle: Part I, origin of composite granitic batholiths: Geol. Soc. America Bull., v. 82, p. 853-868.
- _____ ; and Peterman, Z. E., 1973, Variations in Sr, Rb, K, Na, and initial Sr^{87}/Sr^{86} in Mesozoic granitic rocks and intruded wall rocks in central California: Geol. Soc. America Bull., v. 84, p. 3489-3512.
- Knopf, Adolf, 1921, Ore deposits of Cedar Mountain, Mineral County, Nevada: U.S. Geol. Survey Bull. 725, p. 361-382.
- _____, 1922, The Candelaria Silver District, Nevada: U.S. Geol. Survey Bull. 735, p. 1-22.
- Korzhinskii, D. S., 1965, The theory of systems with perfectly mobile components and processes of mineral formation: Amer. Jour. Sci., v. 263, p. 193-205.
- _____, 1968, The theory of metasomatic zoning: Mineralium Deposita, v. 3, p. 222-231.
- Langenheim, R. L., Jr.; and Larson, E. R., 1973, Correlation of Great Basin Stratigraphic units: Nev. Bur. Mines and Geol. Bull. 72, 36 p.
- Le Conte, Joseph, 1889, On the origin of normal faults

and the structure of the basin region: Amer. Jour. Sci., 3rd Series, v. 38, p. 257-263.

Le Maitre, R. W., 1976, The chemical variability of some common igneous rocks: Jour. Petrology, v. 17, p. 589-637.

LePeltier, Claude, 1969, A simplified statistical treatment of geochemical data by graphical representation: Econ. Geology, v. 64, p. 538-550.

Lincoln, F. C., 1923, Mining districts and mineral resources of Nevada: Nev. Newsletter Publ. Co., 245 p.

Lindgren, Waldemar, 1924, Contact metamorphism at Bingham, Utah: Geol. Soc. America Bull., v. 35, p. 507-534.

Locke, Augustus; Billingsley, P. R.; and Mayo, E. B., 1940, Sierra Nevada Tectonic Pattern: Geol. Soc. America Bull., v. 51, p. 513-539.

Longwell, C. R., 1950, Tectonic history reviewed from the Basin Ranges: Geol. Soc. America Bull., v. 61, p. 431-434.

Lowell, J. D.; and Gilbert, J. M., 1970, Lateral and vertical alteration mineralization zoning in porphyry ore deposits: Econ. Geology, v. 65, p. 373-408.

Mackin, J. H., 1960, Structural significance of Tertiary volcanic rocks in southwestern Utah: Amer. Jour. Sci., v. 258, p. 81-131.

_____, 1968, Iron ore deposits of the Iron Springs District southwestern Utah: Amer. Inst. Mining Metall. Pet. Engineers, Graton-Sales

Vol., v. II, p. 992-1019.

Mangham, J. R., 1977, Geologic reconnaissance of the Santa Fe Mining District, Mineral County, Nevada: Continental Oil Co. Rept. (unPubl.).

McKee, E. H.; and Nash, D. B., 1967, Potassium-argon ages of granitic rocks in the Inyo Batholith, east-central California: Geol. Soc. America Bull., v. 78, p. 669-680.

Middlemost, E. A. K., 1980, A contribution to the nomenclature and classification of volcanic rocks: Geol. Magazine, v. 117, p. 51-57.

Muller, S. W.; and Ferguson, H. G., 1936, Triassic and lower Jurassic formations of west central Nevada: Geol. Soc. America Bull., v. 47, p. 241-252.

_____, 1939, Mesozoic stratigraphy of the Hawthorne and Tonopah quadrangles, Nevada, Geol. Soc. America Bull., v. 50, p. 1573-1624.

Nielsen, R. L., 1965, Right-lateral strike slip faulting in the Walker Lane, west-central Nevada: Geol. Soc. America Bull., v. 76, p. 1301-1308.

Niggli, Paul, 1954, Rocks and mineral deposits: San Francisco, W. H. Freeman and Co., 559 p.

Oldow, J. S., Structure and kinematics of the Luning allochthon, Pilot Mountains, western Great Basin, U.S.A.: PhD Thesis, Evanston, Illinois, Northwestern Univ., 206 p.

Reinhart, C. D.; and Ross, D. C., 1964, Geology and mineral deposits of the Mount Morrison quadrangle Sierra Nevada, California: U.S. Geol. Survey Prof. Paper 385, 106 p.

- Ross, D. C., 1961, Geology and mineral deposits of Mineral County, Nevada: Nev. Bur. Mines Bull. 58, 85 p.
- _____, 1969, Descriptive petrography of three large granitic bodies in the Inyo Mountains, California: U.S. Geol. Survey Prof. Paper 601, 47 p.
- Schilling, J. H., 1965, Isotopic age determinations of Nevada rocks: Nev. Bur. Mines Rept. 10, 79 p.
- Shawe, D. R., 1965, Strike-slip contact of Basin-Range structure indicated by historical faults in western Nevada: Geol. Soc. America Bull., v. 76, p. 1361-1378.
- Sinclair, A. J., 1976, Applications of probability graphs in mineral exploration: Assoc. Explor. Geochemists, Spec. Vol. 4, Richmond, B. C., Richmond Printers Ltd., 95 p.
- Slemmons, D. B.; Van Wormer, D.; Bell, E. J.; Silberman, M. L., 1979, Recent crustal movements in the Sierra Nevada - Walker Lane region of California-Nevada: Part I rate and style of deformation: Tectonophysics, v. 52, p. 561-570.
- Stewart, J. H., 1971, Basin and Range structure: a system of horsts and grabens produced by deep seated extension: Geol. Soc. America Bull., v. 82, p. 1019-1044.
- _____; Albers, J. P.; and Poole, F. G., 1968, Summary for right-lateral displacement in the western Great Basin: Geol. Soc. America Bull., v. 79, p. 1407-1414.

Streckeisen, Albert, 1976, To each plutonic rock its proper name: *Earth Sci. Rev.*, v. 12, p. 1-33.

_____, 1979, Classification and nomenclature of volcanic rocks, lamprophyres, carbonatites, and melilitic rocks: recommendations and suggestions of the IUGS subcommission on the systematics of igneous rocks: *Geology*, v. 7, p. 331-335.

Suschinskiy, P., 1912, Data in studies of contacts between abyssal rocks and limestones in Finland: *Trudy SPb obshch. estestv.*, v. 36, no. 5.

Sylvester, A. G.; Miller, C. F.; and Nelson, C. A., 1978, Monzonites of the White-Inyo Range, California, and their relation to the calc-alkalic Sierra Nevada Batholith: *Geol. Soc. America Bull.*, v. 89, p. 1677-1687.

Tennant, C. B.; and White, M. L., 1959, Study of the distribution of some geochemical data: *Econ. Geology*, v. 54, p. 1281-1290.

Thompson, G. A., 1959, Gravity measurements between Hazen and Austin, Nevada - a study of Basin-Range structure: *Jour. Geophys. Res.*, v. 64, p. 217-229.

_____, 1966, The rift system in the western United States, *Geol. Soc. Canada Paper 66-14*, p. 280-289.

_____; and Burke, B. B., 1973, Rate and direction of spreading in Dixie Valley, Basin and Range province, Nevada: *Geol. Soc. America Bull.*, v. 84, p. 627-632.

Turner, F. J., 1968, *Metamorphic petrology: mineralogical and field aspects*: San Francisco, McGraw-Hill Book Co., 403 p.

- Vance, J. A., 1969, On synneusis: *Contr. Mineral. and Petrol.*, v. 24, p. 7-29.
- Vanderburg, W. O., 1937, Reconnaissance of mining districts in Mineral County, Nevada: U.S. Bur. Mines Information Circ. 6941.
- Washington, H. S., 1917, Chemical analyses of igneous rocks published from 1884 to 1913 inclusive, with a critical discussion of the character and use of analyses; a revision of Prof. Paper 14: U.S. Geol. Survey Prof. Paper 99, 1201 p.
- Whitney, Josiah, 1866, Remarks on the geology of the State of Nevada: *Calif. Acad. Natl. Sci.*, Pr. 3, 266-270.
- Wright, L. A.; and Troxel, B. W., 1970, Summary of regional evidence for right-lateral displacement in the western Great Basin: *Discussion: Geol. Soc. America Bull.*, v. 81, p. 2167-2174.
- Zharikov, V. A., 1968, Skarnovyye mestorozhdeniya (Skarn source fields of ores): in *Genezis endogennykh rudnykh mestorozhdeniy (Genesis of endogenetic ore deposits)*: Moscow, Nedra Press; also in *Intl. Geol. Review*, 1970, v. 12, p. 541-559, 619-647, and 760-775.

APPENDIX

APPENDIX

LABORATORIES AND METHODS USED FOR CHEMICAL ANALYSESMajor Oxides

Samples of volcanic and plutonic rocks

Geology Department, Univ. of Oregon, Eugene
 SiO_2 , TiO_2 , Al_2O_3 , Fe_2O_3^* (total iron
as Fe_2O_3), MgO , MnO , K_2O , P_2O_5 -- X-ray
fluorescence spectroscopy.

Na_2O -- Atomic absorption spectroscopy.

Skyline Labs, Inc., Wheat Ridge, Colorado
 $\text{Fe}_2\text{O}_3/\text{FeO}$ -- Inductively coupled plasma
spectroscopy and potassium dichromate
titration.

Samples of calcareous and calc-silicate rocks

Skyline Labs, Inc., Wheat Ridge, Colorado
 SiO_2 -- Atomic absorption spectroscopy.
 Al_2O_3 , Fe_2O_3^* , CaO , MgO , Na_2O , MgO ,
 Na_2O , K_2O -- Inductively coupled plasma
spectroscopy following HF , HNO_3 , and
 HClO_4 digestion.

Trace Elements

All samples

Rocky Mountain Geochem Labs, Reno, Nevada
 Cu , Zn , Mo , Au , Ag , Mn , Pb -- Atomic
absorption spectroscopy.

WO_3 -- Colorometric analyses.